Mn/Fe reduction in sandy soil during degradation of de-icing chemical

Respiration kinetics and prokaryotic community composition

Gudny Øyre Flatabø

Master thesis in Biology – Microbiology

Department of Biology

UNIVERSITY OF BERGEN

01.06.2017

Gudny Ø. Flatabø, MSc, Department of Biology, University of Bergen, in collaboration with Faculty of Environmental Sciences and Natural Resource Management, Norwegian University of Life Sciences

Supervisors: ***Professor Lise Øvreås (UiB)***
Dr. Peter Dörsch (NMBU)
Associate professor Helen K. French (NMBU)

ABSTRACT

At Oslo airport, Gardermoen, Norway, large quantities of propylene glycol (PG) are used as de-icing fluid during winter, causing high loads of this chemical to infiltrate in surrounding soil during snow melt and increasing concentrations of soluble manganese (Mn^{2+}) and ferrous iron (Fe^{2+}) in the groundwater. Previous studies have suggested that anaerobic microbial Mn and Fe reduction fuelled by PG in deeper soil layers is the primary reason for the observed increase of Mn^{2+} and Fe^{2+} and proposed nitrate (NO_3^-) fertilization as a mitigation measure. However, laboratory and field experiments with NO_3^- addition have yielded inconsistent, partly adverse results.

To better understand the effect PG has on Mn^{2+} and Fe^{2+} release in the Gardermoen soil system, in the presence or absence of moderate NO_3^- concentrations, a series of batch incubation experiments was carried out with non-contaminated top and subsoil sampled at a research site close to Oslo airport. Microbial activity was measured as O_2, CO_2, NO, N_2O and N_2 kinetics, while the release of Fe^{2+} and Mn^{2+} was monitored by subsampling the soil solution through microrhizones. After 26 days of incubation, 16S-rDNA was extracted and sequenced to study the effect of PG and N on microbial community composition.

Both, top- and subsoil released Mn^{2+} and Fe^{2+} in untreated controls but release rates were larger in the presence of PG. Top soil released on average 100 to 1000 times more Mn^{2+} than subsoil, which was attributed to a larger abundance of Mn(IV) reducing bacteria in the topsoil. Unlike in top soil, moderate NH_4NO_3 addition to the subsoil triggered additional Mn^{2+} release, apparently by relieving N limitation of microbial growth. The comparison of 16S rRNA-based taxonomic abundances before and after incubation of subsoil with PG and NO_3^- revealed that the metabolically versatile families *Comamonadaceae*, *Oxalobacteraceae* and *Pseudomonadaceae* increased in relative abundance, likely dominating PG metabolism and Mn and Fe reduction observed at the end of the incubation. Therefore, NO_3^- addition, although providing an alternative electron acceptor, cannot be recommended for mitigation of metal release, as it poses the risk to increase microbial Mn and Fe reduction in the subsoil. In contrast, measures that lead to a better aeration of the top layer, particularly during wet periods, appear to be the more promising approach to avoid Mn^{2+} and Fe^{2+} release.

ACKNOWLEDGEMENTS

First of all I have to thank my supervisor Peter Dörsch at NMBU in Ås for all the late nights and countless hours spent on explaining me the world of respiration kinetics. I have learned an incredible amount in such a short time, and the time spent at the lab in Ås has meant a lot to me. Nothing of this would have been possible without your curiosity and patience, Peter. I would also like to thank Helen French, for her welcoming attitude and for opening up the possibility for me to come to Ås to look into this subject. My supervisor at UiB, Lise Øvreås, thank you for being positive to a collaborative Master project, and for throwing me into the amazing world of geomicrobiology and microbial ecology and pushing me to understand as much as I can of high-throughput sequencing and analysis. Bryan Wilson, who has taught me so much about bioinformatics, and in his cheerful manner have explained the reason behind every command whenever asked. I am so thankful for Hilde and Julia, who went through all the lab work step by step, and patiently answering all questions. I am very grateful for my family, who are always positive and cheering me on. My friends, Anna and Elisabeth, who made my stay in Ås even more interesting. Anja, who is always available and supportive, Cristina, for always being interested and Manuel, who helps in every way possible.

Bergen myrdyrkingsforeningsfond funded the sequencing part of this study, of which I am very grateful. I hope the fund will have continued interest in projects concerning soil contamination in the future.

Bergen, May 2017

Table of Contents

INTRODUCTION

Oslo airport is located at the Gardermoen glacial-contact delta, approximately 40 km north of Oslo in southeastern Norway. The delta forms an aquifer composed of sand with beds of gravel underlain by silty glaciomarine deposits (Jørgensen & Østmo 1990; Tuttle 1997). It is the largest rainfed aquifer in Norway. More than half of the aquifer recharge occurs during snow melt in the spring (Jørgensen & Østmo 1990).

Several chemicals are released during the airport's operations that potentially affect soils and groundwater locally. During the winter months October-April, large amounts of de-icing chemicals, typically glycols, are used to defrost planes, in addition to acetate or formate salts which are used to keep the runways ice-free (Ferguson *et al.* 2008).

When it was decided that Oslo's new main airport was to be built at Gardermoen, concerns were raised about the impact it would have on the groundwater and studies on the transport and degradation of de-icing fluids were initiated before the airport started operating in 1998 (French *et al.* 1994). The most urgent question, whether de-icing fluids would contaminate the groundwater directly or if it would be broken down in the soil profile, was quickly answered when de-icing fluids were detected in the groundwater already in the first year of operation (Samferdselsdepartementet 1999). This led to investment in specialized de-icing platforms designed to collect de-icing fluids from the 1999-2000 winter season onwards (Avinor 2000). Today, Oslo airport collects approximately 80% of fluids used for de-icing airplanes, while the remaining 20% are spread over the area alongside the runways or carried further by the aircraft (Wennberg et al. 2015; Øvstedal & Wejden 2007).

Monitoring of the dispersion of de-icing chemicals at Oslo airport has shown that the largest load occurs close to the runway edge, 400 to 1000 m after the start position for take-off. The total load of propylene glycol (PG) deposited on surrounding soils is 100 - 200 tons per winter. This is a major reduction from the 2 800 tons spread prior to establishing the collection platforms in the winter season of 1998-1999 (Avinor 2000). Still, snow in the area close to the runway can contain up to 6000 ppm of PG, and the cumulative load can be up to 1.8 kg/m^2 in one winter season (Øvstedal & Wejden 2007).

By limiting the use of de-icing fluids, the airport operator mostly complies with the release permit given by the Norwegian Environment Agency. However, concentrations of Mn^{2+} in the groundwater closest to the runway are clearly larger than in the surrounding areas, and concentrations have slightly increased since the start of monitoring in 1999. Likewise, elevated Fe^{2+} concentrations have been reported from groundwater close to the runway, starting to increase in 2006. Mn^{2+} and Fe^{2+} peak concentrations have been observed to occur especially during the summer months (Avinor 2016).

The aquifer underlying Oslo airport is currently not used as a source for drinking water, but there is a general interest to preserve the aquifer as a future resource, which makes avoidance of contamination urgent. Dissolved manganese and iron are generally undesirable in drinking water, as they cause a bad taste and colour as well as precipitates in pipelines, potentially causing pressure build-up and increased maintenance costs (Solheim *et al.* 2008). Hence, in-depth understanding of the conditions supporting Mn/Fe release from the soil to the groundwater and the role of de-icing chemicals therein are crucial for evaluating whether the use of de-icing fluids in its present form is environmentally justified or whether measures to avoid Mn/Fe release should be taken, preferably without compromising the desirable biological degradation of de-icing substances in the unsaturated zone.

1.1 The Moreppen research station and the Gardermoen soil system

The Moreppen research station was established in 1992 as a 2.4 m deep lysimeter trench to monitor environmental data in soil representative for the surroundings of Oslo airport and to perform transport studies with de-icing chemicals (Figure 1.1, French *et al.* 1994). Soils in the unsaturated zone of Moreppen are predominately coarse to medium-sized sands, containing a decreasing amount of gravel with depth, occasional pockets of silt and a layer of fine or laminated sand at the bottom of the profile. The trench and the surrounding area have been used for numerous studies organized in long-term research programs, such as "The environment of the subsurface - Part I: The Gardermoen Project 1992-95" and "Soil Contamination: Advanced integrated characterisation and time lapse Monitoring (SoilCAM) 2008-2012."

The Gardermoen project stated that the Moreppen soil system has a relatively large degradation capacity for different pollutants connected to the airport (French *et al*. 2001) which, however, depends on the residence time of the chemicals in the unsaturated zone. Model studies on meltwater flow suggest that the degradation capacity is additionally controlled by soil heterogeneity (French 1999, Figure 0.1), permeability and micro-topography of the ground surface (Kitterød 2007; French *et al.* 2002).

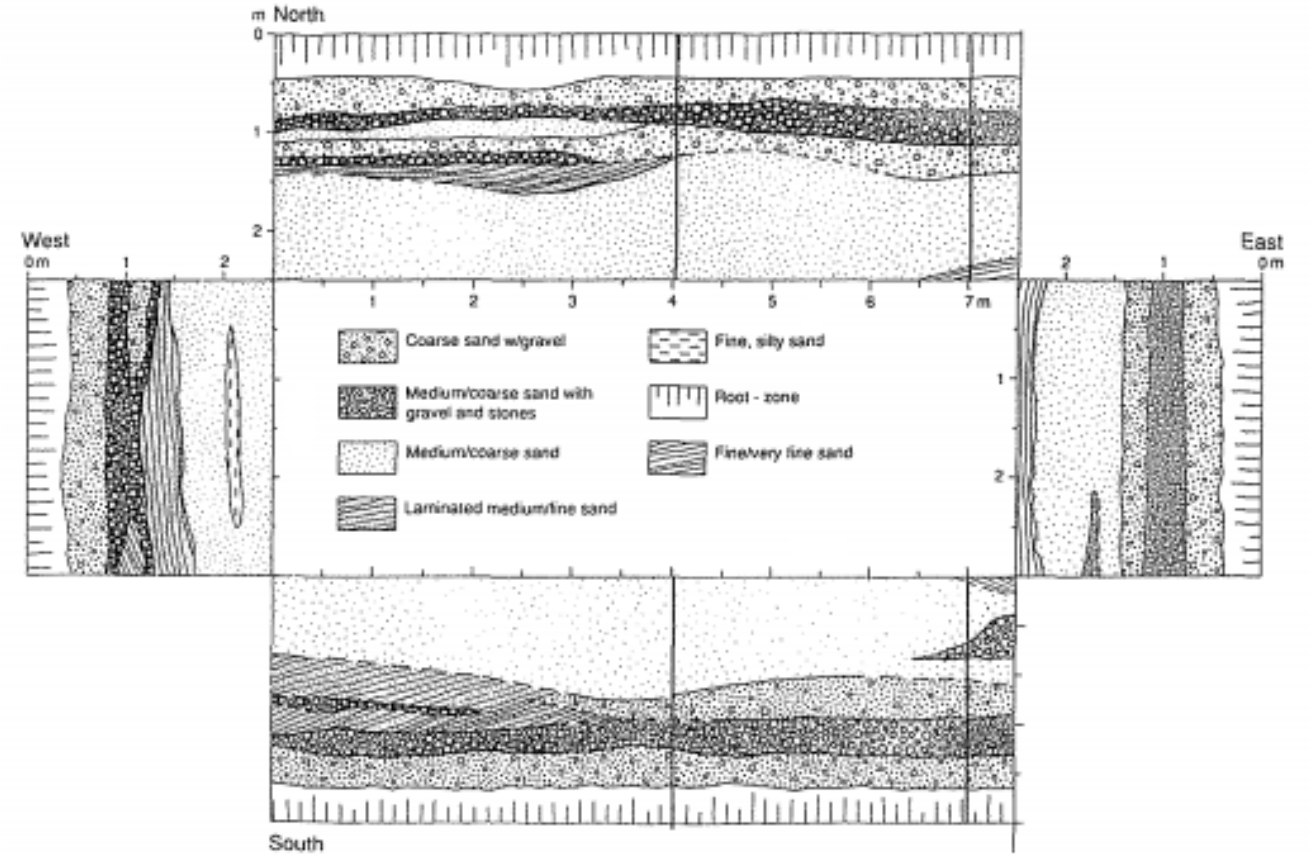

Figure 0.1: Heterogeneity of soils as assessed along the walls of the Moreppen lysimeter trench. From French et al. (1994). The North, West and South walls are equipped with various instrumentation, whereas the East wall was kept as an undisturbed reference profile and was used for soil sample collection in the present study.

De-icing chemicals are typically used during the winter months, allowing the chemicals to mix with the snow alongside the runways. Since de-icing chemicals are liquid at temperatures below 0ºC, they readily infiltrate into the frozen soil. Studies at Moreppen have demonstrated infiltration of melt water with elevated concentrations of de-icing chemicals during the first part of the melting period (French *et al.* 1996). The same study showed that de-icing chemicals accelerated snow melt

relative to snow without de-icing chemicals, resulting in a larger and earlier flush of contaminated melt water infiltrating the soil.

The ground water table at Moreppen before the snowmelt season of 2001 was 3.3 meter below the surface and rose to 2.8 m during snowmelt from early April to early May, despite the temperature in the upper one meter of soil being only between -0.5 and 1ºC, increasing to 2 - 4ºC not before late in April. Concentrations of sodium bromide (NaBr) along the profile, applied as tracer, indicated preferential flow, mediating rapid infiltration of melt water down to 1.5 m depth (French et al. 2002; Kitterød 2007). Simultaneously to the preferential flow, melt water distributed laterally in the surface layers, which became particularly apparent when the ground started to thaw. This infiltration pattern, and the observation that the majority of the de-icing chemicals are infiltrated during the "first flush" of melt water (French *et al*. 1996; French & Binley 2004) suggests that in addition to some infiltration in the upper layers, PG is transported to deeper soil layers bypassing the top soil. Moreover, propylene glycol does not adsorb to the soil particles (French 1999), so that water transport in the profile is the prime factor determining its residence time in the unsaturated zone.

Previous field experiments and airport monitoring found increased concentrations of manganese in the pore water and groundwater during the summer period, when degradation of propylene glycol was fastest (French *et al*. 2001; Avinor 2016). Although not measured, iron was likely also released, as it precipitated as iron oxides in the sampling bottles (French pers. comm.). Since iron and manganese are only mobile in their reduced form (2+), i.e. in the absence of oxygen which quickly oxidize Fe and Mn to immobile forms, this was a strong indication that anaerobic conditions were present during summer also in the unsaturated zone, possible triggered by the high oxygen demand of biological PG degradation. Degradation processes were studied further in the SoilCAM project focusing on degradation products, redox conditions and possible remediation techniques such as adding nitrate (Toscano *et al*. 2014; Lissner *et al.* 2014). Nitrate addition was tested in 1 m long cores with soil from PG-affected areas at Oslo airport. Nitrate addition did not reduce Fe and Mn release nor did it increase PG degradation, and it was concluded that nitrate does not work as an alternative electron acceptor (Lissner *et al*. 2014). However, testing the addition of nitrate to an anaerobic soil slurry of a subsoil (-4 m) from Oslo airport inhibited Mn^{2+} and Fe^{2+} formation and increased PG degradation (Toscano *et al.* 2014).

1.2 Respiration and electron acceptors

All living organisms rely on energy-yielding metabolism for maintenance and growth. Unlike eukaryotes, prokaryotes show a wide metabolic versatility with respect to their substrates and a stunning ability to use widely different electron acceptors for energy conservation. Energy conservation in bacteria is commonly coupled to oxidation-reduction (short: red-ox) reactions, where oxidation is defined as the removal of an electron from a substrate (the "electron donor"), while reduction is defined as the addition of an electron to another substrate (the "electron acceptor"). In aerobic respiration, oxygen is the electron acceptor, being reduced to water (Madigan *et al*. 2014), whereas in anoxic respiration various electron acceptors can be used.

Prokaryotes utilize a large variety of substrates as electron donors, both inorganic and organic ones. *Heterotrophs* or *chemoorganotrophs* oxidise organic compounds, ranging from simple 3-carbon compounds such as glycols (Willetts 1979; Child & Willetts 1978) to more complex molecules such as polyaromatic hydrocarbons (Cerniglia 1984; Johnsen *et al.* 2005). *Chemolithotrophs*, in contrast, oxidize reduced inorganic compounds, such as H_2, NH_4^+, CH_4, H_2S (Schmidt *et al.* 2002; Arp & Stein 2003; Francis *et al.* 2007) or Fe^{2+} (Weber *et al.* 2006).

To yield energy, organisms couple an electron donor to an electron acceptor via metabolic pathways. As mentioned above, in aerobic respiration, O_2 is the terminal electron acceptor. In anoxic respiration, other electron acceptors must be utilized as terminal electron acceptors, such as NO_3^-, Mn(IV), Fe(III), SO_4^- and CO_2 (Madigan *et al*. 2014).

Another option for energy generation is using an organic compound simultaneously as electron donor and electron acceptor, as in *fermentation*. Fermentation creates energy through substrate-level phosphorylation, a process where ATP is synthesized by phosphorylation of ADP directly from energy-rich intermediates during steps in the catabolism of the substrate being fermented. In respiration, ATP is synthesized from a *proton motive force* generated from the electron transport chain of a redox reaction, causing an energized membrane that can drive phosphorylation of ADP to ATP.

Some microorganisms, termed *aerobes*, are only capable of aerobic respiration, while others, termed *anaerobes*, are only capable of fermentation or anaerobic respiration. However, some

microorganisms, termed *facultative aerobes*, are able to switch between different types of energy-yielding metabolism based on environmental conditions, such as denitrifiers (Madigan *et al*. 2014).

Theoretically, the type of prevailing microbial metabolism depends on the organism present, the type and availability of electron donors and acceptors and the achievable energy yield from the metabolic reactions. The "redox tower" (Figure 0.2) is a way to visualize the variety of red-ox reactions that can be utilized for microbial respiration. The listed red-ox couples can be conceptualized as chemical half reactions, which must be combined for a metabolic reaction to occur. When two half reactions are combined, the "tower" predicts metabolism supported by oxidation of the couple with the highest E_0'-value and reduction of the couple with the lowest E_0'. For example the NO_3^-/NO_2^- (0.42 V) couple combined with the CO_2/glucose (-0.43 V) couple yields the following reaction:

$$12NO_3^- + C_6H_{12}O_6 \rightarrow 12NO_2^- + 6H_2O + 6CO_2$$

In this case, NO_3^- is reduced, since it has the highest E_0' value, and glucose is oxidized, since CO_2/glucose has the lowest E_0' value (-0.43 V). In total, 12 × 2 electrons are transferred from glucose to NO_3^-. For a given electron donor, metabolism should be favored involving the electron acceptor yielding the most energy, as predicted from the difference between the two E_0'-values. From the redox tower (Figure 0.2) it can be seen that the O_2/H_2O couple yields the most energy, with an E_0' value of 0.82 V. Thus, when oxygen is present as electron acceptor, aerobic respiration is favoured.

In *denitrification*, the complete reduction of nitrate to molecular nitrogen gas has an E_0' value of 0.74 V, which comes close to the energy yield in oxic respiration. Dissimilatory nitrate reduction to N_2 should thus be the preferred metabolic pathway under anaerobic condition as long as NO_3^- is present. However, not all denitrifiers possess the ability to induce enzymes that can reduce NO_3^- all the way to N_2 via the intermediates NO_2^-, NO and N_2O and truncated metabolic pathways with less energy yield exist Apart from denitrification, many bacteria can perform *nitrate respiration*, i.e. reduce NO_3^- to NO_2^- (E_0' value for NO_3^-/NO_2^- couple: 0.42 V).

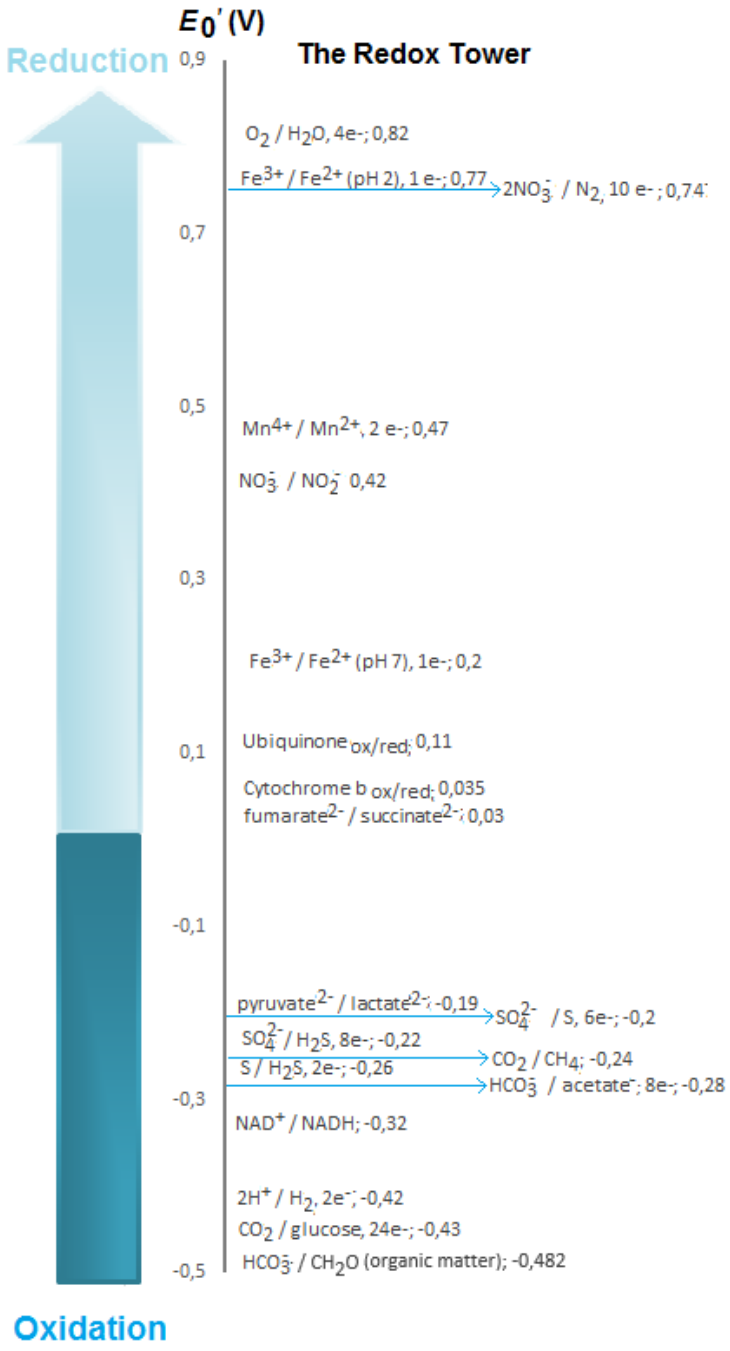

Figure 0.2: The Redox Tower. Redox couples with their corresponding reduction potential at standard conditions (E_0') are listed in descending order, at pH 7 unless otherwise stated. The direction of the electron flow is visualized by the arrow on the left. In theory, any reaction at the bottom of the redox tower can be coupled to the reactions listed on the top of the redox tower, with the amount of energy available from the full reaction (ΔG', proportional to ΔE_0') given as the difference between the two reactions. Modified from Madigan *et al.* (2014), Hinks *et al.* (2017) and Weber *et al.* (2006).

For the Mn(IV)/Mn(II) couple, the E_0' potential is 0.47V, which is larger than that of nitrate reduction to nitrite. However, the E_0' assumes Mn(IV) is readily available in solution, which is not often the case, as Mn(IV) is primarily present as oxides, such as MnO_2, which has a low solubility. The same is the case for the reduction of ferric iron (Fe(III)) to ferrous iron (Fe(II)). Even though the Fe(III)/Fe(II) couple at pH 2 has an E_0 value close to the value of the O_2/H_2O couple (0.77 and 0.81, respectively), Fe(III) exists typically as polymorphic oxide or hydroxide, such as akageneite or magnetite (Hinks *et al*. 2017). Thus, low solubility limits the availability of metal oxides as electron acceptors, as compared with O_2 or NO_3^-, which are readily soluble and can diffuse through soil and into cells. The solid character of Mn(IV) and Fe(III) is likely the reason why the ability for dissimilatory (energy-yielding) iron and manganese reduction is less ubiquitous than nitrate reduction.

Dissimilatory iron and manganese reduction by cultured organisms was first reported in 1988 for an isolate of *Alteromonas putrefaciens* (now named *Shewanella putrefaciens*, Myers & Nealson (1988a) and *Geobacter metallireducens* (first isolated strain named GS-15 by Lovley & Phillips (1988b). To facilitate electron transfer between microorganisms and solid Fe(III) oxide surfaces, three mechanisms have been proposed (Weber *et al.* 2006): i) direct contact between the organism and the oxide surface through conductive extracellular appendages, called 'nanowires' as demonstrated for *Geobacter sp.* (Reguera *et al.* 2005), ii) molecules that serve as electron shuttles produced either endogenously or exogenously (Lovley *et al.* 1996; Newman & Kolter 2000; Turick *et al.* 2002; Hernandez *et al.* 2004) and ii) excretion of complexing ligands that make Fe(III) more soluble, hence more easily available for the microorganism, as demonstrated for *Geothrix sp.* (Nevin & Lovley 2002).

As many bacteria, both anaerobes and facultative aerobes, are able to utilize a range of electron acceptors, the electron acceptor with the highest reduction potential is believed to inhibit the use of electron acceptors with lower reduction potentials (Madigan *et al.* 2014). Consequently, soils may quickly turn anoxic when abundant electron donors with a low reduction potential (high oxidation potential) are added, such as in fresh organic matter (simplified as CH_2O in Figure 0.2) or de-icing fluids. Saturated conditions, such as in unconfined groundwater, with large inputs of dissolved organic carbon , are particularly susceptible to anoxia as the oxygen may be respired before it diffuses from the surface into deeper soil layers. If other electron acceptors are present,

anaerobic respiration will occur, first depleting nitrate, potentially releasing gaseous denitrification products, before reducing available Mn(IV)/Fe(III) to water soluble Mn(II) and Fe(II), and eventually sulphate and CO_2, to H_2S and CH_4, respectively (Madigan *et al.* 2014).

Apart from using substrates for growth, microorganisms need certain elements for growth, especially nitrogen and phosphorous. Nitrate may be assimilated as a source of nitrogen instead of being used as an electron acceptor, however ammonium or urea are usually preferred and inhibit assimilatory nitrate reduction (Jansson *et al.* 1955; Recous *et al*. 1990; Recous *et al*. 1992), even at low concentrations (Rice & Tiedje 1989).

1.3 Degradation of propylene glycol

Propylene glycol (PG), also called propane-1,2-diol (Figure 0.3), is a water-miscible 3-carbon compound ($C_3H_8O_2$) with a molar mass of 76.10 g mol^{-1}. The melting point of pure PG is -60 ºC (Lide 2008), and it can lower the freezing point of water down to -60 ºC in a 60:40 PG:water mixture (DOW 2008). In addition to the use as a de-icing fluid, PG is used for the chemical production of polyester resins (Parker & Moffett 1954), as an additive to food and a solvent for pharmaceuticals, due to its relatively low toxicity (Zar *et al.* 2007).

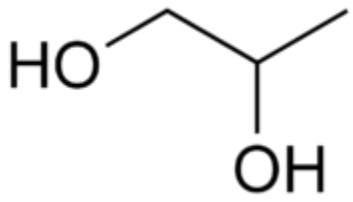

Figure 0.3: Structural formula of propane-1,2-diol, $C_3H_8O_2$.

The compound is generally considered to be easily degradable by microorganisms in both water and soil. Assuming first order kinetics, the Agency for Toxic Substances and Disease Registry in Canada estimated the half-life of propylene glycol in water to be l to 4 days under aerobic and 3 to

5 days under anaerobic conditions, and in soil equal to or shorter than this (Murray & George 1997).

In a microcosm study conducted on a sandy loam sampled close to an airport runway in Michigan, USA, an initial concentration of 400 ppm PG was not measureable after 8 days incubation at 25 ºC or after 12 days incubation at 8 ºC (Klecka *et al.* 1993). Measured CO_2 evolution throughout 34 days at 8 ºC corresponded to 57% of the theoretical CO_2 production assuming complete oxidation of the added PG, demonstrating that mineralization occurred. However, a ten-fold higher initial PG concentration slowed down the degradation rate from 41 to 20 mg PG kg soil^{-1} day^{-1} with 23% of the initial PG concentration remaining after 111 days. Degradation of PG at high load was demonstrated in the same soil at a temperature as low as -2 ºC, however at a much smaller rate of 3.5 mg PG kg soil^{-1} day^{-1} with 86% remaining after 111 days.

The main concern associated with propylene glycol release to the environment is its high chemical oxygen demand (COD). According to the stoichiometry for the complete oxidation of propylene glycol to CO_2 by O_2 (Table 0.1), 4 mol oxygen are consumed per mol of propylene glycol oxidized, corresponding to 1.68 g of O_2 per g of PG. Accordingly, Klecka *et al.* (1993) constantly purged their incubation batches with air to keep O_2 in excess relative to PG. However, O_2 is hardly ever available in excess in soils.

Table 0.1: A selection of catabolic reactions involved in the oxidation or fermentation of propylene glycol ($C_3H_8O_2$).

Aerobic degradation
$C_3H_8O_2 + 4O_2 \rightarrow 3CO_2 + 4H_2O$
Anaerobic, nitrate reduction to N_2
$C_3H_8O_2 + 3.2NO_3^- + 3.2H^+ \rightarrow 3CO_2 + 5.6H_2O + 1.6N_2$
Anaerobic, Mn(IV) reducing bacteria
$C_3H_8O_2 + 8MnO_2 + 16H^+ \rightarrow 3CO_2 + 12H_2O + 8Mn^{2+}$
Anaerobic, Fe(III) reducing bacteria
$C_3H_8O_2 + 8Fe_2O_3 + 32H^+ \rightarrow 3CO_2 + 20H_2O + 16Fe^{2+}$
Anaerobic, fermentative consortia
$C_3H_8O_2 \rightarrow C_3H_6O_2$ (propionic acid) + H_2
$C_3H_8O_2 \rightarrow 0.5C_3H_6O_2$ (propionic acid) + $0.5C_3H_8O$ (n-propanol)
Propionic acid and propanol can be degraded further to acetate, hydrogen and carbon dioxide
Anaerobic, sulphate reducing bacteria
$C_3H_8O_2 + 2SO_4^{2-} + 4H^+ \rightarrow 3CO_2 + 4H_2O + 2H_2S$

Methanogenesis (overall stoichiometry)

$C_3H_8O_2 \rightarrow CO_2 + 2CH_4$

Both aerobic and anaerobic degradation of propylene glycol have been reported in the literature. Willetts (1979) proposed pathways for aerobic and microaerophilic biodegradation of PG by *Xanthobacter autotrophicus* (previously *Flavobacterium* sp.) by an inducible diol-oxidase, which oxidizes PG to lactaldehyde which is subsequently metabolised to pyruvate that enters the tricarboxylic acid cycle (Willetts 1979; Willetts 1983). Under micro-aerophilic conditions, most of the PG is metabolized to propionaldehyde by a diol-dehydratase and subsequently reduced to the endproduct n-propanol (Willetts 1979)(Figure 0.4).

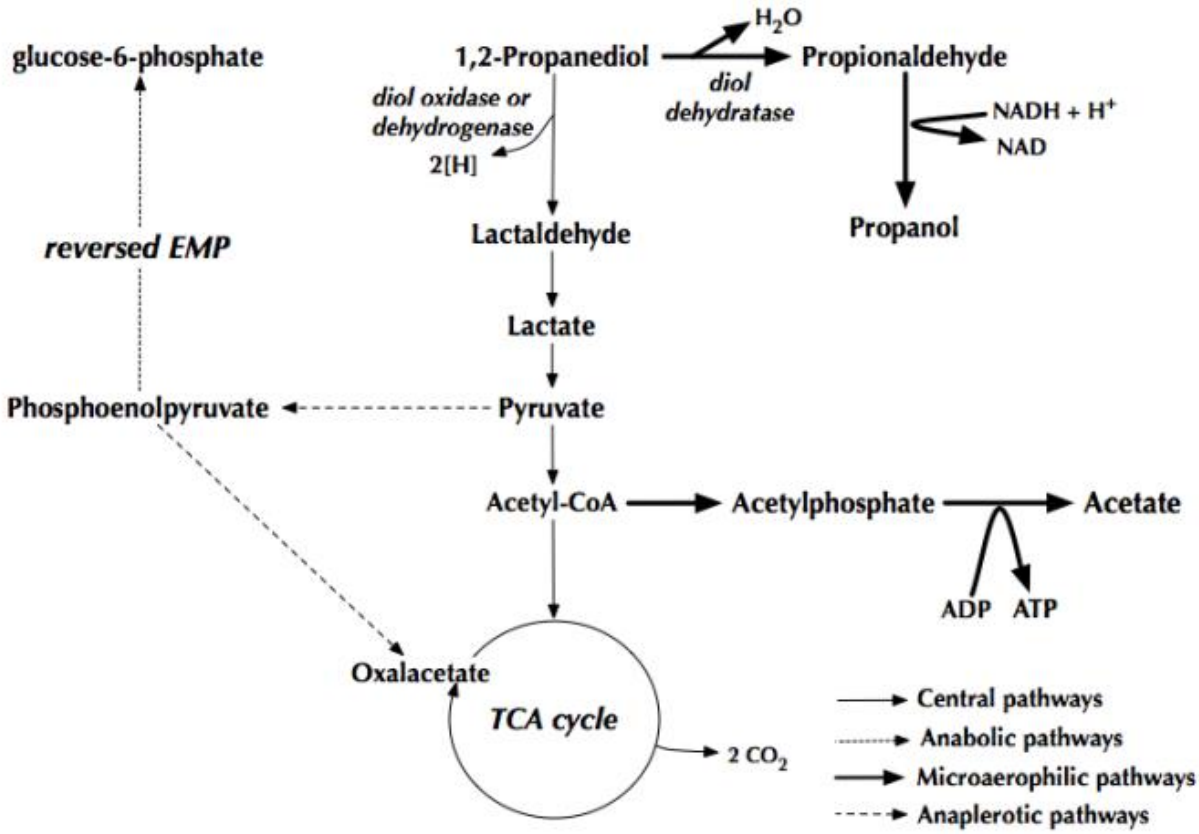

Figure 0.4: Proposed pathways of aerobic and microaerophilic degradation of propylene glycol (1,2-Propanediol) by (Willetts 1979).

In a previous study on aerobic degradation of PG in soil samples from Oslo airport, 19 different strains of *Pseudomonas sp*. were isolated that could grow on PG as a sole carbon source (Toscano et al. 2013).

PG has also been reported to be degraded anaerobically. Under methanogenic conditions (i.e. in the absence of electron acceptors other than CO_2), Veltman *et al.* (1998) proposed that the pathway for PG degradation starts with fermentation via propionaldehyde to equimolar amounts of propionate and 1-propanol, with 1-propanol being converted to propionate. Propionate is then degraded further to acetate, methane and CO_2. A fermentative pathway has also been proposed for the strain *Clostridium glycolicum*, in which the initial step to priopionaldehyde is catalysed by a membrane bound diol-dehydratase, which is then reduced to n-propanol or further oxidised to priopionic acid (Hartmanis & Stadtman 1986). Anaerobic degradation of PG was also studied in column experiments with a gravel-rich Bavarian soil (Jaesche *et al*. 2006), comparing top soil, subsoil and the saturated zone (aquifer). The authors observed an accumulation of propionate and propanol and the formation of iron(II) and manganese(II) in the soil water. Elevated Mn(II) in soil water has also been interpreted as an indirect indicators for PG degradation under field conditions at the Moreppen research station (French *et al.* 2001).

1.4 Analyses of soil microbial communities

Soil represents a highly complex environment due to its heterogeneity in texture. Nevertheless, the soil environment supports a much higher diversity than what can be found in e.g. aquatic or marine environments. In a typical soil sample, the number of prokaryotic cells varies between 10^8 and 10^{10} cells g^{-1} dry weight soil. Soil is also reported to sustain an immense diversity of microbes, much of which still remains unexplored (Torsvik *et al.* 1990; Torsvik & Øvreås 2002). When cultured, microbial organisms can be studied and described in detail, however the minority of environmental bacteria are readily cultured.

By introducing molecular methods in microbial ecology studies it was reported that less than 0.1% of the microorganisms from most environments could be cultivated in the laboratory. Therefore, cultivation based approaches give an unrepresentative view of microbial communities. This was referred to as the "Great Plate Count Anomaly" (Staley & Konopka 1985).

A new era in microbial ecology studies was established by introduction of molecular methods, and the use of the small subunit (16S) ribosomal RNA as a phylogenetic marker gene (Schaup *et al.* 1972; Woese *et al.* 1976). By applying a holistic approach, extracting the DNA from the entire soil microbial community, downstream DNA analyses can provide a snapshot of the diversity of organisms present in the soil microbial community ecosystem at the sampling time.

During the last 30 – 40 years, several methods for microbial community profiling involving the analysis of the 16S rRNA gene have been developed. Initially, fingerprinting methods such as Denaturing Gradient Gel Electrophoresis (DGGE, Muyzer *et al*. 1993; Øvreås *et al*. 1997), gained large interest as a rapid comparison of microbial communities. The advantage of these methods was the possibility for simultaneous analyses of multiple samples for comparison purposes and monitoring. After the introduction of "high throughput sequencing" approaches such as pyrosequencing (454) and Illumina (previously "Solexa"), much larger sequencing depths were possible, and a better cover of the diversity present in various environments could be obtained (Sogin *et al.* 2006; Roesch *et al.* 2007; Caporaso *et al.* 2011).

Both these methods require thousands of copies of each DNA molecule to be sequenced, and therefore require a polymerase chain reaction (PCR) amplification step as part of the sequencing protocol. The PCR method is a very powerful method enabling to multiply the numbers of template sequences exponentially, however errors might be introduced in the first rounds of amplification and therefore are an important pitfall of the PCR reaction and contributes to lower sequencing accuracy (Wintzingerode *et al.* 1997).

The last decade's progress in molecular microbial ecology been enormous, enabling better insight into microbial communities in the environment. Such analyses provides information about community composition and diversity, but only hints to what processes these organisms are doing within the environment. In order to get information about the processes such a snapshot of the microbial environment are involved with, a combined approach is necessary. The use of cultivation and/or incubation experiments, where different chemical or biological measurement are combined, provides a strong basis for the understanding of a microbial community and its role and responses in an environment.

1.5 Project objective and approach

The objective of this study was to investigate the effects of propylene glycol (PG), the dominant component in de-icing fluids, on the kinetics of Mn^{2+} and Fe^{2+} release in soils collected in vicinity of Oslo airport, Gardermoen. In order to obtain information regarding this, 4 specific research questions were addressed:

1. Does propylene glycol increase the amount of Mn^{2+}/Fe^{2+} released to the soil water under anaerobic conditions?
2. Does Mn^{2+}/Fe^{2+} release differ between top soil and deeper layers of the soil profile to which PG leaches?
3. Does the addition of a small amount of nitrate affect the release of Mn^{2+}/Fe^{2+}?
4. How does the microbial community structure in top- and subsoil respond to the addition of PG and/or nitrate, and is the observed release of Mn^{2+}/Fe^{2+} linked to growth of known Mn and Fe reducers?

To address these questions, laboratory experiments were set up in which previously unexposed top- and subsoil was amended with PG and/or nitrate and incubated over 26 days. PG was provided in concentrations relevant to the lower range of measured field conditions (1.3 - 85 mM in snowmelt water, Øvstedal & Wejden 2007; Greco et al. 2012). Nitrate was provided in small concentrations, since the primary goal was not to stimulate PG degradation, but to see how nitrogen affects the metabolic activity of the involved microorganisms, including Mn and Fe reducers. Based on the stoichiometry for denitrification, 3.2 times the amount of nitrate must be added per mol of PG for complete anoxic mineralization (Table 0.1). Mn^{2+} release was in Gardermoen soil was successfully inhibited by this amount of nitrate (Toscano *et al.* 2014; Greco *et al.* 2012). In a field study, nitrate was added in a lower amount (0.26:1 nitrate:PG) and release of Mn^{2+}/Fe^{2+} seemed to increase (Lissner *et al.* 2014).

The soils were incubated in closed, septum-sealed glass bottles and respiration activity was measured by monitoring gas exchange semi-continuously (every 5 hours) in an automated, temperature controlled incubation system. Soil water Fe^{2+}/Mn^{2+} concentrations were monitored less frequently by sampling soil water through microrhizons which were fitted through the septa of

the bottles. At the end of the incubation experiment, each bottle was opened under sterile conditions and soil was sampled for sequencing of 16S rRNA genes from extracted DNA.

The incubations were carried out at 15 ºC and correspond therefore to summer rather than winter or snowmelt conditions. Temperatures in 0.4 – 2.4 m depth reported for Oslo airport soils are in the range of 10 to 17ºC (French *et al.* 2001). The soils used in the experiments were sampled from a trench, which had never been exposed to de-icing chemicals. In this way, short-term effects of PG and/or NO_3^- contamination, rather than chronic exposure, could be targeted, which opens for exploring direct links between relative taxonomic abundances and microbially driven MnO_x/FeO_x reduction. By contrast, microbial responses to the additions would likely be small in long-term exposed soil, as microbial communities might already be adapted to PG as the prevailing carbon substrate.

The study is structured in three parts (Table 0.2); two pilot experiments and one main experiment. The first pilot experiment was designed to assess the aerobic and anaerobic metabolic activity of the soils through gas sampling and another testing the water sampling set-up, prior to the main experiment that combined both sampling approaches and also included molecular microbial community analysis. Subsamples for molecular analyses were taken from the original soil and from all treatments at the end of the main incubation experiment. The experiments are summarized in Table 1.2:

Table 0.2: Overview of experiments performed with soil from the Moreppen research station.

Section	Objectives
Pilot 1, section 2.88	To assess the metabolic activities of top- and subsoil and to test the effect of propylene glycol and nitrate on aerobic and anaerobic respiration by gas kinetics (O_2, CO_2, NO, N_2O, N_2) in batch incubations
Pilot 2, section 2.99	To test repeated soil water sampling during batch incubation by means of microrhizones inserted into the packed soil and to determine the blank and sensitivity for determining Fe^{2+} and Mn^{2+} release
Main experiment, section 2.1010	To study Fe/Mn kinetics together with metabolic activity under the impact of added NH_4^+, PG and PG + NH_4NO_3 and to assess how incubation conditions and amendments affect prokaryotic community structure

2. MATERIALS AND METHODS

2.1 Research site

This research was carried out with soils from the Moreppen research site which is located in close vicinity to the Oslo Airport Gardermoen at 60°13'06.60"N, 011°05'16.08"E. The location was chosen because of its proximity to the airport and a geology that is comparable to that inside the operational area of the airport.

The research site is situated within a low-productive spruce forest with open patches of grass, young birches and small bushes like lingonberry and blueberry in the understory. The mean groundwater level is about 4 meter below the surface (French 1999). The soil profile has previously been characterized for horizon depth, heterogeneity and soil texture. The subsoil is a medium to coarse sand with some gravel and stones, while the top soil is a mixture of root zone soil and coarse soil with gravel (French *et al.* 1994). Chemical properties of the soil have previously been characterized at this location. According to Søvik & Aagaard (2003), total organic carbon (TOC) in the organic horizon comprises 2.5% of the soil, decreasing to 0.5% at 0.5 m below surface and 0.2% with increasing depth. At 1.5 m depth, the total organic carbon has previously been analysed to 0.2-0.4%. The total P was similar in both soil types at ~450 mg kg^{-1} soil. Iron oxides were more abundant in the top layer, ranging from 0.2-0.7%. At 1.5 m depth, the relative concentration of iron oxides was about 0.2%.

The soil was sampled at two locations, one representing "subsoil" (SS), which was sampled in the lysimeter trench (Figure 2.1B) and the other representing the "topsoil" (TS), which was sampled from a mixture of topsoil lying next to the research trench. This mixture had been excavated in 2009 (Lißner *et al.* 2012, Figure 2.2). The topsoil has been previously used for geophysical experiments studying transport and degradation of propylene glycol by PhD student Perrine Fernandez (Revil *et al.* 2015). None of the sites had been subjected to de-icing chemicals previously.

Figure 2.1: A: The prebuilt research trench at Moreppen research station, located at 60°13'06.5208"N, 11°05'15.2268"E, photo G. Flatabø September 14th 2016. The door is normally closed to prevent precipitation and animals from entering the trench. **B**: A hole made in the east wall of the trench. The cover had fallen off, so some soil had collapsed into the trench. The exposed soil was removed prior to sampling. The drawings on the right hand side depicts the geology of the soil profile behind the wall.

Figure 2.2: Sample site for sampling top soil (TS) on September 14th 2016, located at Moreppen, Gardermoen, 60°13'05.8188"N, 11°05'16.1160"E. The soil is a mixture of the first one meter of the top soil, excavated to add a lysimeter for trials in 2009 (Lißner *et al.* 2012).

2.2 Sampling of soil

The soils were sampled on September 14, 2016 together with PhD student Perrine Fernandez. Subsoil was taken using a clean spade from 1.5 m depth from the east wall of the research trench (Figure 2.1) and topsoil from the pile of excavated soil right next to the trench, representing a mixture of soil from 0 - 1 m depth (Figure 2.2). The soils were sampled into clean plastic buckets, each covered by a clean, transparent, plastic sheet to prevent evaporation during transport and storage at NMBU. Extra samples were taken and transferred to a sterile plastic container for

microbial community analyses ("SSfield" and "TSfield"). The buckets were stored at 5ºC in a cooling room, whereas the sterile plastic containers were frozen to -18°C on the day of sampling.

2.3 Pre-treatment of soil

Before experimentation, the soils were sieved through a 3.55 mm mesh-size sieve (Retsch), removing stones and particles. Soil moisture (M_s) of the sieved soil was determined gravimetrically. Maximum water holding capacity (WHC_{max}) was estimated by saturating known volumes of sieved soil in Büchner funnels.

2.4 pH measurements

Three subsamples of sieved and air dried soil (10 mL) were suspended in 25 mL of a 10 mM $CaCl_2$ solution, shaken by hand for about 30 seconds and left standing overnight. In the morning, the vials were briefly shaken again and left standing to settle for 10 minutes before they were measured by a pH-meter (Hach H170).

2.5 Gas measurements

Metabolic activity was measured as O_2 consumption and CO_2, N_2O and NO production in batch incubations using an incubation robot with automatic headspace analysis similar to that described by Molstad *et al.* (2007). The incubations were carried out at the soil biology laboratory of the Faculty for Environmental Science and Natural Resource Management of the Norwegian University of Life Sciences in Ås, Norway (Fig. 2.4). The setup consists of a temperature controlled water bath holding up to 44 serum bottles (120 ml) capped with Butyl septa, which is placed under the robotic arm of an autosampler (GC-Pal, CTC). The autosampler periodically pierces the bottles with a hypodermic needle connected to a peristaltic pump (Gilson 222 XL) and removes ~2 ml which are pumped through dedicated sampling loops of a multi-column GC (Agilent 7890A) and a chemoluminescence NO analyser (Teledyne 200). After each measurement, an equivalent amount of He 6.0 is pumped back to the bottles by reversing the pump to maintain bottle pressure at ~1 atm. The GC is equipped with a poraplot Q column to separate CH_4, CO_2 and N_2O from bulk air and a molesieve column to separate O_2/Ar from N_2. CO_2, O_2/Ar and N_2 were measured by a thermal conductivity detector (TCD), CH_4 by a flame ionization detector (FID) and N_2O by an electron

capture (ECD). A technical description of the set up and of the chromatographic conditions can be found in Molstad *et al.* (2016). Production and consumption rates of gasses were calculated according to Molstad *et al.* (2007), taking account for dilution by He and dissolution in soil water.

2.6 Nitrate measurements

Nitrate (NO_3^-) was measured photospectrometrically at 540 nm in a microplate reader (Tekan Inf F50, Männedorf, Switzerland) by Griess reaction (Keeney & Nelson 1982) after reduction of NO_3^- to NO_2^- by $VaCl_3$ (Doane & Horwáth 2003). Soil pore water samples were amended with Griess reagents (sulfanilamide and N-1-napthylethylenediamine dihydrochloride) in a 1:1:5-ratio and measured at 540 nm to determine NO_2^- concentrations. Thereafter one part of an acid $VaCl_3$ solution was added and the samples were incubated for 90 minutes at room temperature before measuring the $NO_2^- + NO_3^-$ concentration by absorption at 540 nm. The NO_3^- content was calculated by subtracting the NO_2^- from $NO_2^- + NO_3^-$ concentration.

2.7 Iron and manganese quantification

Concentrations of dissolved iron (Fe^{2+}) and manganese (Mn^{2+}) were quantified in water samples. Soil water was sampled by applying underpressure to microrhizones (Rhizosphere Research Products, Wageningen, NL) inserted into the packed soil (see Ch. 2.9), assuming that only reduced species would be in solution. Immediately before analysis, samples were diluted 1:10 with de-ionized water acidified with 10% HNO_3, to dissolve Fe and Mn species that had oxidized during sampling or storage. Concentrations were then analysed by inductively coupled plasma mass spectrometry (8800 ICP-MS Triple Quad, Agilent Technologies) using Germanium as internal standard. All internal solutions like standards and washing liquid were prepared in the same matrix of 10% HNO_3 in de-ionized water. Measured values were corrected for blanks and dilution caused by reinjection of DI water.

2.8 First pilot experiment

To test the metabolic activity of top and subsoil under oxic and anoxic conditions, with and without PG and NO_3^- addition, a first pilot experiment with batch incubations of top (TS)- and subsoil (SS) was undertaken in six different treatments (Table 2.1). No Fe or Mn analyses were performed. Fresh soil corresponding to approximately 60 g dry weight (SS: 60 ± 0.11 g, TS: 59 ± 0.25 g) was added to 120 mL serum bottles. Amendments were scaled to adjust soil moisture to ~60% of WHC_{max} (see section 2.3). PG and KNO_3 was added to final concentrations of 10 and 2 mM in soil moisture, respectively. Due to imprecision of the soil moisture estimates, which could not be determined before the end of the experiment, some variability in initial PG and KNO_3 concentrations occurred. Table 2.1 gives an overview of the treatments and added concentrations. Concentrations are converted to µmol g dryweigh $soil^{-1}$ for the sake of future comparisons.

Table 2.1: Experimental design of the first pilot experiment. PG = propylene glycol. Top- and subsoil were sampled from 0-1 and 1.5 m depth, respectively, at the Moreppen research station (Figure 2.1 and 2.2). Aerobic bottles were incubated in a He/O_2 (80/20) and the anaerobic bottles in a 100% He atmosphere. Each batch consisted of approximately 60 g dry weight soil, adjusted to ~60% water holding capacity (~10 mL). The nominal PG and KNO_3 concentrations and their calculated variability (SD) are given in brackets.

Subsoil aerobic treatment	**Bottle #**	**Top soil aerobic treatment**	**Bottle #**
Control (DI water)	1-3	Control (DI water)	19-21
PG (1.2 ± 0.15 µmol g^{-1})	4-6	PG (1.7 ± 0.01 µmol g^{-1})	22-24
PG (1.5 ± 0.008 µmol g^{-1}) + KNO_3		PG (1.7 ± 0.10 µmol g^{-1}) + KNO_3	
(0.24 ± 0.029 µmol g^{-1})	7-9	(0.33 ± 0.0012 µmol g^{-1})	25-27
Subsoil anaerobic treatment		**Top soil anaerobic treatment**	
Control (DI water)	10-12	Control (DI water)	28-30
PG (1.6 ± 0.41 µmol g^{-1})	13-15	PG (1.6 ± 0.03 µmol g^{-1})	31-33
PG (1.5 ± 0.002 µmol g^{-1}) + KNO_3		PG (1.7 ± 0.06 µmol g^{-1}) + KNO_3	
(0.37 ± 0.083 µmol g^{-1})	16-18	(0.32 ± 0.006 µmol g^{-1})	34-36

All bottles were incubated at 15°C for two weeks, while monitoring headspace concentrations of O_2, N_2, CO_2, N_2O and NO four times per day as described in Ch. 2.5. Figure 2.3 gives an overview over sample processing in the 1st pilot experiment.

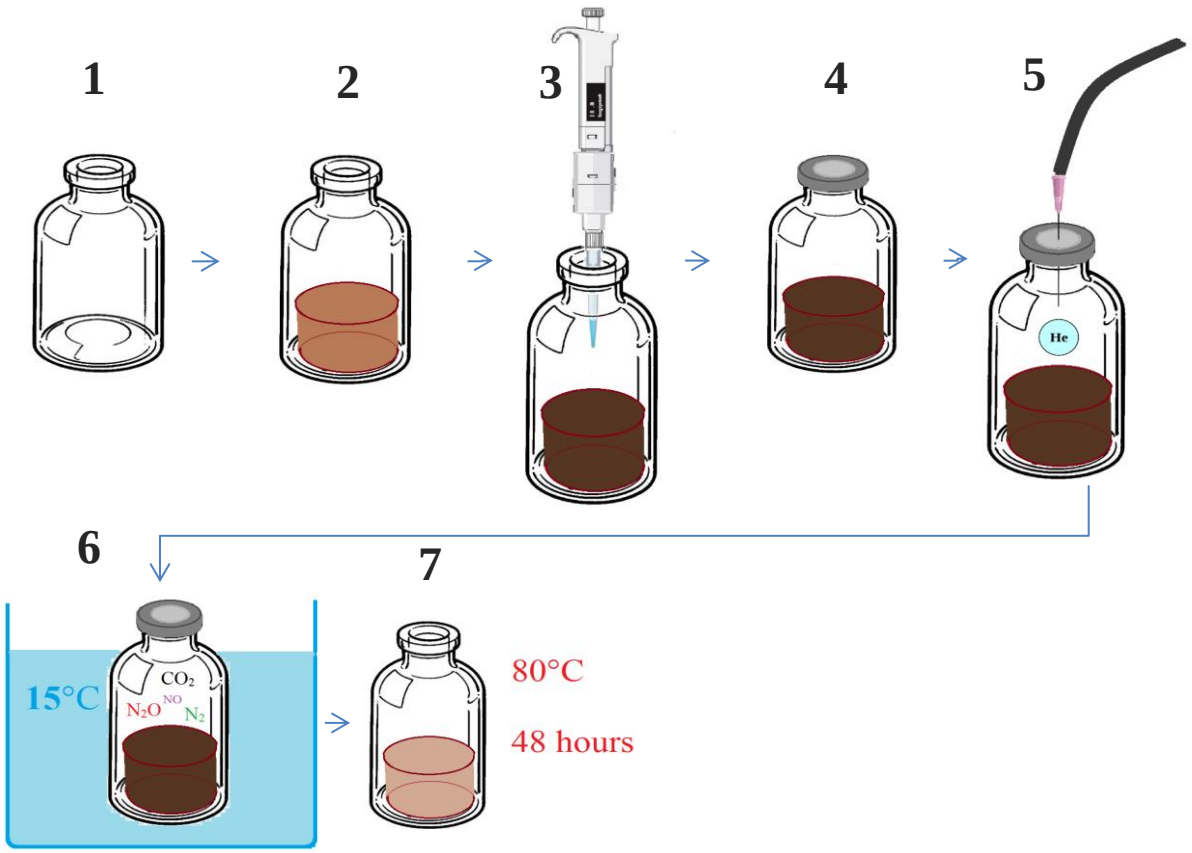

Figure 2.3: Scheme of sample processing in the first pilot experiment. **(1)** A clean glass serum bottle of 120 mL is pre-weighed and **(2)** fresh soil equivalent approximately 60 g dry weight is added, with the exact weight noted. **(3)** DI water, propylene glycol or propylene glycol and KNO_3 are added and the total weight is noted. **(4)** The bottle is crimp sealed and **(5)** He-washed (anaerobic treatment) or washed with a 80/20 He/O_2 mixture (aerobic treatment), using six cycles of three minutes vacuum and 20 seconds of He-filling. **(6)** After releasing the overpressure (resulting from He-washing), the bottles are placed in a water bath at 15℃ (up to 40 bottles at once) and the headspace is sampled for gases four times every day throughout two weeks. **(7)** After terminating the incubation experiment, the bottles is opened and dried at 80℃ for at least 48 hours to determine the actual amount of dry weight soil in each bottle.

2.9 Second pilot experiment

A second pilot experiment was set up to test the feasibility of analysing Fe^{2+} and Mn^{2+} release in batch incubations. No gas measurements were performed. Serum bottles were filled with subsoil, adjusted to 80% WHC_{max} and equipped with polymeric microrhizones (Rhizosphere Research Products, Wageningen, NL). The increase of water from 60% WHC_{max} in the first pilot experiment, to 80% WHC_{max} was chosen to reduce water sampling time. The microfiltration membrane has a nominal pore size of 0.12 - 0.18 µm and a length of 40 mm with 2.5 mm OD and 1.5-1.6 mm ID. The membrane was connected to a 800 mm long PEEK tube (1.6 mm OD, 0.75 mm ID) without any metal enforcement, making them well suited for metal research.

Figure 2.4: A microrhizon (Rhizosphere Research Products, Wageningen, NL) used for taking water samples directly from the soil. The membrane provides filtration so that water samples can be analysed directly on instruments such as ICP-MS (section 2.7).

After inserting the membrane vertically into the loosely packed soil, the PEEK tubing was protruded through the fringe of the septum (Figure 2.5). The bottles were crimp sealed and incubated aerobically and anaerobically for 10 days at room temperature, during which soil water was sampled periodically from the microrhizones by applying under-pressure with a disposable syringe and a blocked plunger. After retrieving 0.8 to 2 mL soil solution, the syringe was detached, the amount of sampled water determined by weighing and an equivalent amount of de-ionized water reinjected to maintain the water balance throughout the experiment (Figure 2.6). Care was taken to avoid intrusion of air into the microrhizones by using two-way stopcocks or tube clamps. The sampled water was frozen immediately prior to analysis of NO_3^-, Fe^{2+} and Mn^{2+} as described in Ch. 2.66 and 2.77.

The subsoil was amended with 100 µL PG or DI water only, in anaerobic or aerobic atmosphere. Controls without soil, containing a similar volume of DI water was tested to evaluate input of ions from the used water and sampling procedure. The different treatments are outlined in Table 2.2.

Figure 2.5: A microrhizon protruded through the butyl rubber septum of the serum bottles, further attached to a viton tubing and a two-way stopcock.

Table 2.2: Experimental design of the 2nd pilot experiment. PG = propylene glycol. Top- and subsoil were sampled from 0 - 1 and 1.5 m depth, respectively at the Moreppen research station (Figure 2.1 and 2.2). The aerobic treatment was in laboratory air, the anaerobic treatment in He. Each batch consisted of approximately 60 g dry weight soil adjusted to ~80% of maximum water holding capacity. Given are the amount of PG added and its variation (SD) in brackets. Note that bottle 1-3 contained pure de-ionized water in an anaerobic atmosphere (analytical blanks).

Subsoil anaerobic	**Bottle #**
Blank: 50 mL de-ionized water (no soil)	1-3
Water to 80% WHC_{max} + PG (104 ± 1.37 µmol)	4-6
Subsoil aerobic	
Water to 80% WHC_{max}	7-9
Water to 80% WHC_{max} + PG (104 ± 2.24 µmol)	10-12

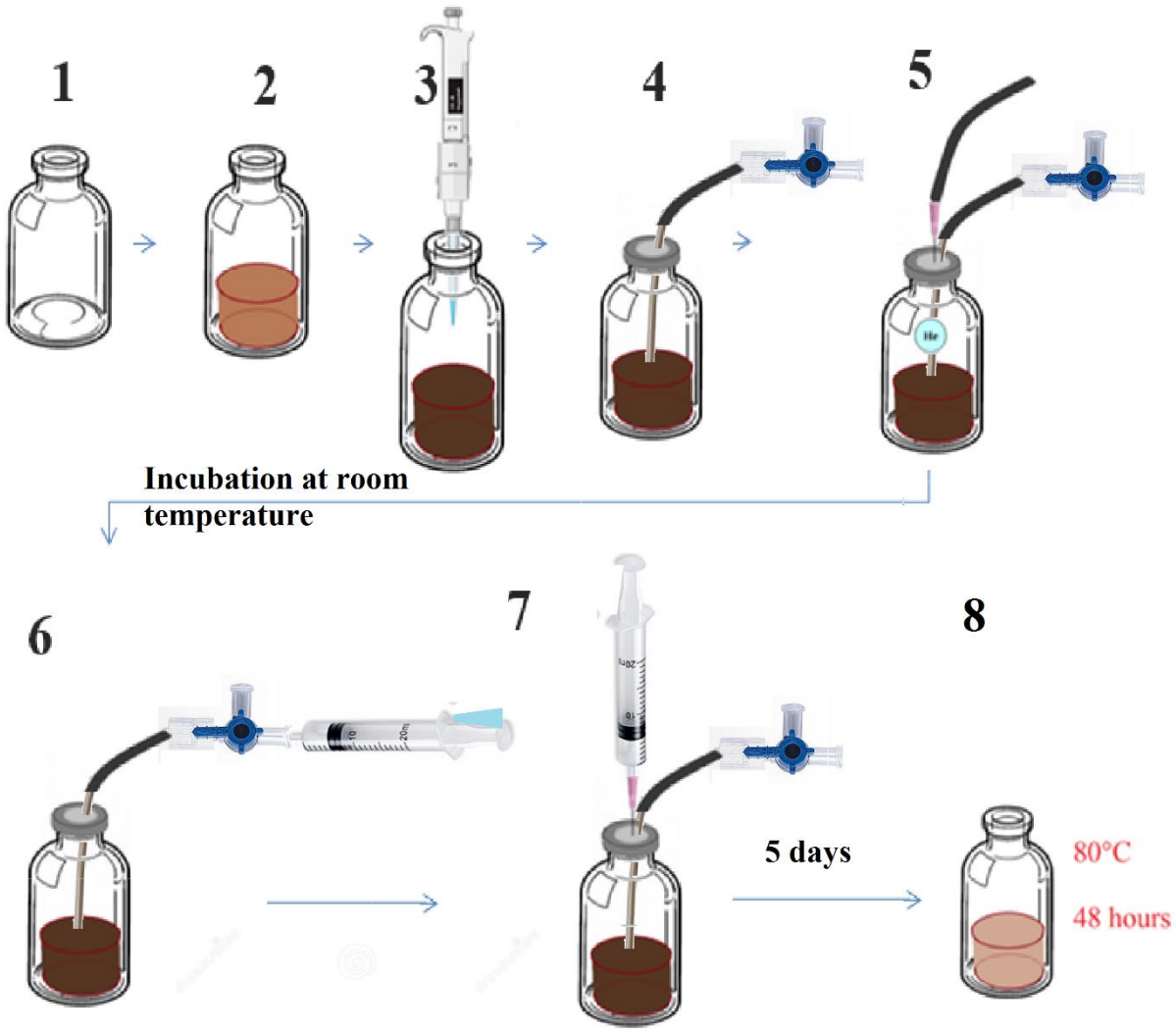

Figure 2.6: Scheme of sample processing in the second pilot experiment. **(1)** A clean glass serum bottle of 120 mL is pre-weighed and **(2)** fresh soil equivalent approximately 60 g dry weight, or DI water equivalent to 50 mL is added, with the exact weight noted. **(3)** DI water, or diluted propylene glycol are added and the total weight is noted. **(4)** The bottle is attached with a microrhizon protruded through the septum and a closed three-way stopcock, crimp sealed and some are **(5)** He-washed (anaerobic treatment), using six cycles of three minutes vacuum and 20 seconds of He-filling. **(6)** the overpressure is released (resulting from He-washing), and water samples are obtained through underpressure from a 5 mL syringe that fits the attached three-way stopcock. **(7)** The water sampled is replenished with DI water using a syringe. Note that the water used to replenish the samples was He-washed to avoid dissolved oxygen. The bottles are incubated at room temperature and sampled every day for five days. (**8)** After terminating the incubation experiment, the bottles is opened and dried at 80°*C* for at least 48 hours to determine the actual amount of dry weight soil in each bottle.

2.10 Main experiment

The goal of the main experiment was to measure metabolic activity by gas exchange while simultaneously probing the soil pore water for released Fe and Mn. For this, serum bottles were filled with soil, equipped with microrhizons as described in chapter 2.9, adjusted to 80% WHC_{max} and placed into the incubation robot (Figure 2.7) with the microrhizone tubings orientated into one direction to avoid collision with the autosampler needle. Since the three-way stopcocks were too large for the autosampler needle, these were replaced with tube clamps. The syringe was then attached directly into the viton tubing for water sampling, as seen in Figure 2.7. Care was taken to keep viton tube filled with water up to the clamp to minimize diffusion of air through the tubing.

Figure 2.7: Placement of incubation bottles equipped with microrhizones in the incubator during the main experiment. Some of the bottles are being sampled for soil water through attached syringes.

Amendments were water, NH_4Cl, PG or PG + NH_4NO_3. NH_4^+ was chosen, as results from the first pilot experiment revealed severe N limitation of subsoil metabolism, both oxic and anoxic. To further study this phenomenon, addition of a minor amount NH_4^+ (10 µmol $bottle^{-1}$) was included as a treatment of its own and in combination with PG + NO_3^-. In the latter treatment, NH_4^+ was added to avoid immobilization of NO_3^- during microbial growth, which would affect electron acceptor availability under anoxic conditions.

The sample set included controls without any treatment, where only DI water was added. No sterile controls were used in this sample set, to control for chemical release of gases or Mn^{2+} or Fe^{2+}. It is assumed that any chemical release would also occur in the control flask and can thus be corrected for. However, to account for metal contamination from sampling procedures and glass bottles, blanks where the soil was exchanged for DI water were used to evaluate contribution of Mn^{2+} and Fe^{2+} from the sampling procedures, which was subtracted from the results of Mn^{2+} and Fe^{2+} release. Details about the experimental setup are given in Table 2.3.

Table 2.3: Experimental design of main experiment. PG = propylene glycol. Top- and subsoil were sampled from 0 - 1 and 1.5 m depth, respectively at the Moreppen research station (Figure 2.1 and 2.2). Each batches consisted of approximately 60 g dry weight soil adjusted to ~80% WHC_{max}. All bottles were initially He-washed.

Treatments	**Symbol in figs.**	**Subsoil Bottle #**	**Top soil Bottle #**
Water (80% WHC_{max})	H2O	1-3	13-15
NH_4Cl (10 µmol)	NH4Cl	4-6	16-18
PG (100 µmol)	PG	7-9, 33	19-21
PG + NH_4NO_3 (100 µmol PG, 10 µmol NH_4NO_3)	$PGNO_3$	10-12	22-24
De-ionized water, 40 mL	Blank*		25-27

* Used for calculation purposes.

All bottles were made anaerobic by He washing. However, due to the microrhizone tubing being protruded through the septum, variable amounts of laboratory air leaked into the bottles, making the headspace less strictly anaerobic than in the first pilot experiment (Ch. 2.88). Since the measured oxygen only reflected the concentration in the headspace at any given point of time, the measured O_2/N_2 ratio was compared to the known atmospheric O_2/N_2 ratio to provide a better estimate of O_2 influx. The O_2 influx was then estimated by multiplying the measured concentration of N_2 with the known atmospheric O_2/N_2 ratio, equation 2.1:

$$[O_{2tot}] = \frac{[N_{2hs}] \times [O_{2air}]}{[N_{2air}]} \qquad (2.1)$$

where $[N_{2hs}]$ is the concentration of N_2 measured in the headspace, $[O_{2air}]$ and $[N_{2air}]$ are the concentrations of O_2 and N_2 in a standard bottle containing air, all in µmol $bottle^{-1}$.

To evaluate the influence of oxygen leakage on respiration activity, the concentration of oxygen respired by the soil [O_{2resp}] at any time point during the incubation was estimated as the difference between leaked and measured O2 based on the known atmospheric O2/N2 ratio, equation 2.2:

$$[O_{2resp}] = \frac{[N_{2hs}] \times [O_{2air}]}{[N_{2air}]} - [O_{2hs}] \qquad (2.2)$$

where [N_{2hs}] is the concentration of N_2 measured in the headspace, [O_{2air}] and [N_{2air}] are the concentrations of O_2 and N_2 in a standard bottle containing air and [O_{2hs}] is the concentration of O_2 measured in the headspace of each bottle, all in µmol bottle^{-1}.

.

2.11 Cell enumeration

Viable cells were enumerated in the original soils frozen on the day of sampling (Ch. 2.2) and after incubating the soils in the main experiment (Ch. 2.10). For this, subsamples of soil were retrieved from the incubation bottles, frozen at -20ºC and shipped to the Department of Biology, UiB. At UiB, the soil samples were stored at -80ºC. Cell enumeration followed the standard protocol of the UiB Marine Microbiology Group, consisting of diluting the soil in distilled and sterile filtered water (0.22 µm syringe filter, Whatman FP30) in a 1:10 weight:volume ratio, followed by fixation in a 25% glutaraldehyde solution, which was incubated for 30 minutes at 4°C. The suspension was vortexed, left to stand for a few seconds to sediment the largest particles, before siphoning off the supernatant. 10-fold dilutions was made using sterile distilled water and an aliquot of the 10^{-4} dilution was filtered through a black polycarbonate filter (0.22 µm, Osmonics Inc) and washed, following a standard protocol, in sterile buffered PBS.

The polycarbonate filters were placed backside down on a drop of SYBR Green dye (2.5 vol%) in a petri dish, and incubated at room temperature in the dark, allowing the dye to diffuse through the filter and to stain the cells. After one hour, the backside of the filter was washed in a drop of buffer, slightly air dried, counter stained with a drop of ethidium homodimer-1 (EthD-1, 0.58 vol%) and kept in the dark at room temperature for 30 minutes. The backside of the filter was then rinsed in

a drop of buffer, slightly air dried and mounted on a glass slide with a drop of anti-fade solution (1:1 glycerol:PBS with 10% p-phenylenediamine). Viable cells were counted using an epifluorescence microscope (Zeiss Axio Imager Z.1) with a blue excitation (AF488) filter, while dead cells were estimated through a green excitation (DsRed) filter. On each filter, 10 fields were counted and extrapolated by equation 2.4:

$$[Cells] = \frac{N \times \frac{A_{filter}}{A_{counted}} \times dil}{m_{soil}} \quad (2.3)$$

where [Cells] is the number of cells per g soil, N is the number of cells counted, A_{filter} is the total filter area, $A_{counted}$ is the total area counted in the microscope, dil is the dilution factor and m_{soil} is the dry mass of soil weighed out. The slides were analysed and enumerated within two days of preparation, and were otherwise stored in a dark box at 4°C.

2.12 DNA extraction

DNA was extracted using the PowerSoil DNA Isolation Kit (Mo Bio Laboratories, Inc.), following the manufacturers protocol. A subsample of 0.3 ± 0.07 g from each soil was weighed into provided PowerSoil® Bead Tubes using a pre-sterilized spatula. A list of extracted samples is provided in the appendix, Table A.1. The bead tubes were used to homogenize the samples on a flat-bed vortexer for further extraction of DNA in the supernatant. The DNA was purified by precipitation with a salt solution provided in the kit before loading the mixture on silica spin filters for centrifugation. The DNA attached to the silica filters was washed using an ethanol solution before elution from the silica filter into 100 µL of the provided elution buffer.

The extracted DNA was analysed on a 0.75% agarose gel and visualised using 0.01% GelRed. The DNA concentration of the extracts was quantified photospectrometrically using a Qubit™ Fluorometer (Invitrogen, USA) together with a high sensitivity dsDNA assay. Extracts were stored at 4 ºC before further analysis on the same or the following day, or at -20 ºC when analysed later.

2.13 PCR and Illumina sequencing

To target prokaryotes in the DNA extracts, 16S rRNA genes were amplified in two steps using polymerase chain reaction (PCR). To prepare for Illumina sequencing, the first amplification was performed using the HotStar PCR Master Mix Kit (Qiagen, Hilden, Germany). A prokaryotic primer-pair was included in the reaction, containing Illumina adapters: (FAdapter)-N5-519F/(RAdapter) 806RB, and targeting the 16S rRNA V4 region.

Table 2.4: Primer sequences for relevant primers used for PCR amplification of 16S rRNA genes.

Primer	Target	Sequence (5′ – 3′)	Annealing t° (°C)	Reference
519F	16S rRNA gene, V4 region	CAGCMGCCGCGGTAA	55	(Øvreås *et al.* 1997)
806RB	16S rRNA gene, V4 region	GGACTACNVGGGTWTCTAAT	55	April *et al.* (2015)

(M=A/C , N=G/A/T/C , V=A/C/G, W=A/T)

To minimise PCR drift, the first amplification was performed in triplicate. Each sample comprised in total 20 µL reaction mixture: 10 µL Qiagen HotStar master mix, 0.5 µL of each of the primers (10 µM), 0.5 µL BSA (100%) and 1 or 2 µL DNA, depending on the concentration of the extract, ranging from 1 - 10 ng DNA per PCR reaction. The triplicates were pooled and visualized on a 1.5% agarose gel containing 0.01% GelRed. Pooled triplicate PCR products were cleaned using Zymo DNA Clean & Concentrator (Zymo Research Corp, USA) and quantified using a Qubit™ Fluorometer prior to the second PCR.

The second amplification targeted the overhanging Illumina adaptors with barcode sequences. Each sample was amplified using a unique combination of forward and reverse-primers. For this sample set, four different forward primers and 12 different reverse primers were used providing 37 different combinations. The total reaction volume of 50 µL consisted of 25 µL Qiagen HotStar master mix, 1 µL of each of the two barcoded primers (10 µM) and 10 or 20 µL pooled and cleaned PCR product from the first PCR, providing 3-16 ng DNA per reaction.

The first PCR reaction was initiated by a denaturation step (95°C, 15 min), followed by 25 cycles of denaturation (95°C, 20 s), annealing (55°C, 30 s) and extension (72°C, 30 s), with a final extension of 7 min at 72°C. The second PCR had the same conditions, except for an annealing temperature of 62°C, and 15 cycles (17 of the samples were run using 13 cycles). PCR products were subsequently purified using AMPure XP magnetic bead PCR purification protocol (AMPureXP, Beckman Coulter), eluted in 25 µL of DNase-free water, before quantifying the amount of DNA. The purified samples were then mixed in equimolar amounts and the DNA concentration of the mixture was quantified using a Qubit™ Fluorometer, before sending the mixture for sequencing analyses by the Illumina 'MiSeq v2 sequencing system' (Illumina, USA) at the Norwegian High-Throughput Sequencing Centre in Oslo (Norway).

2.14 Statistical and bioinformatical methods

phiX internal control was removed using the BBDuk (Decontamination Using Kmers) version 37.02 tool from the BBTools package (Bushnell 2017). Paired-end reads were merged using the BBmerge tool from the same package. Linkers and primers were removed, and merged reads were quality trimmed from both the left and right to exclude base calls with PHRED scores below 27. Obtained 16S rDNA amplicons were categorized and assigned to operational taxonomic units (OTUs) using QIIME (Quantitative Insights into Microbial Ecology; Caporaso *et al.* 2010) version 1.9.1, with the *pick_de_novo_otus* script at 97% sequence identity. The script generated an OTU table BIOM file, which was converted to a tab separated text file including taxonomic information using the script *biom convert* with taxonomy classified using the GreenGenes database (DeSantis *et al.* 2006).

Statistical tests were performed using the statistical software environment R (R Core Team 2015). Samples of the communities were rarefied to the minimum number of reads obtained in the sample set. Rarefaction curves were plotted to evaluate if the number of reads used for rarefaction would give a representative subsample of the whole attainable community. To avoid bias from differing numbers of reads, the rarefied sample set was used to estimate Shannon diversity index (H) and Evar evenness index (Smith & Wilson 1996). To test for significant differences in the prokaryotic communities based on the various treatments, permutational multivariate analysis of variance

(PerMANOVA) using the function *adonis* with Bray-Curtis distance matrices and 999 permutations was performed on the rarefied sample set. Relationships at OTU level between different treatments and community structure from the main experiment was assessed by non-metric multidimensional scaling (NMDS; Kruskal 1964) using the *vegan* package (Oksanen *et al.* 2017) based on Bray-Curtis dissimilatory measure and 999 permutations to two dimensions.

Rates To compare for significant treatment effects on metal dissolution, the continuous rates were approximated and subjected to linear models using Tukey Contrasts Multiple Comparisons of Means from the *multcomp* package (Hothorn *et al.* 2008). To test for correlations between the average rates of gas, nitrate and water soluble metals a Pearson's product-moment correlation test was used.

3. RESULTS

3.1 Soil characteristics

Both soils sampled for this study were sandy, with only few stones, which were removed by sieving the soils through a 3.55 mm sieve. The sieving also removed most of the plant roots contained in the top soil. The WHC_{max} was estimated to be 29±3% and 35±2% for sub- and topsoil, respectively. Measured pH after sieving averaged 4.63 for subsoil and 4.40 for topsoil (n=3; Tab. 3.1). The pH was also measured in each sample bottle after the main experiment and showed a significant decrease all subsoil treatments except PGNO3 ($p<0.02$) and an insignificant increase in pH for top soil.

Table 3.1: Measured pH values from soil suspended in a $CaCl_2$ solution.

pH values	Subsoil	Topsoil
Before main experiment	4.63 ± 0.061	4.40 ± 0.021
After main experiment		
H2O1	4.55	4.46
H2O2	4.17	4.49
H2O3	4.17	4.45
NH4Cl1	4.25	4.41
NH4Cl2	4.24	4.46
NH4Cl3	4.27	4.44
PG1	4.34	4.43
PG2	4.38	4.47
PG3	4.43	4.49
PG4	4.46	-
PGNO31	4.51	4.5
PGNO32	4.55	4.49
PGNO33	4.63	4.53

3.2 Pilot 1: Oxic and anoxic metabolism of Moreppen soils

To explore the indigenous and substrate-induced oxic and anoxic metabolic potentials of Moreppen top and subsoil, a batch incubation experiment was carried out (Pilot 1, Ch.2.8). Oxic respiration

was quantified as the rate of CO_2 accumulation in a He/O_2 atmosphere and corrected for pH-dependent bicarbonate dissolution (Molstad et al. 2007). Figure 3.1 shows the maximum inducible oxic respiration rates in top and subsoil without amendment or with PG or KNO_3 addition.

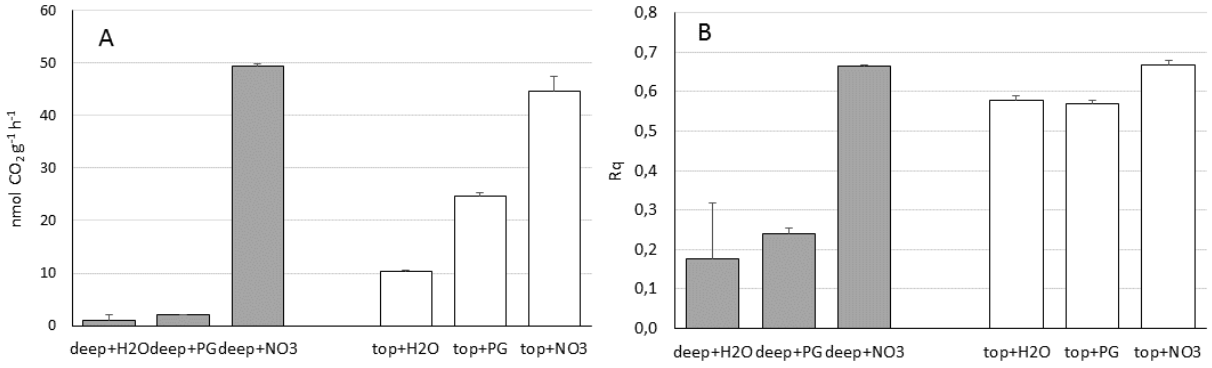

Figure 3.1: A Maximum inducible respiration rates in oxic treatments with and without PG or KNO_3 addition (for details, see tab. 2.3) and **B** respiratory quotient Rq (mol CO_2 released per mol O_2 consumed). Shown are mean values (n=3). Error bars are SD.

Without amendments, subsoil had a ~10 lower metabolic activity than topsoil (Fig. 3.1A). PG addition increased respiration by 88% in subsoil and by 140% in topsoil, illustrating the greater responsiveness to carbon addition in top- than in subsoil. KNO_3 addition to subsoil resulted in a 45 times larger inducible respiration activity while the corresponding increase in topsoil was only 4.3 fold, resulting in an overall larger inducible respiration in subsoil than topsoil. The respiratory quotient (R_q) of maximum inducible topsoil respiration was around 0.6 mol CO_2 per mol O_2 consumed, irrespective of amendment. By contrast, the R_q of non-amended subsoil was much smaller (~0.2), reflecting more reduced and/or recalcitrant substrates in the subsoil. PG addition to subsoil did not increase R_q, whereas KNO_3 addition increased the R_q to the level of topsoil (Fig. 3.1B).

A severe nitrogen limitation of Moreppen soil was also seen when inspecting the respiration kinetics in more detail (Figure 3.2). Non-amended soil (not shown) and soil amended with PG showed linear CO_2/O_2 kinetics for subsoil and quasi-linear kinetics for topsoil (Figure 3.2, left panel). In contrast, both soils responded with pronounced exponential kinetics when amended with KNO_3, indicating a microbial growth response upon relieving N limitation. This response was stronger in sub- than in topsoil.

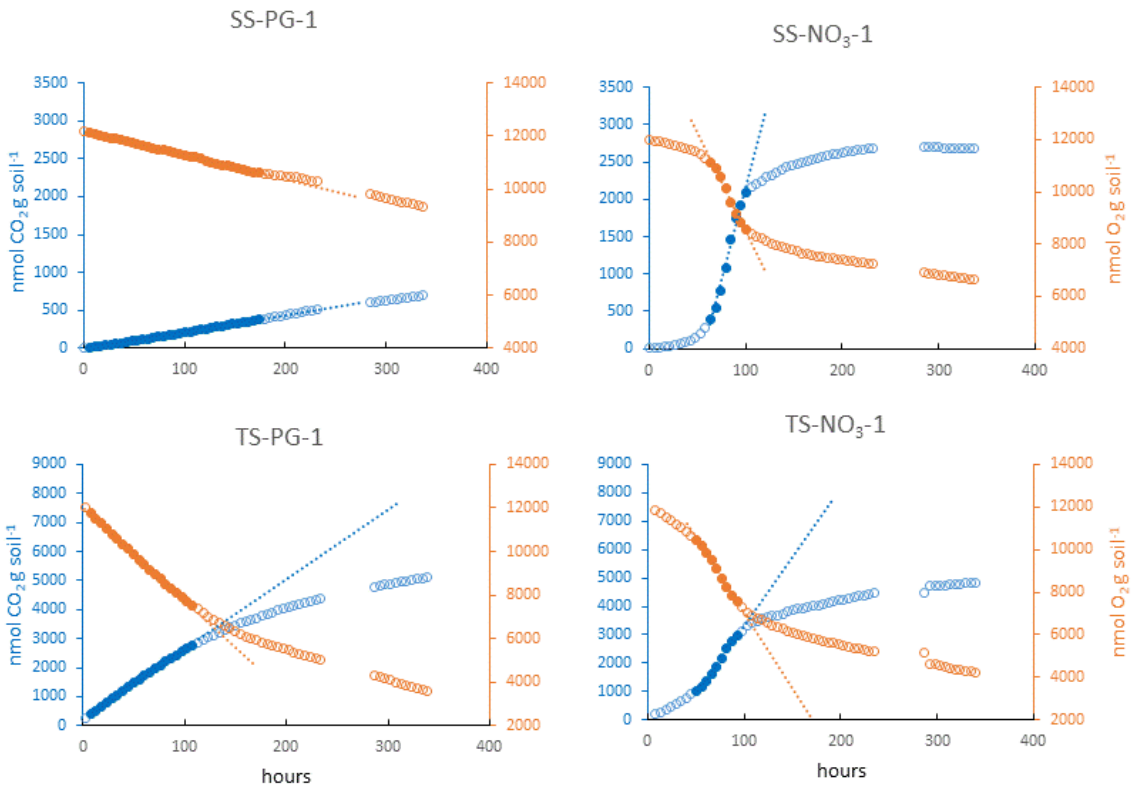

Figure 3.2: Respiration kinetics in the first replicate of oxically incubated sub(SS)- and topsoil (TS) with PG (left panel) and KNO_3 addition (right panel). Regression lines indicate maximum inducible respiration. Note different y-axis scaling for sub- and topsoil.

To study anoxic respiration and denitrification, a subset of bottles was incubated in pure He-atmosphere. Denitrification activity, i.e. N gas accumulation in subsoil samples was small and repeated piercing increasingly compromised N_2 measurements due to influx from the atmosphere in some bottles. Therefore denitrification activity was estimated from product accumulation during the first 100 h of incubation and compared to CO_2 production from the same period of incubation. Mean CO_2 production rates for the different treatments are shown in Figure 3.3A, together with estimated rates of total N gas production (Figure 3.3B).

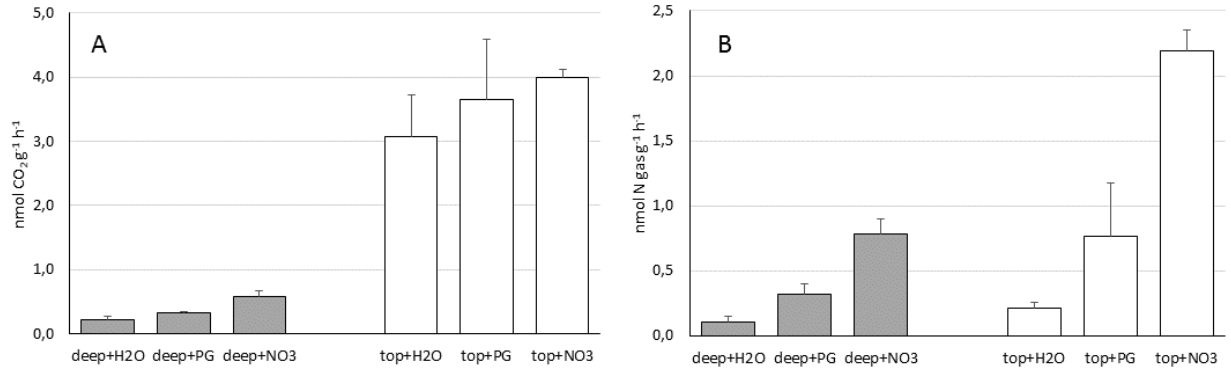

Figure 3.3: Initial respiration rates in sub- and topsoil under anoxic conditions with and without PG or KNO3 addition (for details, see tab. 2.3), measured as (**A**) rate of CO_2 accumulation and (**B**) rate of total N gas accumulation (for denitrification kinetic, see Fig. 3.6). Shown are mean values (n=3). Error bars are SD.

Anoxic CO_2 production was less responsive to PG or NO_3^- addition than oxic CO_2 production (compare Fig. 3.1 and 3.3). Respiration kinetics measured as CO_2 accumulation (Figure 3.4) showed that only subsoil amended with NO_3^- had apparent growth. Unlike under oxic conditions, topsoil did not show growth kinetics, irrespective of treatment.

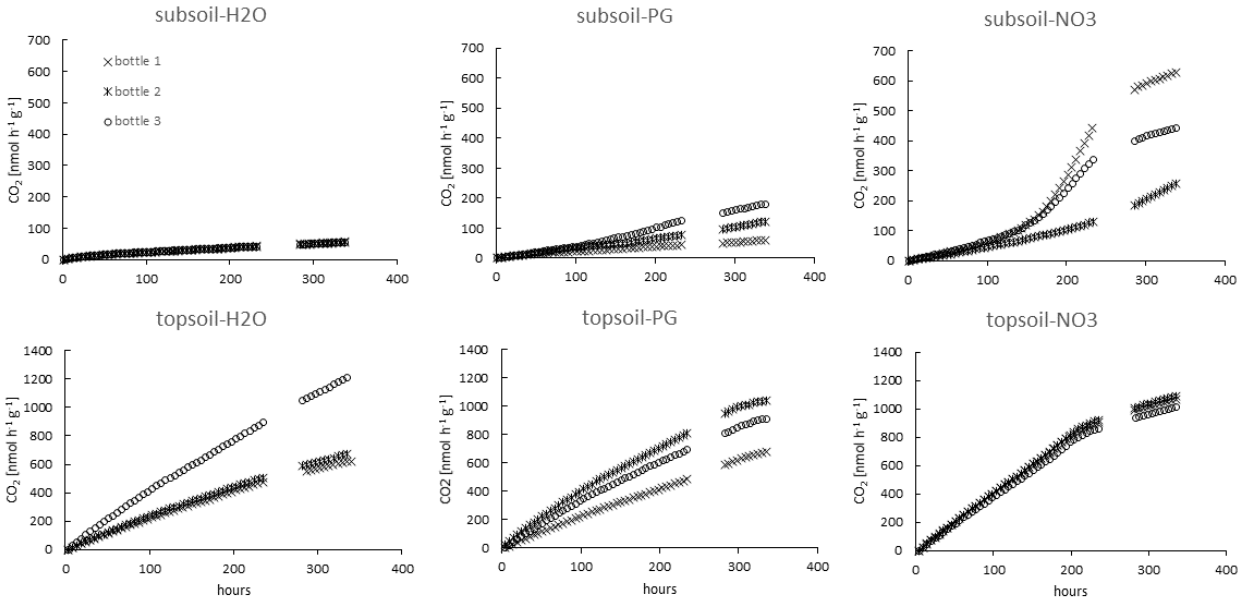

Figure 3.4: Kinetics of CO_2 accumulation in subsoil (upper panel) and topsoil (lower panel) without amendemnet (left panel), PG addition (middle panel) and NO_3^- addition (right panel). Shown are single bottle values (n=3) for each treatment.

Anoxic respiration reached 19,6% (subsoil) and 30% (topsoil) of oxic respiration observed in untreated control soils (compare Fig. 3.1A and 3.3A). The corresponding values for the PG treatment were 15.4% (subsoil) and 14.8% (topsoil) and for the NO_3- treatment 5.9% (subsoil) and 9.0% (topsoil). For the NO_3^- treatments, maximum CO_2 production rates during exponential growth were compared. The small ratios of anoxic over oxic respiration in the NO_3^- treatments reflect the strong N limitation in both the top- and the subsoil. As oxic growth is faster than anoxic growth, the same N addition provoked a relatively larger increase in CO_2 production under oxic conditions, which was not compensated by the stimulation of denitrification as a respiratory process ion under anoxic conditions. Monitoring of CH_4 and H_2 concentrations in the bottles revealed small concentrations in the pico-molar range, but a conspicuous pattern of small H_2 production in the subsoil in presence of NO_3^- and some CH_4 production in the top soil.

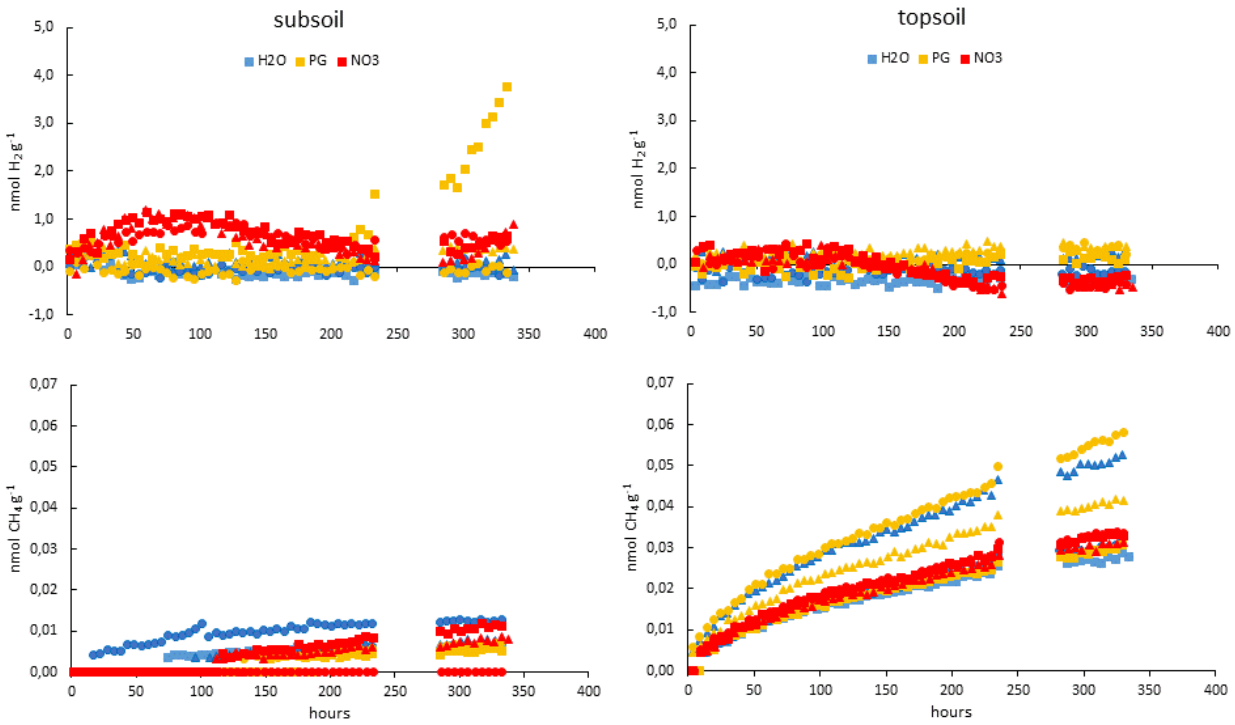

Figure 3.5: Kinetics of H_2 (upper panel) and CH_4 (lower panel) in subsoil (left panel) and top soil (right panel) in the 1st pilot experiment. Shown are single values of three replicates for unamended control soil (blue), PG amended soil (yellow) and NO_3^- amended soil (red). The detection limit of the H_2 analyser under

the given experimental conditions was app. 500 pmol H_2 g soil^{-1}. 1 nmol H_2 g^{-1} corresponds to ~10 ppm H_2 in the headspace.

Denitrification in unamended and PG-amended soils was short-lived and dominated by N_2 production (not shown), suggesting that native NO_3^- concentrations in both sub- and topsoil were small. Figure 3.6 shows the denitrification kinetics in three single bottles each for the NO_3^- treatments of sub- and topsoil. Both soils accumulated NO to small amounts (< 3 nmol g^{-1} soil) which was depleted towards the end of the incubation. In the subsoil, N_2O accumulated almost linearly, before accelerating towards a sharp peak after 150 – 200 h and being taken down to zero rapidly. Although similar in magnitude, N_2O accumulation in topsoil was smoother and depleted much earlier than in subsoil. All three bottles with subsoil had problems with leakage from 100 h into the incubation onwards. Therefore, only the first 100 h of N_2 accumulation are shown.

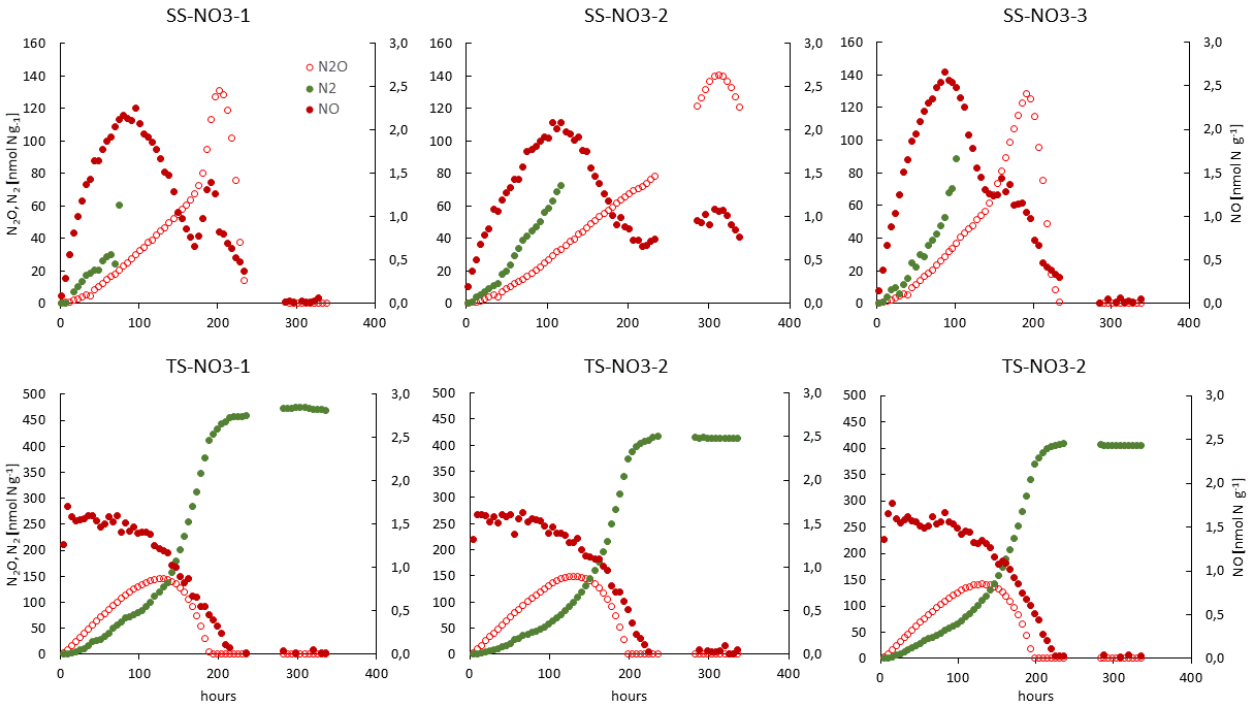

Figure 3.6: Denitrification kinetics in NO_3^- treatments of subsoil (SS, upper panel) and topsoil (TS; lower panel). Shown are three replicate bottles for each soil and treatment. Note different y-axis scaling for unamended/PG and NO_3^- amended.

.

3.3 Pilot 2: Release of Mn and Fe in soil water

When setting up the second preliminary experiment (pilot 2), the water content of the soil was increased from ~60% to ~80% WHC_{max} to have enough soil water for sampling ~1 mL for metal analysis through the microrhizons within a reasonable time. Sampling times required for ~1 ml soil solution ranged from 6 to 138 minutes. No obvious reason for the large range of sampling time was observed, but when the soil was packed more tightly around the microrhizones, the sampling time seemed to decrease. As the microrhizones have a high "bubble point" (the suction at which air enters the lysimeter), they do not sample air with underpressures achieved by a disposable syringe. Thus, air inclusion at the interface between microrhizon and soil reduce the contact area for water movement and increase the sampling time. For efficient sampling, it is therefore important to pack sieved soil slightly. Other factors influencing the sampling time could be clogging, as fine particles and possibly precipitated iron oxides were observed on the membrane after the experiment (Figure 3.7).

Figure 3.7: Microrhizon after second pilot experiment, with fine particles on the outside of the membrane.

The water samples were analysed for iron, manganese and nitrate. For the anaerobic treatment, initial concentration levels of dissolved Mn^{2+} ranged from from 0.007-0.02 pmol g^{-1} soil, before starting to increase after two days, reaching 0.76 pmol g^{-1} soil by the end of the experiment. The increase in Mn^{2+} coincided with the depletion in NO_3^- (Figure 3.8A). Nitrate concentrations at the start of the experiment were between 4 and 7 nmol g^{-1} soil, and dropped quickly throughout the first two days. For the oxic control treatment, the nitrate concentration remained stable between 0.8 and 1 nmol g^{-1}, before dropping to concentrations below the detection limit at the end of the experiment. In PG treatments, both aerobic and anaerobic, NO_3^- concentrations dropped to 0 - 0.1 nmol g^{-1} soil already after two days, indicating denitrification. In contrast to Mn^{2+}, Fe^{2+} levels seemed to reach a peak after one day in all treatments, with largest values of 0.18 pmol g^{-1} soil in the unamended control (Figure 3.8B). This peak was transient and disappeared after two days, after

which Fe^{2+} in the control slowly declined to zero, while slightly elevated concentration between 0.04 and 0.1 pmol g^{-1} soil were observed in the oxic and anoxic PG treatments.

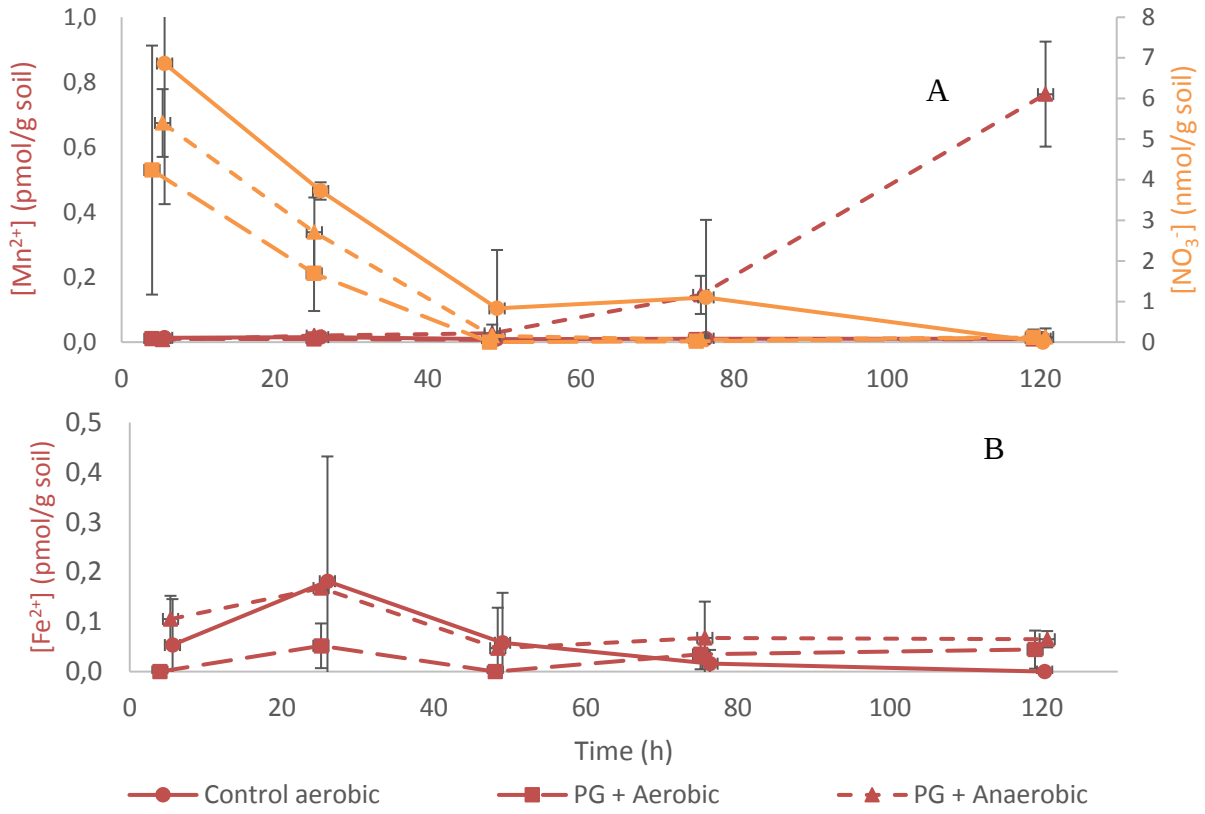

Figure 3.8: Dynamics of dissolved Mn (A) and Fe (B) in the different treatments of the second pilot experiment. The dynamics of nitrate are shown in both A and B. Symbols indicate treatment, as provided in legend and Table 2.2, orange shows nitrate, plotted in the upper panel. Note different scaling of y-axis for Mn^{2+} and Fe^{2+}.

3.4 Main experiment: Metal respiration

3.4.1 Oxygen

In the pilot experiment 1, the amount of O_2 leaking into the bottles was small and constant enough to be corrected for. In the main experiment, the protruding the microrhizones through the septa of the bottles resulted in a more variable amount of O_2 and N_2 entering the bottles, either through the septum or through the microrhizon itself, particularly when sampled. The total amount of O_2 entering the individual bottles was estimated from equation 2.1, assuming that biological N_2

production was negligible, and is plotted in Figure 3.9. There was no obvious trend in O_2 influx across treatments, since this had to do with factors other than treatment, such as the angle and placement of the microrhizone through the septum and crimping of the metal ring.

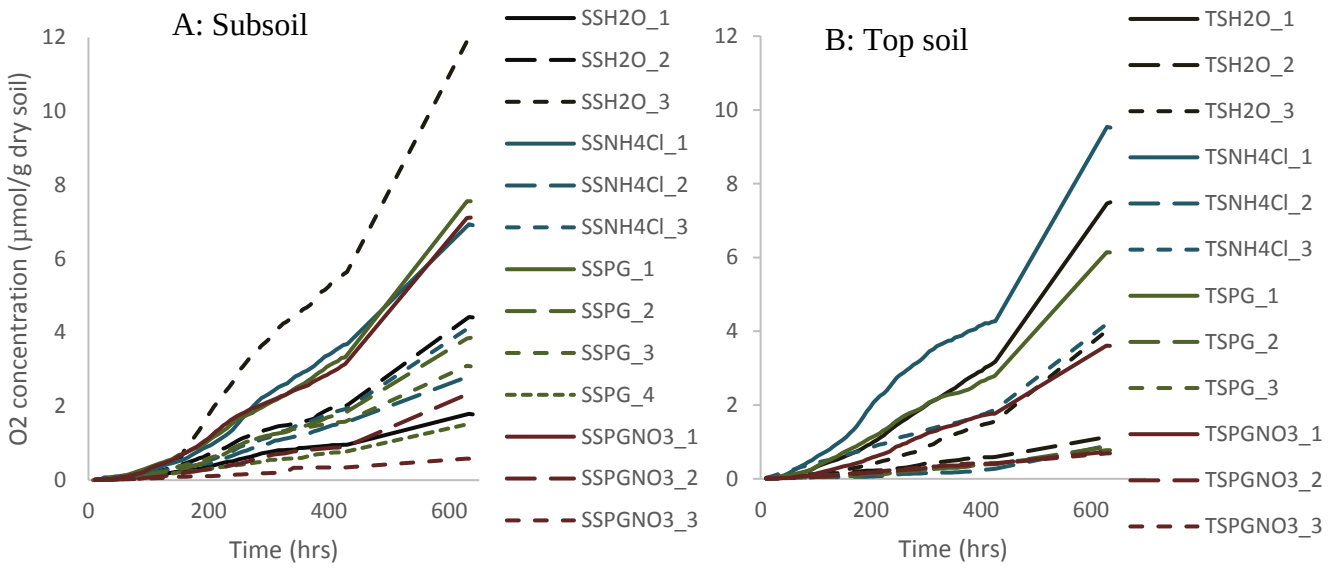

Figure 3.9: Net oxygen influx per bottle over time, estimated by linear equation 2.1. Bottles containing subsoil (SS, Figure 2.1B) to the left (A), bottles containing top soil (TS, Figure 2.2) to the right (B). H2O = soil only added de-ionized water, NH4Cl = soil amended with ammonium chloride, PG = soil amended with propylene glycol, PGNO3 = soil amended with propylene glycol and ammonium nitrate.

When investigating how much of the total O_2 had been used for respiration (eq. 2.2), there was less variation between replicates of the same treatment. Figure 3.10 compares the average rates of O_2 influx with the average rates of oxygen respiration. As expected, for most of the bottles, the rate of O_2 respiration and influx were positively related, i.e. the more O_2 leaked into the bottle, the more was respired. This was particularly evident for the topsoil with amendments, but did not apply for subsoil without PG amendments, obviously because the metabolic activity was limited by electron donors (and probably N) and not by the electron acceptor O_2. The bottle SSH2O_3 had the largest rate of O_2 influx among all bottles (18 nmol O_2 g^{-1} h^{-1}) and the third smallest average rate of O_2 respiration (0.19 nmol g^{-1} h^{-1}). Only bottles SSH20_1 and SSNH4Cl_3 had smaller rates with 0.17 and 0.18 nmol O_2 g^{-1} h^{-1}, respectively.

Ammonia added to the soils to relieve N limitation did not result in larger respiration rates in subsoil, whereas in topsoil, two of three bottles responded positively. In the subsoil, the largest average O_2 respiration rate with added ammonium was 0.6 nmol O_2 g^{-1} h^{-1} (SSNH4Cl_1), while the smallest respiration rate estimated for topsoils with ammonium was 0.8 nmol O_2 g^{-1} h^{-1} (TSNH4Cl_2).

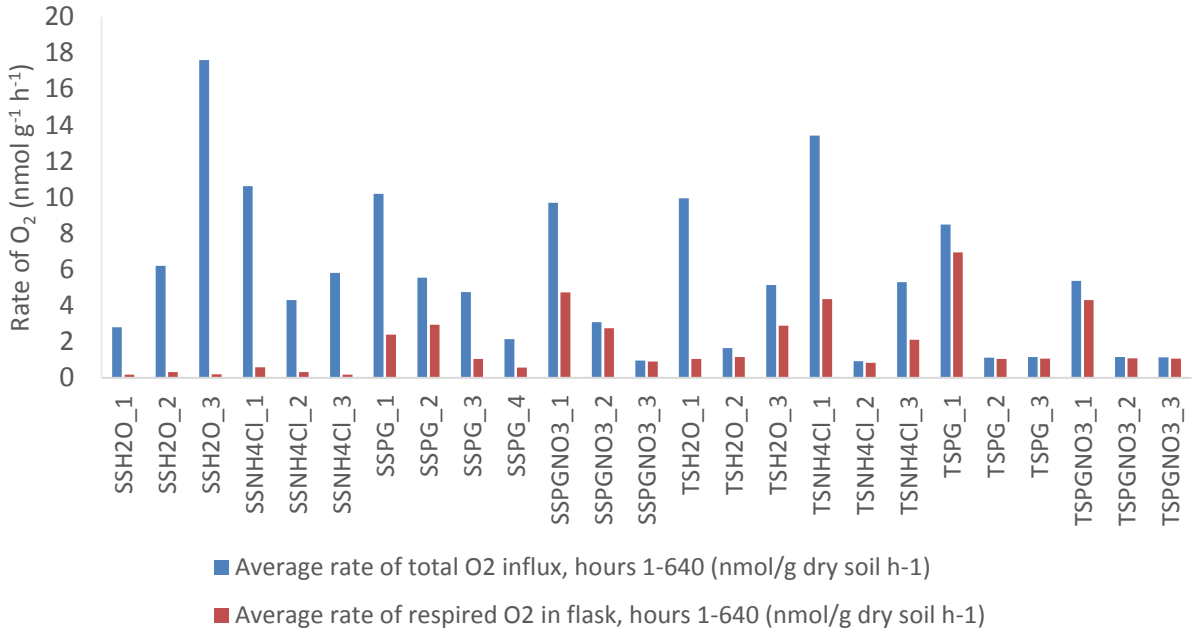

Figure 3.10: Average rates (nmol g^{-1} dry soil h^{-1}) of O_2 flux into the bottles (blue) and O_2 respiration (red) during 400 h of initially anoxic incubation. SS = subsoil (Figure 2.1), TS = top soil (Figure 2.2), H2O = control, NH4Cl = soil amended with ammonium chloride, PG = soil amended with propylene glycol, PGNO3 = soil amended with propylene glycol and ammonium nitrate.

3.4.2 CO_2

Figure 3.11 shows CO_2 accumulation over time in subsoil (Figure 3.11A) and topsoil (Figure 3.11B). In general, subsoil produced less CO_2 than topsoil, similar to what was found in pilot experiment 1 (Figure 3.1). CO_2 accumulation by subsoils after 600 hours was quite variable but clearly larger in PG and PG+NO_3^- treatments than in control or NH4 treatments, reaching a maximum of 1.5 µmol CO_2 g^{-1}. Maximum CO_2 accumulation in topsoil was almost twice as large (2.6 µmol g^{-1}). Also here, final CO_2 accumulation was very variable between replicates of the NH_4, PG and PG+NO_3^- treatments, where one bottle of each treatment reached large values, while the other bottles scaled closer together.

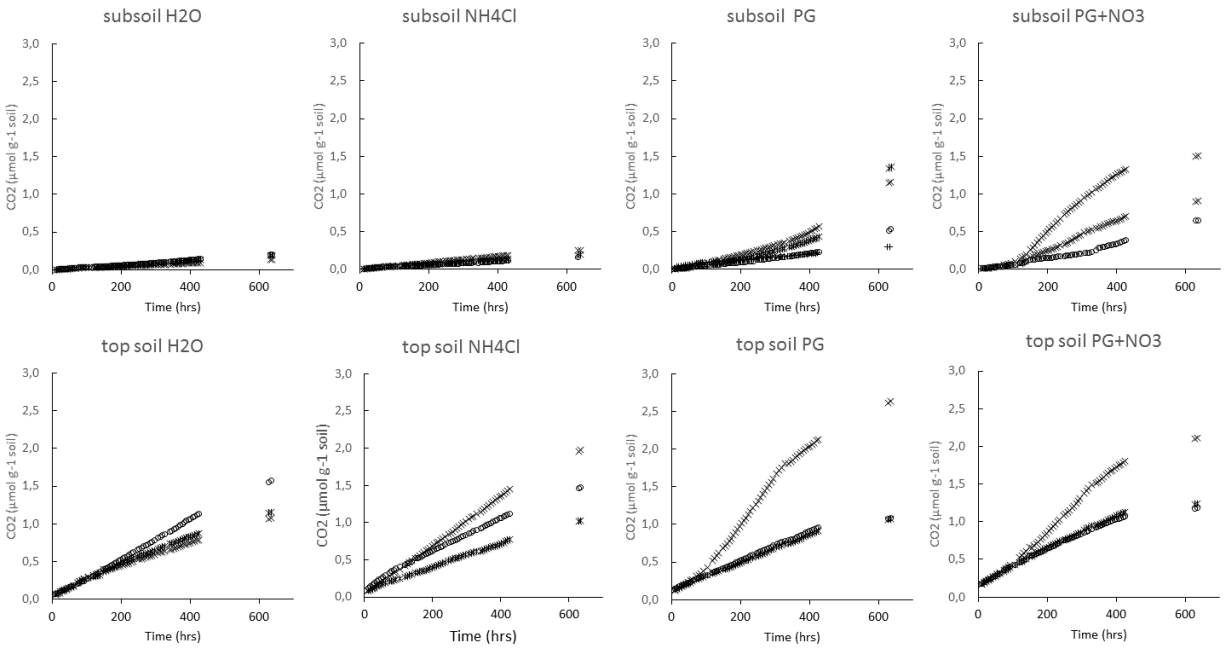

Figure 3.11: CO_2 accumulation for each bottle in the main experiment normalised to dry weight of soil. (A) Bottles containing subsoil (SS) and (B) bottles containing top soil. H2O = control, NH4Cl = with ammonium chloride, PG = with propylene glycol, PGNO3 = with propylene glycol and ammonium nitrate.

Based on the initial addition of 300 µmol PG-C bottle^{-1}, a complete mineralization of PG should have resulted in a total excess CO_2 accumulation (PG treatment minus control treatment, assuming no priming takes place) of 5 µmol CO_2 g^{-1}. Because replicate bottles of PG and control treatments were exposed to different amounts of O_2, the excess CO_2 accumulation attributed to PG degradation could not be estimated based on treatment averages. To solve this problem, excess CO_2 production was calculated from single control and treatment bottles that were exposed to approximately equal amounts of O_2. For the subsoil, the observed excess in CO_2 production accounted for a relatively small fraction of the theoretical amount of CO_2 which would have been generated assuming complete PG degradation, with 3-23% for the PG treatment and 11-25% for the PG + NO3 treatment, indicating that PG was not completely mineralized 26 days after the addition. For the topsoil, this fraction was in the same order of magnitude with 5-26% for the PG treatment and a somewhat lower 13-14% for the PG + NO3 treatment (Figure 3.13).

In Figure 3.12, average rates of CO_2 accumulation are plotted together with average rates of O_2 respiration, revealing a clear positive relationship with a larger rate of O_2 respiration when rates of CO_2 accumulation in are high.

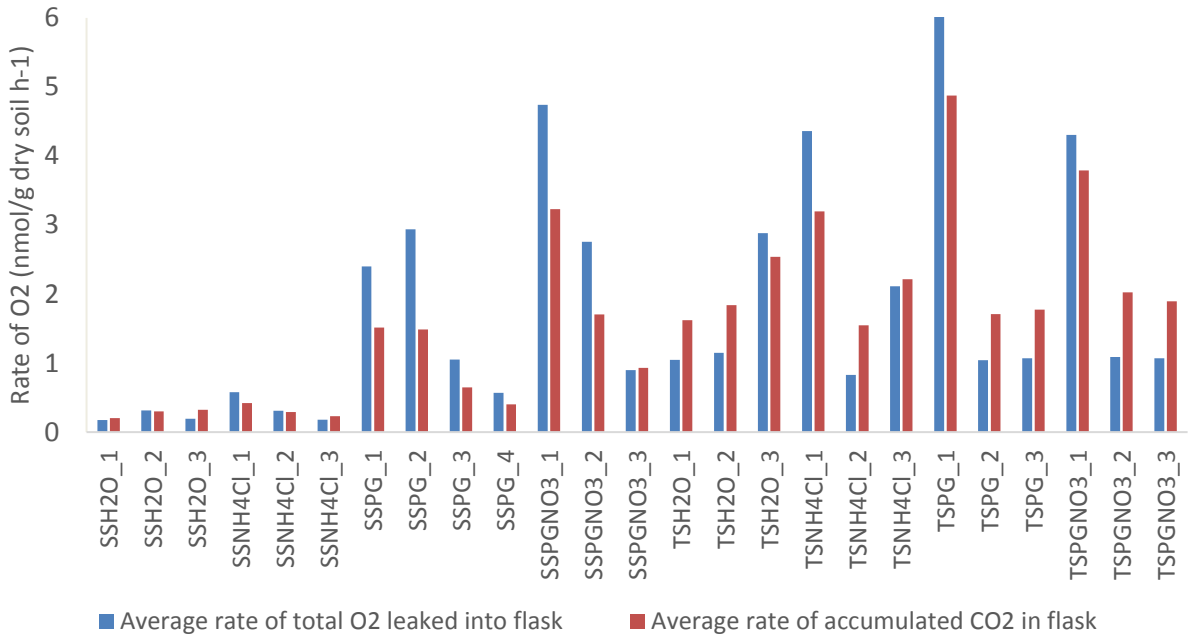

Figure 3.12: Average rates (nmol/g dry soil h^{-1}) of respired O_2 in bottle (blue colour, left column) and of accumulation of CO_2 in bottle headspace (red colour, right column). SS = subsoil (Figure 2.1), TS = top soil (Figure 2.2), H2O = soil only added de-ionized water, NH4Cl = soil amended with ammonium chloride, PG = soil amended with propylene glycol, PGNO3 = soil amended with propylene glycol and ammonium nitrate.

To further visualize the extent of correlation between CO_2 and O_2, the maximum value of respired oxygen was plotted together with the relative degradation of PG (Figure 3.13). The soils which respired the most oxygen showed the highest relative degradation of PG.

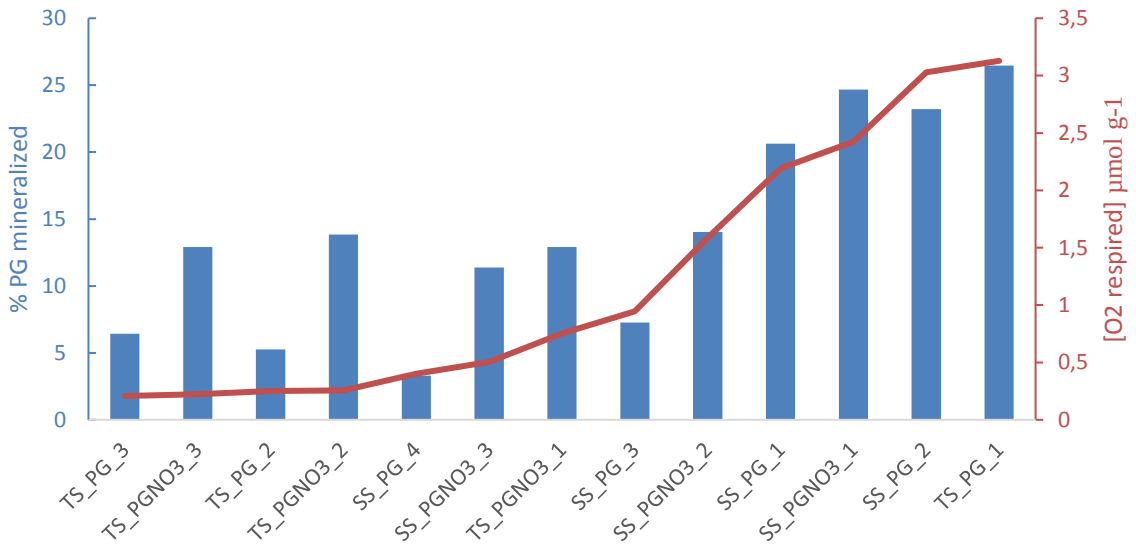

Figure 3.13: The calculated relative degradation of PG (blue bars) and the respired O_2 (red line) after end of experiment on day 26. Note that samples are sorted by increasing O_2 respiration.

3.4.3 Denitrification: N_2, N_2O, NO and NO_3^-

Because of variable leakage from the atmosphere, contaminating the bottle headspaces with N_2, total denitrification rates could not be estimated. The cumulative influx of N_2-gas into the individual bottles can be found in the appendix in section A.A.2 (Figure A.1).

Unlike the presence of N_2, the presence of N_2O and NO may be taken as indicators for denitrification (section 1.2), as they only occur at trace concentrations in ambient air so that leakage does not play a role. All bottles showed transient N_2O and NO accumulation of varying duration (Figure 3.14). In treatments with no extra NO_3^- or NH_4^+ addition, the N_2O and NO peak seemed to be controlled by the NO_3^- initially present in the soil, which was depleted within <100 hours (Fig, 3.8, A, B and E, F). With added ammonium (but also in the subsoil control), N_2O accumulation was biphasic, with a pronounced initial peak (0 – 100h) and a shoulder of elevated N_2O persisting throughout the entire incubation (Figure 3.14C, D). This probably suggests that added ammonium together with the O_2 leaking into the bottles stimulated nitrification including N_2O production. Nitrification is also supported by the finding of increasing NO_3^- concentrations in the ammonium treatment.

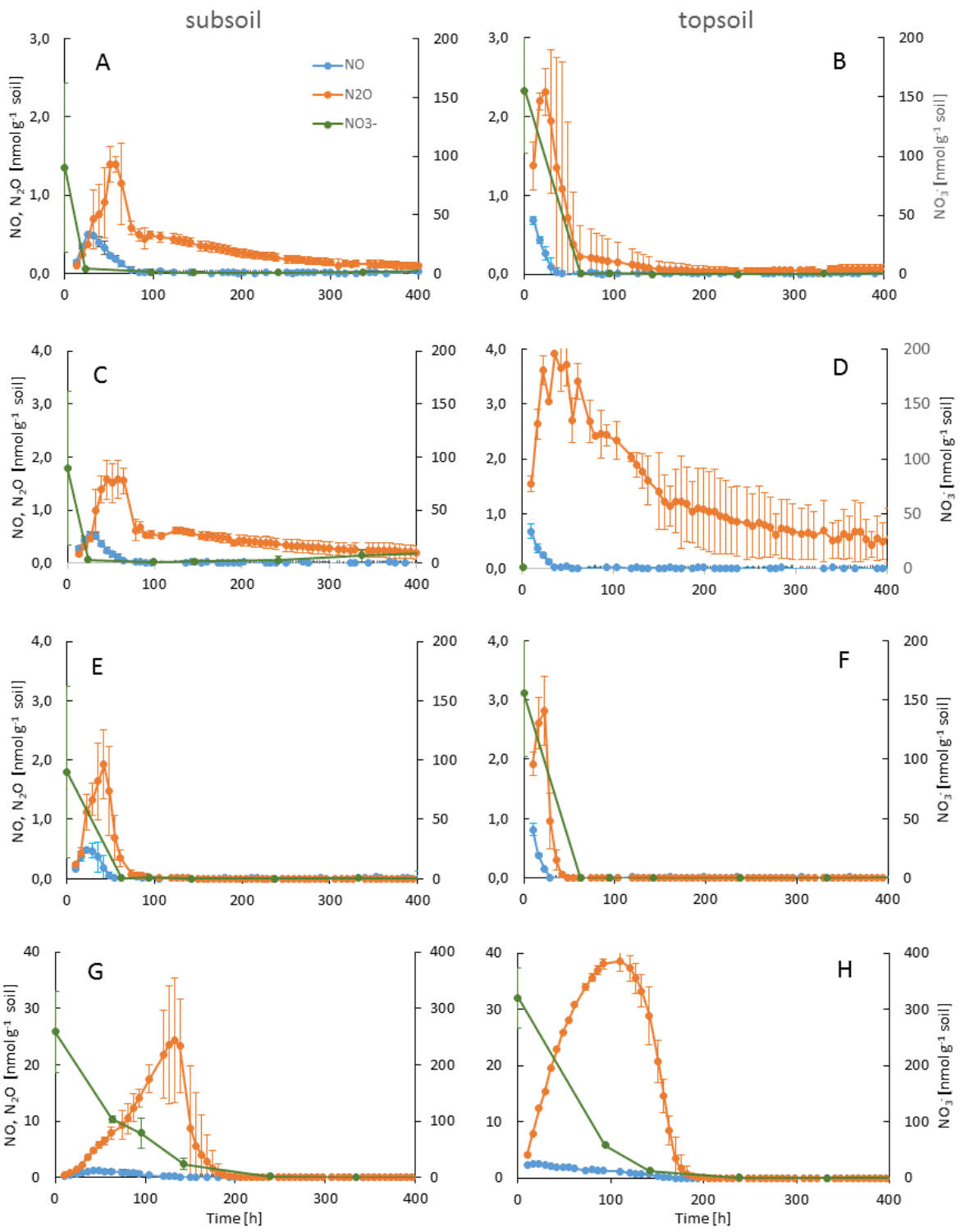

Figure 3.14: Dynamics of NO (blue), N_2O (orange) and NO_3^- (green) in subsoil (left panel) and topsoil (right panel) in control treatments (A, B), with NH_4Cl addition (C, D), with PG addition (E,F) and with PG and NO_3^- addition (G, H). Shown are average values with standard deviation as error bars. More details about the NO_3^- dynamics can be found in the Appendix section A.3.

N_2O accumulation was most pronounced and more persistent in the NO_3^- treatments. Both sub- and topsoil accumulated and depleted N_2O within 200 h. As in the preliminary experiment (pilot 1, Ch. 3.2), N_2O accumulated somewhat faster and to a larger amount in top- than in subsoil.

The background concentration of NO_3^- in subsoil and topsoil was 90 ± 72 nmol and 160 ± 53 nmol g^{-1}, respectively (Table A.2 and Figure 3.14A, B). Initially measured NO_2^- was small with 1.8 ± 1.1 and 1.5 ± 0.61 nmol g^{-1} soil in the subsoil and top soil, respectively (Table A.3). The high standard deviation of the initially measured NO_3^- concentration in the soils could indicate that NO_3^- was initially unevenly distributed within the soils. Measured NO_3^- and NO_2^- concentrations over time are listed in the Appendix, Table A.4. Unamended subsoil accumulated about 2 nmol N_2O g^{-1} soil (Figure 3.14A), and unamended topsoil about 3 nmol N_2O g^{-1} (Figure 3.14B). This is about 1/10 of the maximum value compared to that of the NO3- amended soils, which accumulated 25 and 40 nmol N_2O/g soil in the subsoil and top soil, respectively (Figure 3.14G, H). This shows that the addition of a relatively small amount of NO_3^-(160 nmol g^{-1} soil) stimulated denitrification largely.

3.4.4 Iron and manganese

Fe^{2+} and Mn^{2+} concentrations measured in soil water, and recalculated per g dry weight soil are plotted in Figure 3.15 and Figure 3.16 for subsoil and top soil, respectively. In the subsoil, Fe^{2+} release was quite small irrespective of treatment (<0.3 nmol g^{-1} soil). Peaks of elevated Fe^{2+} concentrations were variable and short-lived, pointing at variable reduction - reoxidation kinetics in single bottles. Only in the PG+NO_3^- treatment, all three parallels showed a consistent increase of Fe^{2+} towards the end of the incubation (Figure 3.15D).

Iron release from the top soil was on average ten times larger, reaching a maximum of 2.4 nmol g^{-1} in one bottle of the PG treatment (Figure 3.16C). In general, Fe^{2+} release in the top soil was steadier over time in comparison than in subsoil, reaching highest values at the end of the incubation. Both PG and PG+NO_3^- addition stimulated Fe^{2+} release, whereas NH_4^+ addition did not seem to have any effect.

As with Fe^{2+}, Mn^{2+} release from subsoil control or the NH_4^+ treatment was small and inconsistent. When amended with PG or PG+NO_3^-, significant Mn^{2+} release from subsoil occurred towards the end of the incubation. There was one outlier in the latter treatment, reaching an extraordinary large value of 15 nmol Mn^{2+} g^{-1}.

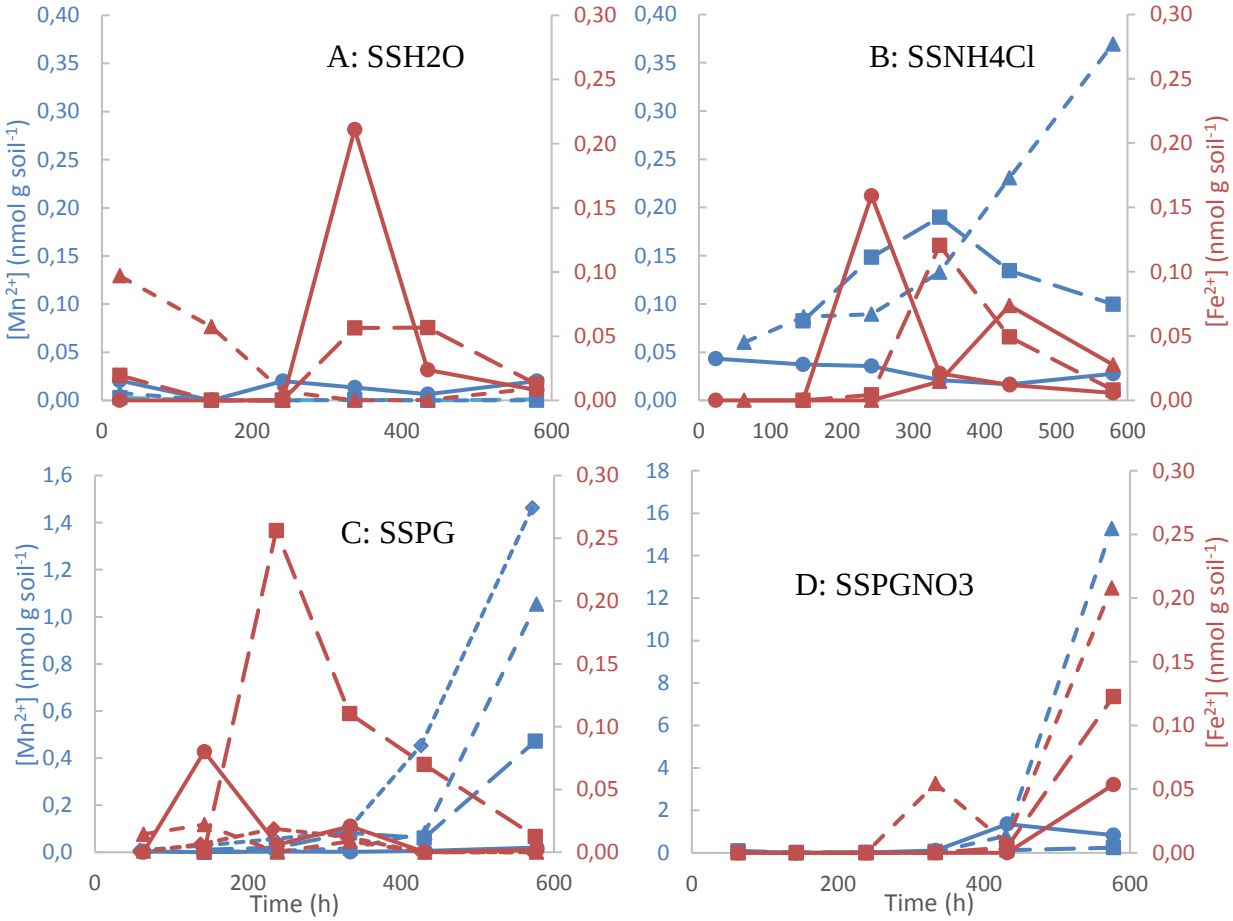

Figure 3.15: Dynamics of released manganese (blue colour) and iron (red colour) measured in water samples taken from bottles containing subsoil. Subsoil with only DI water (A), subsoil amended with NH_4Cl (B), subsoil amended with PG (C) and soil amended with PG and NH_4NO_3 (D). Solid line and circles represent replicate bottle no 1, dashed line and squares represent replicate bottle number 2, dashed lines and triangles represent replicate bottle no 3. Notice the difference in scaling of Mn between the two top and the two bottom graphs. In D, the last measured Mn-concentration of SSPGNO3_3 (15 nmol g soil $^{-1}$) is omitted for visualization purposes.

Whereas the difference in Fe^{2+} release between subsoil and topsoil was only 4 to 8 fold, topsoil released up to 100-1000 times more Mn^{2+} than subsoil in the same treatment, and even larger differences in the controls. Largest release was observed in the PG treatment. PG + NO_3^- addition

resulted in only marginally smaller Mn^{2+} accumulation, whereas control and NH_4^+ treatment accumulated about half of the Mn^{2+} found in the PG treatments.

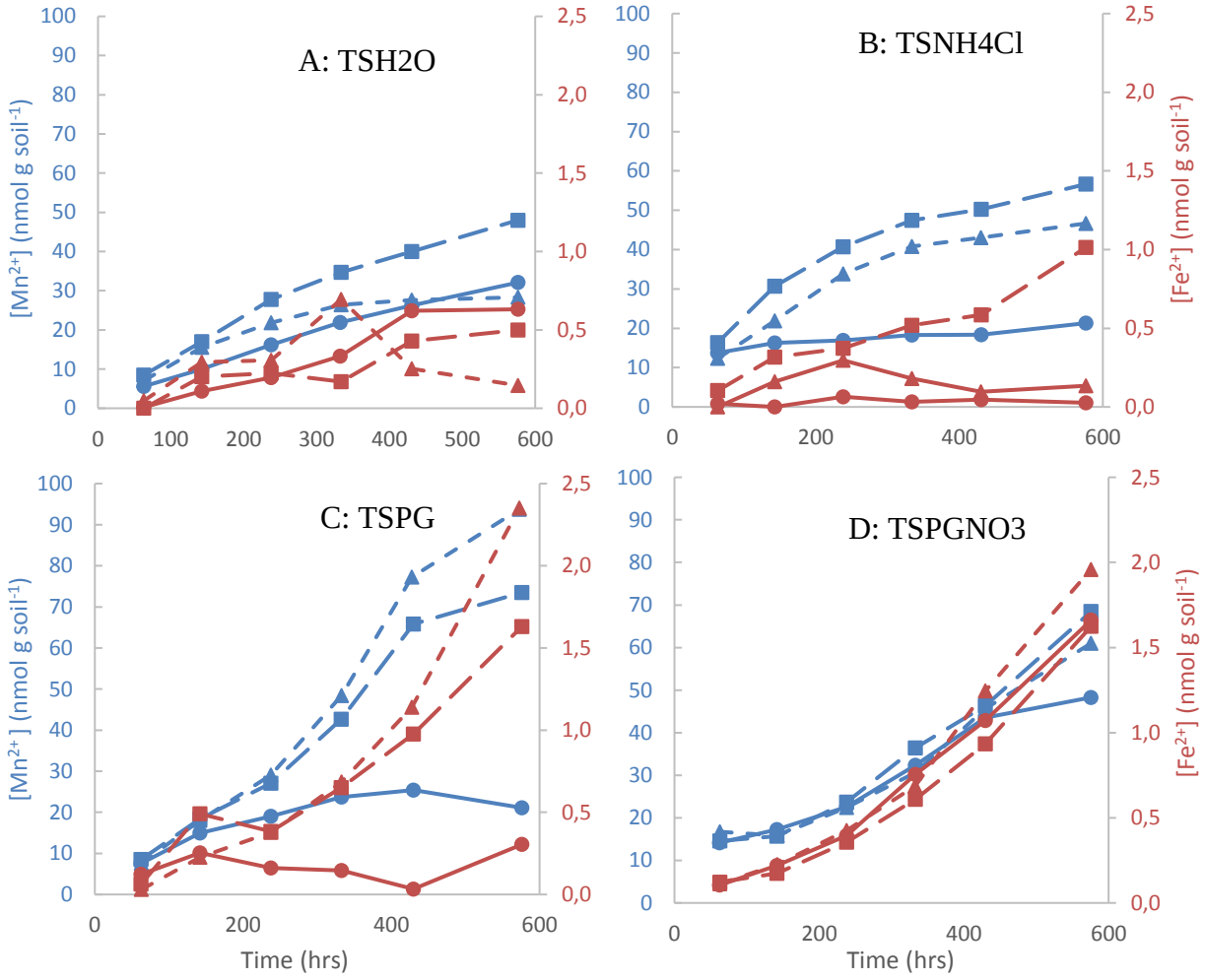

Figure 3.16: Dynamics of released manganese (blue colour) and iron (red colour) measured in water samples taken from bottles containing topsoil. Topsoil with only DI water (A), subsoil amended with NH_4Cl (B), subsoil amended with PG (C) and soil amended with PG and NH_4NO_3 (D). Solid line and circles represent replicate bottle no 1, dashed line and squares represent replicate bottle number 2, dashed lines and triangles represent replicate bottle no 3.

To visualize the impact of O_2 availability on $Fe^{2+}$and Mn^{2+} release, the average rates of Fe^{2+} and Mn^{2+}accumulation were plotted together with the average rates of oxygen respiration (Figure 3.17). From this it becomes clear that the rate of metal release was negatively related to oxygen availability, meaning that O_2 was chosen over metals as terminal electron acceptor.

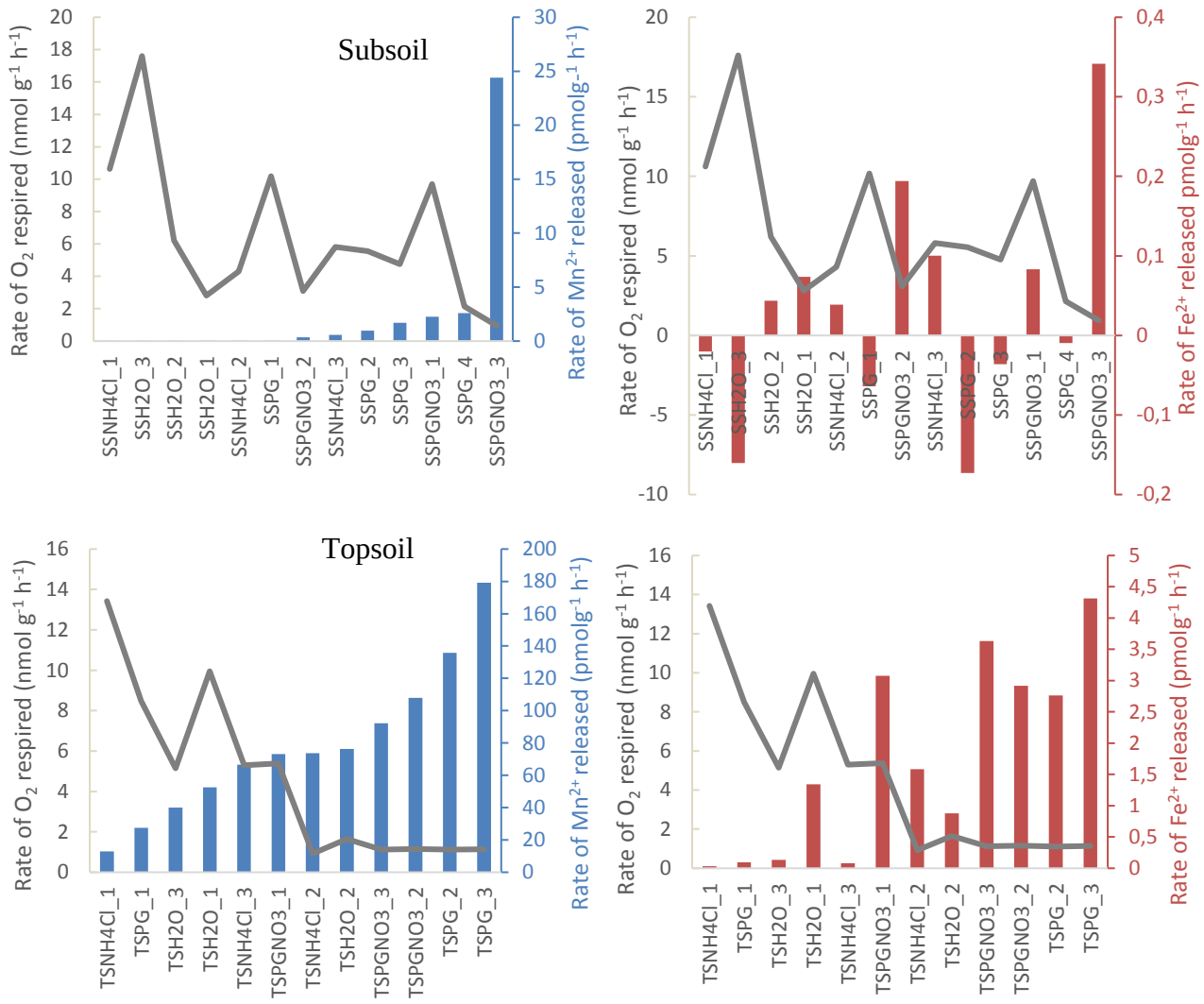

Figure 3.17: The average rates of released Mn2+ (blue) and Fe2+ (red) in subsoil (top panels) and top soil (lower panels) based on linear regression. The average rates of oxygen respired were included (grey line). Note that samples are sorted in order of increasing rates of Mn2+ release. Notice that the scaling of the secondary y-axes is different.

3.5 Microbial community analysis

A total of 37 soil samples was subjected to DNA extraction and analysed for prokaryotic community composition using metabarcoding of the 16S rDNA gene. All batches from the main experiment were included, providing at least three replicates for each treatment. In addition, three replicates of native subsoil and top soil (section 2.2), and three replicates from each of the sieved soils directly before distributing them into the flasks were analysed. An overview of the samples is given in Appendix 1, Table A.1.

Based on the estimated number of cells, an assumed DNA concentration of 10^{-15} g per cell (1 Mbp chromosome × the average mass of a one base pair), and the measured DNA concentrations after extraction from the soil, the DNA yield ranged from 6% to 29% for subsoil, and from 10% to 77% for top soil. It is noteworthy that there was a large variability in estimated cell numbers and these were only estimated for the native soils (labelled "field"). This might have led to an underestimation of the number of cells and thus an overestimation of DNA extraction yield.

3.5.1 Cell enumeration

The total number of cells estimated by fluorescence microscopy varied from 0.6×10^9 to 4.1×10^9 in the native subsoil, and 1.8×10^9 to 9.3×10^9 in the native top soil from two dilution levels (Table 3.2). The purpose behind enumerating the cells was to make this study comparable with other studies and to approximate the DNA extraction yield, and was therefore not prioritized for the entire sample set. The results showed that topsoil harboured approximately double as many cells than the subsoil, even though this difference was not statistically significant due to lack of replicates. Viable cells were estimated to account for 64 - 92% of cells enumerated in both soil types. Note that the "topsoil" is a mix of several horizons of the sand and may contain fewer cells than what could be expected for an organic soil horizon.

Table 3.2: Amount of cells enumerated by fluorescence microscopy in native samples of the subsoil and the topsoil. The average numbers are based on two dilutions from the same sample ± standard deviation.

Soil type	[Cells] g^{-1} soil	[Dead cells] g^{-1} soil	Fraction live cells (%)
Subsoil	$2.3x10^9 \pm 2.5x10^9$	$3.8x10^8 \pm 2.9x10^8$	68-86 %
Top soil	$5.5x10^9 \pm 5.3\ x10^9$	$6.9x10^8 \pm 0.70x10^8$	64-92 %

3.5.2 Community composition

Community profiles were analysed by amplification of the 16S rRNA genes using Illumina amplitag sequencing. A total of 3 762 904 reads were generated from the entire sample set with an average quality phred score of 37. During initial filtering and merging, 405 110 reads were removed, and the average quality phred score increased to 40. The number of reads per sample ranged from 57 970 to 152 329, and the recovery rate of the reads after merging ranged from 85% to 91%. The length of the sequences were 251 base pairs before merging and trimming, and ranged

from 200 to 421 base pairs after trimming. Table 3.3 provides an overview of the total sample set, while the individual data are listed in Appendix 4, Table A.5.

Table 3.3: Overview of quality parameters for the sequencing of the total sample set, subsoil and topsoil.

	Total reads	Reads after filtering	Taxonomically assigned reads	16S rRNA OTUs	Sequence length range (bp)	Classified at Genus level	Classified at Class level	16S rRNA OTUs after rarefaction
Total	3762904	3357794	3309757	117854	200-421	17 %	96 %	82218
Subsoil	1905962	1689679	1661829	74404	200-421	18 %	97 %	48784
Top soil	1856942	1668115	1647946	74977	200-418	16 %	95 %	47658

After analysis, a total of 117 857 operational taxonomic units (OTUs) were picked. Out of the total OTUs picked, 31 527 were shared by the two soil types, as illustrated in Figure 3.18.

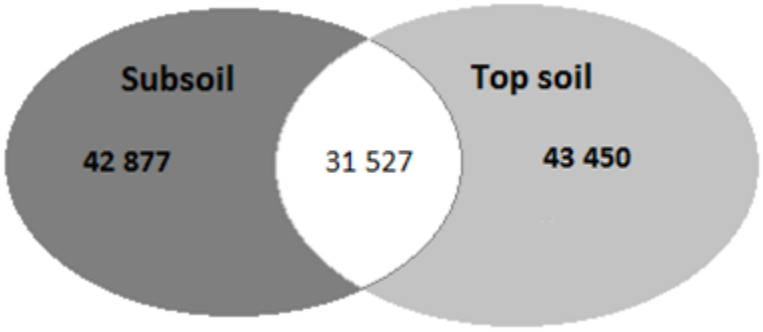

Figure 3.18: Simple Venn diagram illustrating the distribution of the total picked OTUs between sub- and topsoil.

Out of these, 64 742 singletons were observed. The singletons were kept for initial analysis, however 35 636 OTUs were removed by rarefaction to the lowest amount of reads. Prior to rarefaction analyses, the rarefaction curves of the sample set were inspected (Figure A.4), to decide whether the sequencing depth chosen for the rarefaction (52 079 reads) would be sufficient for comparison between samples.

In total, 99% of all reads from tagged 16S rRNA genes could be assigned at the phylum rank and 96% at the class rank (Appendix 4, Table A.6). The most abundant phyla were *Proteobacteria*

(30%) and *Acidobacteria* (21%) and the candidate phylum "*AD3*" (15%), followed by *Actinobacteria* (5.9%), *Chloroflexi* (4.9%) and *Verrucomicrobia* (4.6%).

The relative abundances of all identified phyla assigned to all samples are shown Figure 3.19. In the subsoil, the archaeal phyla *Euryarchaeota* decreased from a relative abundance of 13-15% in the native ("field") samples compared to 0.37-3.6% at the end of the incubation, irrespective of treatment. The most obvious difference between incubated samples was the large increase of *Proteobacteria* in the treatments using PG, particularly when applied together with NO_3^-. In the subsoil, the relative abundance of *Proteobacteria* increased from 24-28% in the native soil and the untreated control to 31-43% in the PG treatment and to 68-81% in PG+NO3 treatment. The increase in *Proteobacteria* was accompanied by a decrease in the relative abundance of *Acidobacteria* and the candidate phyla "*AD3*", which ranged from 5-10% and 3-6% in the PG+NO3 treatment respectively, while in the native soil and the control treatment these phyla ranged from 22-28%, and 12-16%, respectively.

In the top soil, differences at phylum rank were less obvious than in subsoil. In TSfield1 and TSstart1, the relative abundance of *Cyanobacteria* was at 5% compared to the other TS-samples ranging from 0.3 to 1.2%. In the PGNO3 treatments, *Proteobacteria* seemed to have a higher relative abundance (30-33%) than in the control treatment (22-25%), while the PG treatment had intermediate abundences (25-29%). However, one replicate of the native soil (TSfield2) and the sieved soil (TSstart3) had similar relative abundances of *Proteobacteria* than the PG+NO3 treatment (33 and 30%, respectively).

If the number of reads differ between samples, comparing relative abundances might overestimate the value of differences. In this sample set, most of the samples had around 90 000 reads, so when directly comparing the OTU richness of the assigned phyla (Figure 3.20), the same pattern can be seen: *Proteobacteria* had a larger OTU richness in PG-treated subsoil samples compared to controls, while *Acidobacteria* had a smaller OTU richness compared to controls.

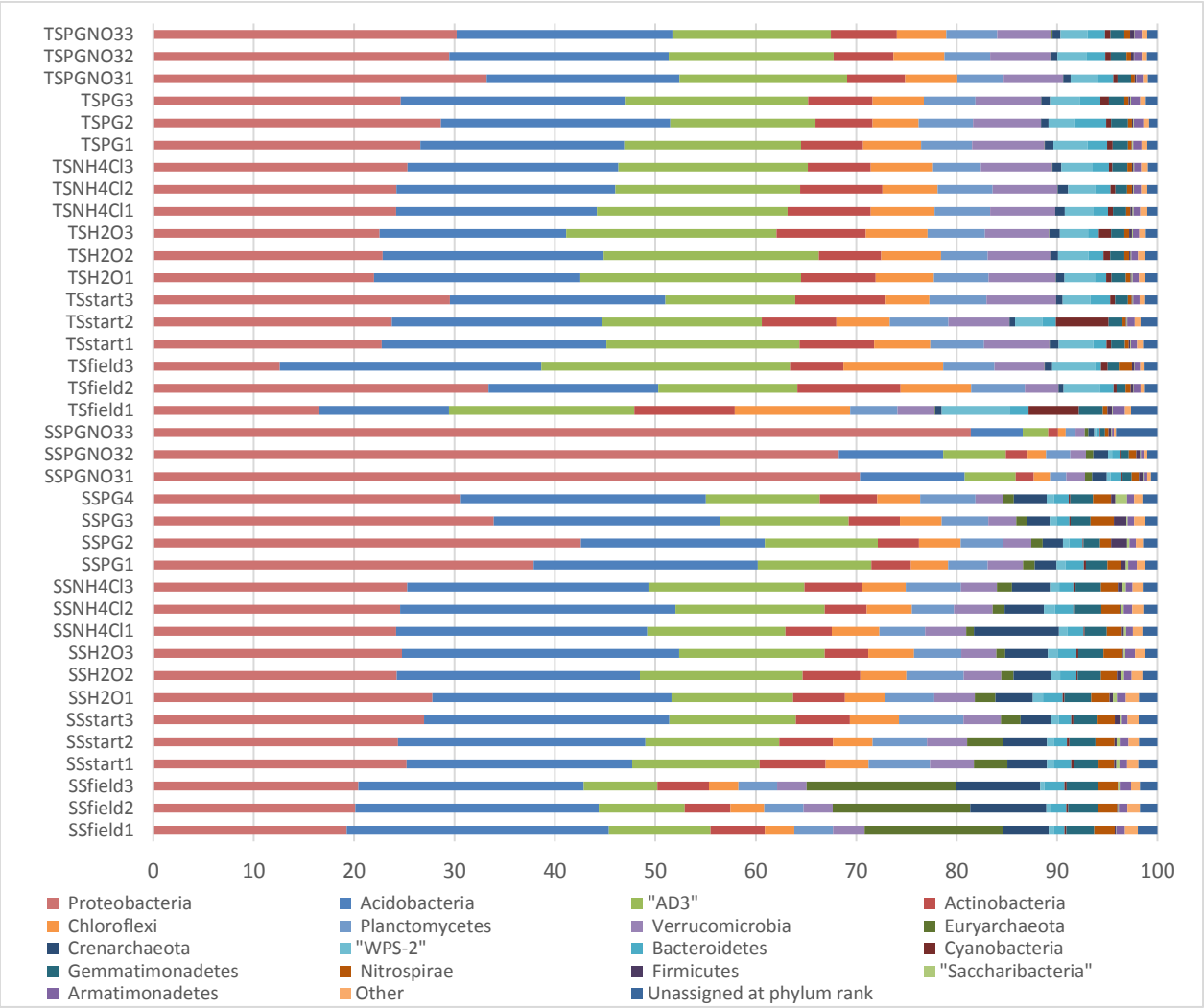

Figure 3.19: The relative abundances of assigned phyla in the different samples ordered by treatment. Candidate phyla are denoted by apostrophes. All phyla which contributed <1% in all the samples are pooled in the "Other" category. SS = subsoil (Figure 2.1), TS = top soil (Figure 2.2), field = native samples (from field), start = soil sampled directly before distributing into flasks, H_2O = soil with de-ionized water, NH_4Cl = soil amended with ammonium chloride, PG = soil amended with propylene glycol, $PGNO_3$ = soil amended with propylene glycol and ammonium nitrate.

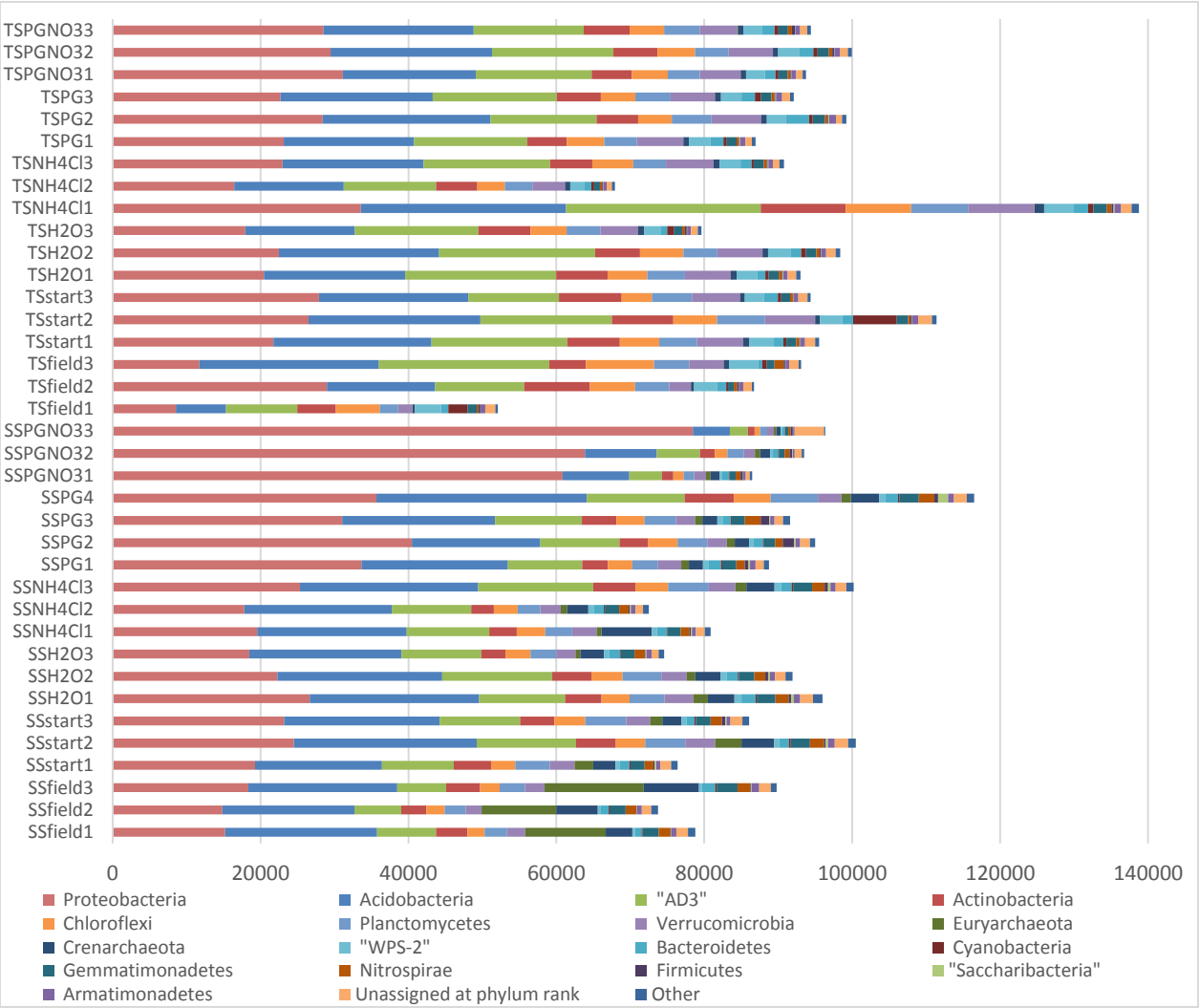

Figure 3.20: OTU richness of assigned phyla in the different samples. Candidate phyla denoted by apostrohes. All phyla which contributed <1% in any samples are pooled in the category "Other". SS = subsoil (Figure 2.1), TS = top soil (Figure 2.2), field = native samples (from field), start = soil sampled directly before distributing into flasks, H2O = soil with de-ionized water, NH4Cl = soil amended with ammonium chloride, PG = soil amended with propylene glycol, PGNO3 = soil amended with propylene glycol and ammonium nitrate.

Further dividing the *Proteobacteria* into classes, it was observed that *Beta-* and *Gammaproteobacteria* were the dominating this phylum in the PG+NO3 of subsoil (combined 62-79% relative abundance). In the top soil, *Alphaproteobacteria* were the dominating class in phylum *Proteobacteria* (11-14% relative abundance).

From the entire dataset, only 17% of the OTUs could be classified down to genus rank. When investigating the 10 most abundant OTUs of the dataset, only two of them could been assigned to genus rank, while six of them were classified down to family rank (appendix 4, Table A.7). Upon comparison of the relative abundance of these six families, the families *Oxalobacteraceae*, *Comamonadaceae* and *Pseudomonadaceae* were found to account most for the increase in *Proteobacteria* in the PG+NO3 of the subsoil. Note that only 52% of the dataset was classified down to the Family rank, while 79% were classified at the Order rank. The two orders representing the three families mentioned (*Burkholderiales* and *Pseudomanadales*) showed the same pattern when compared across treatments, thus the low relative abundance of these families in the control treatments cannot be explained by a lack of classification at this rank. Combined, these three families represented 58-76% of the relative abundance in the SS-PGNO3 treatments, compared to 1.5-4.9% in the control treatment (Figure 3.21). An increase in the relative abundance of the families was also noted in the SSPG and TS-PGNO3 treatments.

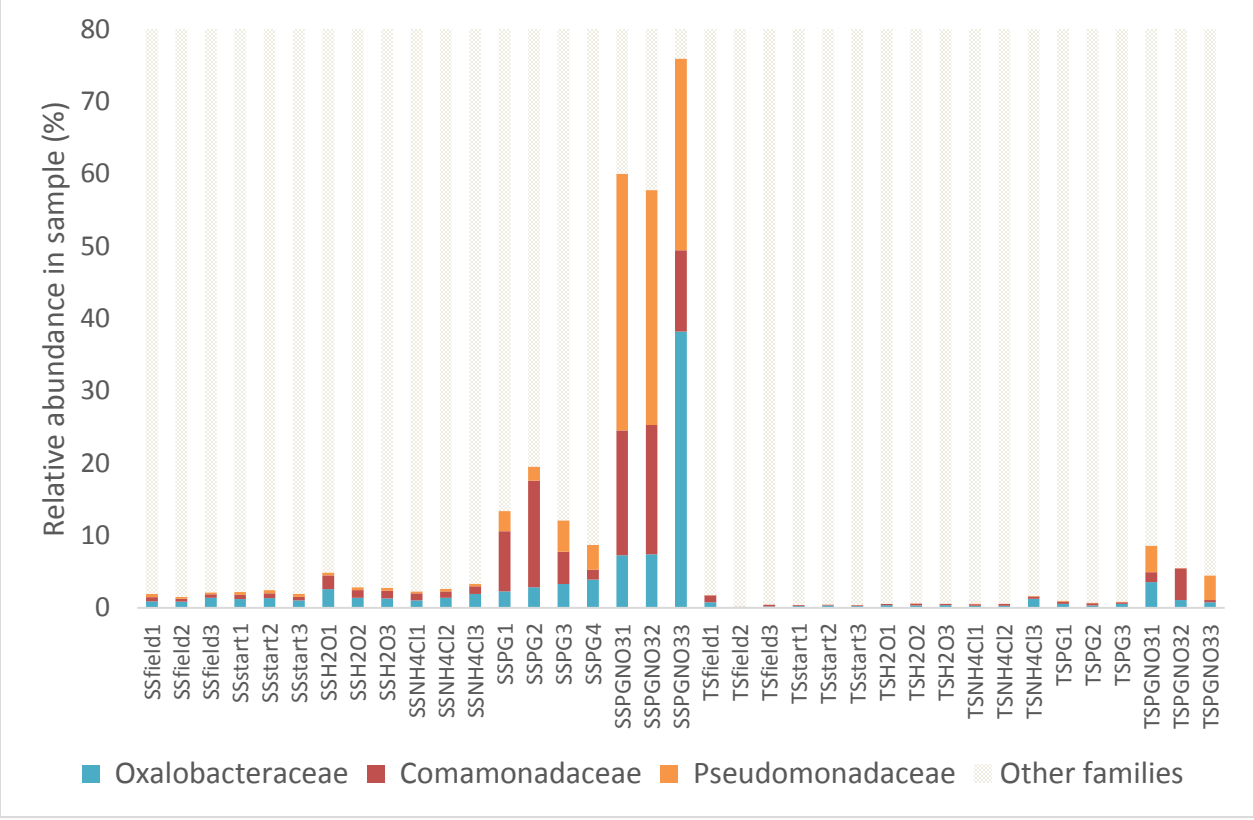

Figure 3.21: Relative abundance of the families *Comamonadaceae* (class *Betaproteobacteria*), *Oxalobacteraceae* (class *Betaproteobacteria*) and *Pseudomonadaceae* (class *Gammaproteobacteria*).

3.5.3 Diversity

Two diversity indices were calculated to provide information about rarity and commonness of species in the various samples. A diversity index is a mathematical measure of species diversity in a given community. Species diversity is superior to species richness (i.e., the number of species present) when evaluating microbial community structure, as it takes the relative abundances of different species into account (e.g. Simpson index 1-D; Simpson (1949)). In communities dominated by a few species, the diversity is low, whereas in communities with a more even relative abundance of species, even if the number of different species would be the same, diversity is high.

The Simpson index (1-D) ranges from 0 to 1, where 1 represents perfect evenness. From Figure 3.22, it can be seen that the diversity and evenness for all treatments was high, with Simpson values ranging from 0.97-0.99, with the exception of the PG+NO3 treatment in subsoil, which ranged from 0.81 to 0.89. Comparing with the chao1 values of richness (Figure 3.23), the two native samples, especially the one from the subsoil ("SSfield") had a species richness similar to that of SS-PGNO3 treatment. However when comparing the two indices, it can be assumed that the SS-PGNO3 community was more skewed towards a few dominant species than the native sample. This aligns well with the observations of a large increase in relative abundance of *Oxalobacteraceae, Comamonadaceae* and *Pseudomonadaceae* (Figure 3.21) in this treatment.

The larger species richness in treated samples than in the native soils might be caused by contamination and growth of species from the laboratory environment, as the experiment was not performed under strictly sterile conditions. However, all taxa dominating after the incubation had respective representatives in the native soils, so that it is unlikely that the observed change in community composition was due to contamination. Individual for each sample are listed in Appendix 4, Table A.5.

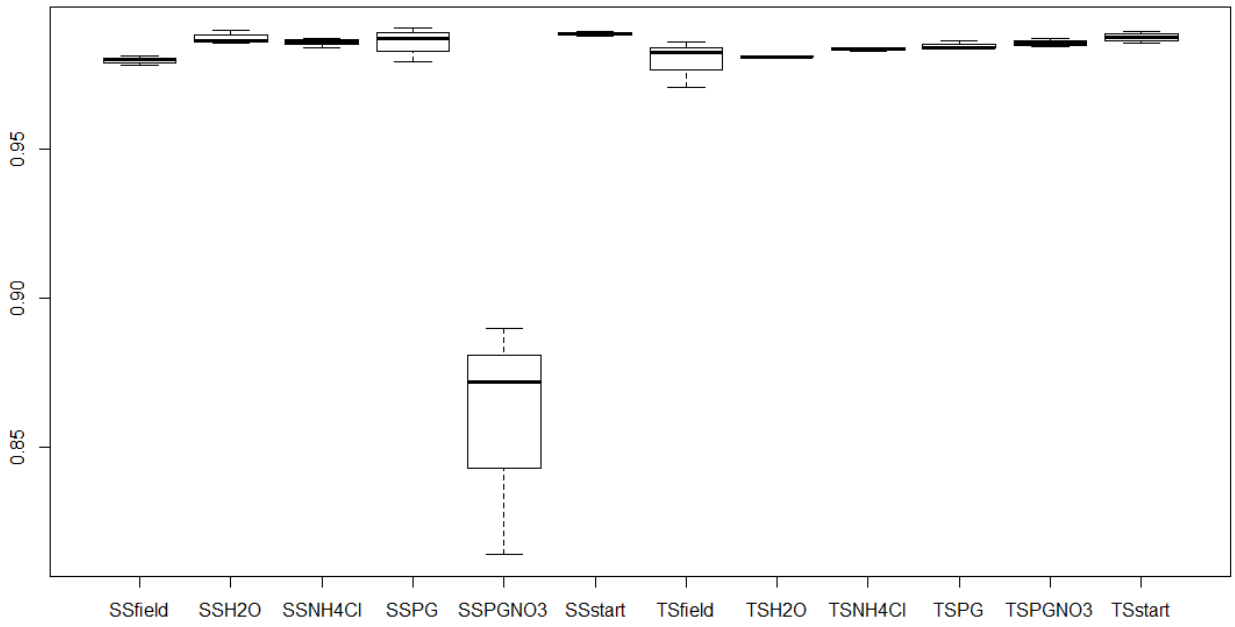

Figure 3.22: Alpha diversity of the samples, represented by the Simpson index (1-D), which also accounts for evenness in the samples. The black line of the box plot shows the median of the samples for each treatment (n=3, and n=4 for SSPG), the vertical line shows the distribution of the data, and the end horizontal lines shows the minimum and maximum values of the sample set. Indices were calculated from rarefied data.

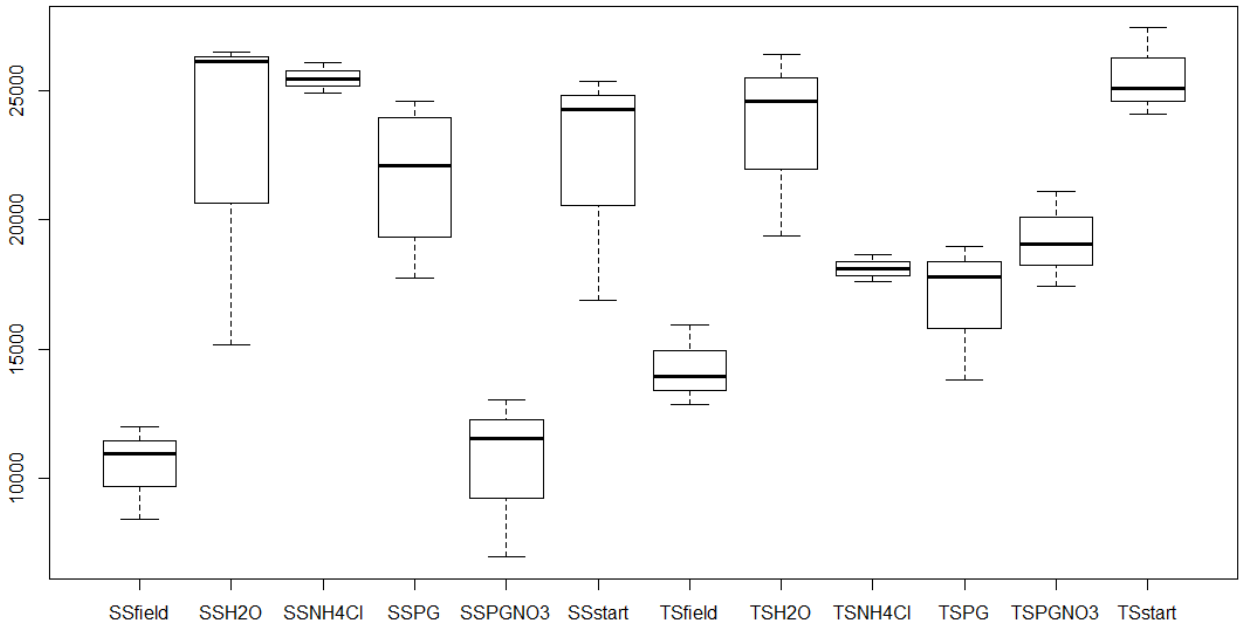

Figure 3.23: Extrapolated richness of the samples, given as Chao1 index. The black line of the box plot shows the median of the samples for each treatment (n=3, and n=4 for SSPG), the vertical line shows the

distribution of the data, and the end horizontal lines shows the minimum and maximum values of the sample set. The indices were calculated from rarefied data.

Comparing the *chao1* index with the amount of observed OTUs after rarefaction (Table A.5, not plotted), the same pattern by treatment was followed. This suggest that there were similar amounts of rare species in all samples so that the chao1 index mirrors the sampled richness using extrapolated values.

To evaluate differences in community structure, a 2D NMDS-plot was constructed, based on the distribution of OTUs in the samples after rarefaction (Figure 3.24). The clustering revealed a clear difference between the two soil types along MDS 1. In addition, "field" samples were separated from incubated samples by MDS2. The most pronounced difference in community structure was seen in the PG+NO3 treatment in the subsoil, which clustered far away from other subsoil samples along both MDS 1 and 2.

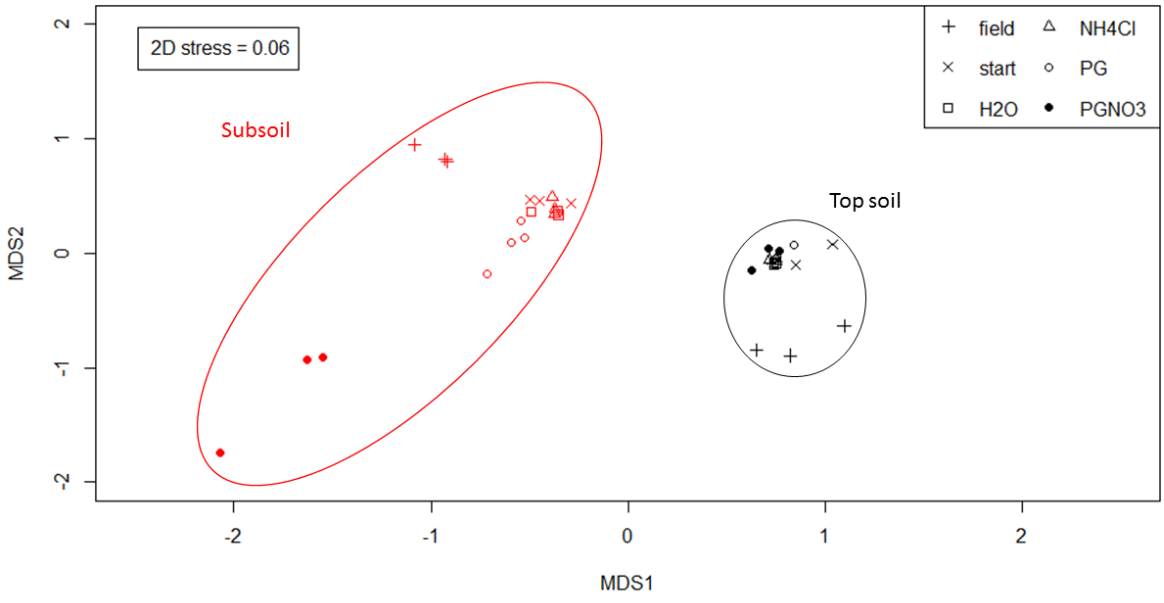

Figure 3.24: NMDS-plot in two dimensions, based on Bray-Curtis distances of OTUs in the dataset after rarefaction. Subsoil samples in red, and top soil samples in black.

To further visualize differences in community structure, a dendrogram showing the branching of the samples was constructed using the same Bray-Curtis distances as for the NMDS plot. Figure

3.25 show that at 50% similarity, three distinct branches form. The subsoil samples amended with PG and nitrate (SSPGNO3) are placed on a separate branch, while the rest of the subsoil and the topsoil samples are placed on two individual branches each.

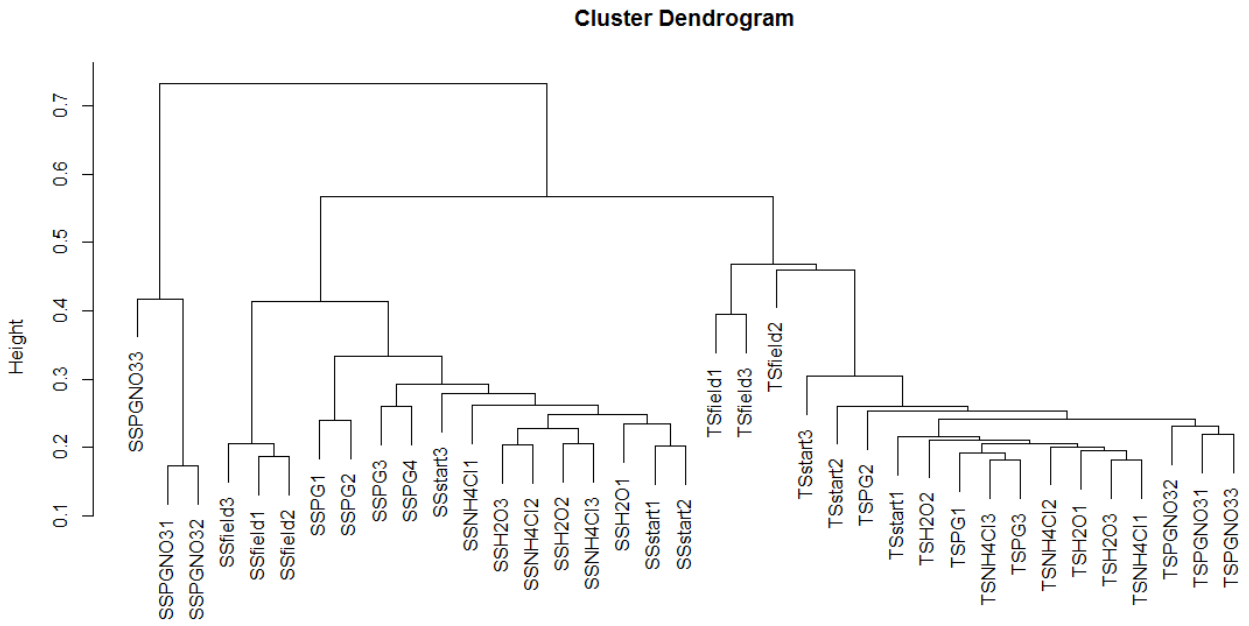

Figure 3.25: Dendrogram showing clustering of the samples based on Bray-Curtis distances of the OTU composition of each sample. At 50% similarity, three distinct clusters are forming, one for the PG and NO_3^- treated subsoils, one for the rest of the subsoils and one including all the top soil samples.

4. DISCUSSION

4.1 Metabolic activities

Ex situ incubation of sieved soil is one of several methods commonly employed to study metabolic activity in soils, and combined with high-resolution subsampling techniques, it can give a good picture of actual and/or inducible microbial activities in a small subsample of a soil taken from the field. One of the advantages of bottle experiments over *in situ* studies is the possibility to manipulate conditions and control factors that are difficult to control in field experiments, while at the same time holding other parameters constant (e.g. temperature, soil moisture, soil structure). In

the present study, batch incubations, i.e. incubation of soil in closed bottles, were employed to study the effect of PG and NO_3^- on respiration rates, kinetics and prokaryotic community structure. In the first preliminary experiment (ch. 2.8), a well-tested standard method was used, which has a small, but constant and reproducible leak of O_2 and N_2 that can be corrected for, thus allowing for quantification of denitrification rates (Molstad *et al.* 2016).

To allow for simultaneous sub-sampling of soil pore water, this system was modified by equipping the bottles with microrhizons which were protruded through the butyl septum. Despite preliminary successful tests, this system turned out to suffer from non-reproducible leaks, resulting in variable O_2 influx into the initially anoxic bottles in the main experiment, so that no strictly anoxic conditions could be obtained. Accordingly, a variable part of the observed PG-degradation was driven by oxic respiration (Figure 3.13), which in turn depended on O_2 influx (Figure 3.11). Oxidation of PG with O_2 as an electron acceptor is the by far most efficient way of PG degradation, as could be seen from comparing CO_2 production rates in PG amended soil under oxic and anoxic conditions in experiment 1 (Ch. 3.2). Anoxic CO_2 production in non-amended subsoil reached only ~20% of the CO_2 production obtained in oxically incubated soils (Figure 3.3). When amended with PG, this share decreased further to ~15%, revealing the limited metabolic potential of the subsoil for anoxic PG degradation. Nitrogen addition increased respiration after some lag phase both under oxic and anoxic conditions (Figure 3.2Figure 3.4), illustrating that the metabolic potential of the subsoil is strongly N limited.

The impact of oxygen on Fe/Mn dynamics was more difficult to assess, as the kinetics of Fe(II)/Mn(II) release were more variable. In the main experiment, the initially He-washed soil was incubated at ~80% WFPS, leaving only ~20% air-filled pores for O_2 diffusion into the soil. Since gaseous diffusion in water-filled pores is very slow, it is likely that "anoxic microsites" developed throughout the incubation, which acted as "hot spots" for Fe/Mn reduction. A part of the large variability in Fe(II)/Mn(II) dynamics across treatment replicates may thus be due to differences in the distribution of anoxic microsites resulting from uneven packing of soil or uneven distribution of organic matter.

4.2 The effect of propylene glycol on Mn^{2+}/Fe^{2+} release

The premise of the proposed research question, whether propylene glycol increases the amount of Mn^{2+}/Fe^{2+} released to soil water under anaerobic conditions, was to create anaerobic conditions. Even though this goal was not fully reached, Mn^{2+} and Fe^{2+} were detected in all treatments. A relatively low pH, between 4.4 - 4.6 (Table 3.1), combined with the high saturation level of the samples (~80 $\%WHC_{max}$) might have altered the effective redox potential to be more favourable towards iron reduction compared to the standard conditions described by the redox tower (Figure 0.2). The degradation of PG by Mn(IV) or Fe(III) consumes protons (16 and 32 mol H^+ per mol PG, respectively, Table 0.1) and for each unit decrease in pH, the redox potential of the Fe(III)/Fe(II) redox couple increases by ~59 mV per the Nernst equation (Levar et al. 2017).

To evaluate the effect of PG on Mn^{2+}/Fe^{2+} release, treatment replicates with similar O_2 conditions had to be compared. For the top soil, the six bottles with the lowest average rate of respired oxygen, had the highest rates of Mn^{2+} release (Figure 3.17). Of these, the four bottles with the highest Mn^{2+} release rate, were treated with PG and the bottle with the highest rate of Mn^{2+} release more than doubled that of the control sample incubated under comparable O_2 conditions (179 and 76 pmol g^{-1} h^{-1} for PG3 and H2O_1; Figure 3.17). Ammonium addition did not seem to have any significant effect. Among the four PG-treated samples with similar rates of O_2 respiration, the two amended with nitrate had slightly smaller rates of Mn^{2+} release, 92-108 and 136-179 pmol g^{-1} h^{-1}, respectively. Irrespective of O_2 respiration, when removing outliers (i.e. the smallest and largest metal release rate in each treatment), PG treated samples showed significantly larger Mn^{2+} and Fe^{2+} release than controls ($p=0.04$ for Mn^{2+} , $p=0.005$ for Fe^{2+} by Welch Two-Sample t-test).

For the subsoil, the sample with the highest rate of Mn^{2+} release was also the one with the lowest rate of respired O_2, and also for subsoil there was a significant increase in Mn^{2+} release by PG when outliers were removed ($p=0.02$). Interestingly, when comparing the two bottles with lowest rate of respired O_2 (Figure 3.17), PGNO3_3 released Mn^{2+} at a rate almost tenfold (24 pmol g^{-1} h^{-1}) than that of PG4 (2.6 pmol g^{-1} h^{-1}). The first Pilot expriment had shown that only NO_3^- amended subsoils showed growth under anaerobic conditions, and the CO_2 kinetic of PGNO3_3 (Figure 3.11) showed similarity to the results from pilot 1, indicating growth.

Ultimately, soil samples from the 0-1 m top layer showed a much larger potetial for Mn^{2+} and Fe^{2+} release than soils from below 1.5 m depth. Mn^{2+} release from untreated controls throughout the

incubation was in the range of 5-48 nmol g^{-1}, while PG treatments released 8-94 nmol g^{-1} (Fig. 3.16). Oxygen limited the release of Mn^{2+}, as suggested by the small rates of release in samples with large O_2 respiration (Figure 3.17). The release of Fe^{2+} also seemed to be limited by oxygen (Figure 3.17), but followed a less clear pattern. Mn^{2+} concentration levels measured in the top soil were only reached by one subsoil sample belonging to PG+NO_3 treatment (~15 nmol g^{-1}; Figure 3.15D). Both Mn^{2+} and Fe^{2+} in this sample increased towards the end of the incubation, probably owing N-dependent bacterial growth, similar to that documented in pilot experiment 1. In general, the much smaller potential of subsoil than top soil to release Mn^{2+}/Fe^{2+} can be assumed to be due to the low abundance of bacteria in subsoil. Biró *et al.* (2014) showed decreasing cell abundances by two orders of magnitude from surface to 1.5 m subsurface in soil from Oslo airport, by counting aerobic and anaerobic colony forming units and measuring a number of different enzyme activities. The cell enumeration performed in the present study suggested that there resided at least double as many cells in the top- than in the subsoil (Table 3.2).

4.3 Microbial community structure

Change in diversity

The combined input of PG and NH_4NO_3 to subsoil decreased microbial diversity in the subsoil. This is often observed in hydrocarbon-polluted soils (Madigan et al. 2014), as degraders are able to grow, and increase in relative abundance. The diversity in the top soil was not affected by PG according to the Simpson index (Figure 3.22). More diverse soil communities are considered to be more resilient to inputs of pollution or nutrients (Giller *et al.* 1997), but according to the Simpson index, the top soil was initially not more diverse than the subsoil.

The calculation of the Simpson index also includes evenness, so even if a sample has fewer species, the value increases if their relative abundances are similar. Other indices try to estimate the total richness of the community (often called “extrapolated richness”), giving more weight to the number of rare species sampled. The Chao1 index (Chao 1987; Chiu *et al.* 2014) has this intention, thus the value of the index is usually greater than the number of species actually sampled. According to

this index (Figure 3.23), the richness of top soil was reduced with treatments compared to the start soil.

When comparing the species richness between the samples (Figure 3.23), the native ("field") samples had less diversity than the "start" samples, while the only difference was transport, handling and storage. Since the transport, handling and storage was not performed under sterile conditions, the increased richness of the starting soil may be because the prokaryotes present in the soil responded to these storing conditions. Investigating this in more detail, it was found that about 5% of the total sample set consisted of OTUs that were not observed in the native samples. However, the ten most abundant OTUs were all found to be present in the native samples, and all of the most abundant phyla were represented (Figure 3.19), so this did not seem to interfere with the observed changes in community composition by treatment.

Community response to treatments

The largest response observed in the community composition was the response in subsoil to combined propylene glycol and nitrate addition. In the Cluster Dendrogram (Figure 3.25), all samples from this treatment formed a separate branch showing more than 50% similarity.

Statistical testing (PerMANOVA) showed a significant difference between the soil types ($p=0.001$), and statistically significant change in OTU composition by the PG+NH_4NO_3 treatment ($p=0.002$). Since the subsoil nitrate treatment was clearly distinguished from the other samples, this was excluded when testing for significance further. The native samples were found to differ significantly from the other controls ($p=0.006$, SS, $p=0.007$, TS), so these were also excluded from further significance testing. In both the top- and subsoil, PG treated samples had a significantly changed OTU composition compared to the controls ($p=0.002$).

The most pronounced difference in the community composition was found in the subsoil, in which a large increase in the relative abundance of *Proteobacteria* occurred, increasing from 27% in the control sample with the largest relative abundance to 81% in one of the PGNO3 samples (Figure 3.19). *Proteobacteria* are often found as dominating groups in hydrocarbon contaminated soils (Madigan et al. 2014; Saul et al. 2005; Viñas et al. 2005), as it is a metabolically diverse phylum which includes many heterotrophs. The three *Proteobacteria* families found to represent up to 76% of the relative abundance in PG treated soils, *Oxalobacteraceae, Comamonadaceae* and

Pseudomonadaceae (Figure 3.21), all represent aerobic and facultative organotrophs that likely degrade PG or its fermentation products.

The *Oxalobacteraceae* represent mostly aerobic/microaerophilic species, with a few facultative aerobic and one obligate anaerobe genus (Baldani *et al.* 2014).

The *Comamonadaceae* is a highly metabolically diverse family, including aerobic organotrophs, anaerobic denitrifiers, Fe^{3+}-reducing bacteria, hydrogen oxidizers, photoautotrophic and photoheterotrophic bacteria as well as fermentative bacteria (Willems 2014). The most abundant OTU from this family was assigned as *Rhodoferax sp.* The *Rhodoferax* genus include three species, two facultatively anaerobic photoheterotrophs, while one, *Rhodoferax ferrireducens*, is classified as a facultatively anaerobe, using oxygen, nitrate, Fe(III), Mn(IV) or fumarate as electron acceptors while oxidizing fermentation products such as acetate and propionate and is capable of growth at temperatures as low as 4 ºC (Finneran *et al*. 2003).

The *Pseudomonadaceae* contain chemoorganotrophs that carry out respiratory metabolisms. All species can grow as aerobes, but some are also capable of anaerobic respiration with nitrate as a terminal electron acceptor. Reduction of Fe(III) has also been observed for some species within the Pseudomonadaceae (Naganuma *et al*. 2006). Many of the aerobic PG degraders isolated from Oslo airport, Gardermoen, were from the genera Pseudomonas (Toscano *et al.* 2013).

The largest change by treatment was observed when PG and NH_4NO_3 were added together. Even though nitrate was added only in a small quantity, this seems to have been enough for the aforementioned bacterial families to grow. In an anaerobic slurry of a soil sampled close to the same location as in the present study (Greco *et al.* 2012), linear PG degradation kinetics (zero order) was measured suggesting maintenance metabolism. When supplied with sufficient KNO_3 to degrade the amount of PG present, the rate of degradation increased, but no sign of growth was observed. The same result was found for an aerobic slurry. With the amendment of ammonium chloride, PG degradation changed to first order kinetics, recognized by an initial lag phase, then a fast exponential degradation or "growth" phase until PG was depleted. When comparing the CO_2 accumulation kinetics in Figure 3.2 (aerobic, first pilot), Figure 3.4 (anaerobic, first pilot) and Figure 3.11 (main experiment), several of these CO_2 accumulation curves display zero order kinetics when only PG is added, but first order kinetics for NO_3^- treatments, implying growth.

The growth kinetics displayed in nitrate-amended subsoil in this study indicated nitrate assimilation, which could be of either ammonium or nitrate, since both were supplied. The supply of ammonium chloride without PG was tested, but did not lead to significant differences in growth from untreated controls (Figure 3.11). This suggests that the subsoil is both carbon and nitrogen limited. In the study by Greco *et al.* (2012), nitrate was found to increase the rate of anaerobic PG degradation. The influx of oxygen in the main experiment, which gives more energy than nitrate as a terminal electron acceptor increased PG degradation yields across all treatments in both soil types (Figure 3.13). However, when comparing four top soil samples that were exposed to similar rates of oxygen, the PG degradation yields were larger for two nitrate amended samples (13-14%), compared to two PG amendment alone (5-6%). Comparing two treated subsoil samples exposed to similar rates of oxygen also display larger PG degradation yields in the presence of nitrate (11 and 3% for NO3 and PG, respectively). This suggests that even small inputs of nitrate can increase PG degradation in the unsaturated zone in the depths investigated.

PG or PG and nitrate addition altered the top soil community composition less than that of the subsoil. Statistical testing showed significant differences with addition of PG in number and distribution of OTUs. The relative abundance of the previously mentioned families (Figure 3.21) also increased in PG treated topsoil, but by far not as much as in the subsoil.

Euryarchaeota and possible methanogenesis

In In the subsoil, the archaeal phylum *Euryarchaeota* decreased from a relative abundance of 13-15% in the native (“field”) samples compared to the rest of the samples ranging from 0.37 to 3.6%. This phylum includes the *methanogens,* i.e. archaea that are obligate anaerobes (Madigan *et al.* 2014). Upon sampling the subsoil, it was exposed to air, which is a probable explanation for the decrease in reolative abundance of this phylum in all treated samples. All *Euryachaeota* represented in the sample set belonged to the class *Thermoplasmata* and order *Methanomassiliicoccales* (Iino *et al.* 2013). A few were classified to family, and belonged to the family *Methanomassiliicoccaceae*. Members of this family are described as strictly anaerobic and methanol-reducing hydrogenotrophic methanogens.

Toscano *et al.* (2014) performed soil slurry experiments under anaerobic conditions with a soil sample from 4.5 meter below the surface, close to the groundwater table of Oslo airport. This

experiment showed a lag phase of 200 hours before PG started being degraded and propionic acid formed. The production of priopionic acid did not match fermentation stoichiometrically (Table 0.1) and Mn^{2+} release accounted for only 1% of the electron acceptor demand of observed PG degradation. The authors therefore hypothesized that metabolic pathways other than fermentation to propionate and Mn reduction may have been involved in PG degradation, such as acetoclastic methanogenesis. A similar conclusion was drawn by the same authors from a study on soil samples from the Moreppen trench (Greco *et al.* 2012). However, which specific depth the Moreppen soil was taken from (labelled "refill") was not specified, and it was probably a mixture of the top 1.5 m. When handling the deep airport soil (Toscano *et al.* 2014), care was taken to avoid oxygen during storage, so the obligate anaerobes, for example native methanogens, should have survived. As mentioned, 13-15% relative abundance of *Euryarchaeota* were found in the native subsoil samples in this study, and it is likely that deeper parts of the soil, where even less O_2 is available, might have similar abundances or larger abundances of methanogens, so methanogenesis is a possible pathway that could have reduced PG or its fermentation products (propionic acid, n-propanol and acetate: Table 0.1) to methane and CO_2, with H_2 becoming available as an electron donor through fermentation by other bacteria.

The care taken to avoid O_2 was not the case for the Moreppen subsoil used by Greco *et al.* (2012), as it was taken from an excavation and further handling and storage details were not provided. Still, the natural abundance of methanogens may have survived to a larger degree than what was found in this study. If, however, the soil was exposed to air in a similar manner as in this study, the methanogens might not have survived and another explanation is needed to explain the observed respiration kinetics. Only minor amounts of methane was produced from the experiments of this study (Figure 3.5, maximum 0.06 nmol g-1 in TS, approximate rate 0.17 pmol h^{-1} g^{-1}), so it cannot explain degradation of PG.

Toscano *et al.* (2014) did not find any release of Fe^{2+}, and this was not mentioned by Greco *et al.* (2012). However, Fe^{2+} is very oxygen sensitive, and the procedure used for sample preparation of water samples analysed for reduced metal species included centrifugation for 15 minutes and filtration, so it is likely that Fe^{2+} could have oxidized during such a sample preparation. Under anaerobic conditions, Fe^{2+} is reported to be rapidly oxidized by Mn(IV) oxide (stoichiometry 2:1) at neutral pH (Myers & Nealson 1988b; Lovley & Phillips 1988a). When Fe(III) was added to the

media of Fe/Mn reducing organism *Shewanella putrefaciens* together with Mn(IV), no Fe^{2+} could be measured, while the concentration of Mn^{2+} increased when compared to Mn(IV) alone. This makes "re-reduction" of the iron oxides possible, and direct analysis of reduced Fe^{2+} unreliable. If sampling and filtering is performed with minimal contact with oxygen, like by using saturated microrhizons, the results are more reliable but probably still underestimated. Thus, reduction of Fe/Mn is likely a more important respiration pathway than what was concluded by Toscano *et al.* (2014).

Analysing microbial community composition using high-throughput sequencing, comprises many stages at which errors may occur. Evaluating the composition of a soil system from a 0.5 g subsample obviously does not give the complete richness of this system, however by tools such as rarefaction (Figure A.4), the sequencing depth can be evaluated, and from richness indices such as Chao1, the richness can be estimated and compared between samples. With this sampling design we are not able to capture all the specific prokaryotes present in the soil, however this is less important, as changes in the community structure still can be assessed from smaller subsamples. Amplicon-based community analysis also requires the use of polymerase chain reaction and selective primers for DNA amplification, which also might cause errors and biases (Wintzingerode *et al.* 1997). However, since all samples were processed the same way, the amount of errors and biases should be equal for all samples, thus the change in the community structure can be assumed to essentially be an effect of treatment and incubation conditions.

When sampling DNA from soil, it has been shown that large amounts of "relic DNA", from organisms no longer active may also be extracted (Carini *et al.* 2016). This can obscure treatment effects and amplify diversity estimates. Taking this into account, only the largest changes in relative abundance should be considered as treatment effects.

4.4 Summary and Conclusion

Propylene glycol (PG) addition to a sandy soil representative for the Gardermoen soil system significantly increased the release of Mn^{2+} and Fe^{2+} throughout 26 days of incubation under variable microaerophilic conditions. Mn^{2+} release without amendments was by a factor of 100-1000 larger in soil from 0-1 m depth (48 µmol kg^{-1}) than in soil sampled below 1.5 m (0.02 µmol

kg^{-1}), suggesting that Gardermoen soils hold a high natural potential for Mn^{2+} release in the upper 100 cm. Addition of PG to topsoil increased Mn^{2+} release to a maximum of 94 µmol kg^{-1} throughout 24 days.

Estimated numbers of bacterial cells in the top soil doubled those in the subsoil, and the taxonomic composition of the microbial communities differed greatly between top and subsoil, probably explaining smaller Mn^{2+} release rates in the subsoil by differences in microbial abundance and functional diversity. A small addition of NH_4NO_3 together with PG to the subsoil promoted community change by triggering growth of metabolically diverse *Comamonadaceae*, *Oxalobacteraceae* and *Pseudomonadaceae,* and the release of Mn^{2+} from the subsoil to concentrations comparable to those in unamended top soil (16 µmol kg^{-1}) appeared to be linked to this community shift. In comparison, community change in the topsoil and in subsoil incubated with PG alone, was negligible.

Fe^{2+} release from the subsoil was variable and obviously influenced by re-oxidation with O_2 leaking into the bottles, while in the topsoil, which likely respired O_2 more efficiently, Fe^{2+} accumulated more steadily. Maximum Fe^{2+} accumulation in unamended top soil roughly doubled that in subsoil, but remained at low concentration levels in both soils (0.2 - 0.7 µmol kg^{-1} soil). PG addition (with or without additional NH_4NO_3) resulted in a tenfold increase of Fe^{2+} in the top soil with PG amendment (~2.3 µmol kg^{-1}).

In summary, Fe^{2+}/Mn^{2+} release from the Gardermoen soil system seems to be dominated by upper soil layers. The metabolic activity in soil below 1.5 m depth, particularly under strictly anoxic conditions as tested in experiment 1, appears to be too small to generate enough electrons for fuelling significant Fe^{2+}/Mn^{2+} release. Leaching of de-icing fluids to lower layers therefore poses little risk for Mn^{2+} release from deeper soil, suggesting that the reported contamination of ground water with Mn^{2+} stems from anoxic metabolism in the top layers during anoxic spells such as during snowmelt or after heavy rainfalls.

Addition of NO_3^- as an alternative electron acceptor has been discussed and tested for mitigating Fe^{2+}/Mn^{2+} release in Gardermoen soils. Unlike in soil slurry experiments with well-distributed NO_3^- in excess of what is necessary for complete PG degradation, a field experiment with NO_3^- addition could not confirm a mitigation effect but increased Fe^{2+} and Mn^{2+} release was found. This

thesis confirms that nitrate, when added in low concentrations, does not efficiently lower Fe^{2+} and Mn^{2+} release in the top 1 m of Gardermoen soil and poses a risk to trigger Fe^{2+} and Mn^{2+} release in the subsoil through inducing functional community shift.

Oslo airport is currently testing an aeration scheme for soils being affected by de-icing chemicals. This is very positive, as good aeration seems to be crucial to promote PG degradation and avoid accumulation of Fe^{2+} and Mn^{2+} in the ground water. In this study, aerobic degradation of PG outnumbered anaerobic degradation by far, irrespective of soil depth, suggesting that soil aeration can lead to a win-win situation, i.e. speeding up PG degradation while preventing Fe^{2+} and Mn^{2+} release.

Aeration could make the current fertilization scheme using $Ca(NO_3)_2$ redundant, but might be continued to avoid nitrogen limitation in the upper part of the soil. In areas where the ground water has public interest as a potential source of drinking water, fertilization should be avoided, especially during seasons with high water transport to the lower parts of the soil, such as during spring conditions.

In conclusion, as nitrate promotes growth of metabolically versatile bacteria in deeper soil layers, the effect as an alternative electron acceptor for Fe^{2+} and Mn^{2+} requires a large and continuous supply of nitrate to the subsoil, which is not desirable in terms of ground water protection. Aeration appears to be the better alternative.

REFERENCES

Appril, A. et al., 2015. Minor revision to V4 region SSU rRNA 806R gene primer greatly increases detection of SAR11 bacterioplankton. *Aquatic Microbial Ecology*, 75, pp.129–137. Available at: https://darchive.mblwhoilibrary.org/bitstream/handle/1912/7426/a075p129.pdf?sequence=1&isAllowed=y [Accessed May 11, 2017].

Arp, D.J. & Stein, L.Y., 2003. Metabolism of Inorganic N Compounds by Ammonia-Oxidizing Bacteria. *Critical Reviews in Biochemistry and Molecular Biology*, 38(6), pp.471–495. Available at:

http://www.tandfonline.com/doi/full/10.1080/10409230390267446 [Accessed May 23, 2017].

Avinor, 2016. *BR29 Fe og Mn - Unpublished monitoring data*, Nannestad, Norway.

Avinor, 2000. *Oslo airport Annual Report 2000*, Available at: https://avinor.no/globalassets/_oslo-lufthavn/om-oslo-lufthavn/om-oss/rapporter/en/annual/annual_report_2000_tcm181-73687.pdf [Accessed May 21, 2017].

Baldani, J.I. et al., 2014. The Family Oxalobacteraceae. In E. Rosenberg, ed. *The Prokaryotes - Alphaproteobacteria and Betaproteobacteria*. Berlin: Springer-Verlag, pp. 919–972. Available at: http://download.springer.com/static/pdf/815/chp%253A10.1007%252F978-3-642-30197-1_291.pdf?originUrl=http%253A%252F%252Flink.springer.com%252Freferenceworkentry%252F10.1007%252F978-3-642-30197-1_291&token2=exp=1496171726~acl=%252Fstatic%252Fpdf%252F815%252Fchp%2525253A10.1007%252 [Accessed May 30, 2017].

Biró, B. et al., 2014. Vertical and horizontal distributions of microbial abundances and enzymatic activities in propylene-glycol-affected soils. *Environmental Science and Pollution Research*, 21(15), pp.9095–9108. Available at: http://link.springer.com/10.1007/s11356-014-2686-1 [Accessed June 1, 2017].

Bushnell, B., 2017. BBTools. *DOE Joint Genome Institute*. Available at: http://jgi.doe.gov/data-and-tools/bbtools/ [Accessed May 10, 2017].

Caporaso, J. et al., 2010. QIIME allows analysis of high-throughput community sequencing data. *Nature Methods*, 7(5), pp.335–336. Available at: http://www.nature.com/nmeth/journal/v7/n5/full/nmeth.f.303.html [Accessed May 10, 2017].

Caporaso, J.G. et al., 2011. Global patterns of 16S rRNA diversity at a depth of millions of sequences per sample. *Proceedings of the National Academy of Sciences of the United States of America*, (Supplement 1), pp.4516–22. Available at: http://www.ncbi.nlm.nih.gov/pubmed/20534432 [Accessed June 1, 2017].

Carini, P. et al., 2016. Relic DNA is abundant in soil and obscures estimates of soil microbial diversity. Available at: http://fiererlab.org/wp-content/uploads/2014/09/Carini_etal_NatMicro_2016.pdf [Accessed May 30, 2017].

Cerniglia, C.E., 1984. Microbial Metabolism of Polycyclic Aromatic Hydrocarbons. In pp. 31–71. Available at: http://linkinghub.elsevier.com/retrieve/pii/S0065216408700522 [Accessed May 23, 2017].

Chao, A., 1987. Estimating the population size for capture-recapture data with unequal catchability. *Biometrics*. Available at: http://www.jstor.org/stable/2531532 [Accessed May 18, 2017].

Child, J. & Willetts, A., 1978. Microbial metabolism of aliphatic glycols bacterial metabolism of ethylene

glycol. *Biochimica et Biophysica Acta (BBA) - General Subjects*, 538(2), pp.316–327. Available at: http://linkinghub.elsevier.com/retrieve/pii/0304416578903598 [Accessed May 23, 2017].

Chiu, C. et al., 2014. An improved nonparametric lower bound of species richness via a modified good–turing frequency formula. *Biometrics*. Available at: http://onlinelibrary.wiley.com/doi/10.1111/biom.12200/full [Accessed May 18, 2017].

DeSantis, T.Z. et al., 2006. Greengenes, a chimera-checked 16S rRNA gene database and workbench compatible with ARB. *Applied and environmental microbiology*, 72(7), pp.5069–72. Available at: http://www.ncbi.nlm.nih.gov/pubmed/16820507 [Accessed May 10, 2017].

Doane, T.A. & Horwáth, W.R., 2003. Spectrophotometric Determination of Nitrate with a Single Reagent. *Analytical Letters*, 36(12), pp.2713–2722. Available at: http://www.tandfonline.com/doi/abs/10.1081/AL-120024647 [Accessed November 8, 2016].

DOW, 2008. Engineering and Operating Guide for DOWFROST and DOWFROST HD Inhibited Propylene Glycol-based Heat Transfer Fluids. Available at: http://msdssearch.dow.com/PublishedLiteratureDOWCOM/dh_010e/0901b8038010e417.pdf?filepath=heattrans/pdfs/noreg/180-01286.pdf&fromPage=GetDoc [Accessed May 26, 2017].

Ferguson, L. et al., 2008. Formulations for aircraft and airfield deicing and anti-icing: aquatic toxicity and biochemical oxygen demand. *ACRP, Transportation Research Board*. Available at: http://www.trb.org/Publications/Blurbs/155765.aspx [Accessed September 15, 2016].

Finneran, K.T., Johnsen, C. V & Lovley, D.R., 2003. Rhodoferax ferrireducens sp. nov., a psychrotolerant, facultatively anaerobic bacterium that oxidizes acetate with the reduction of Fe(III). *International Journal of Systematic and Evolutionary Microbiology*, 53, pp.669–673. Available at: http://www.geobacter.org/publication-files/12807184.pdf [Accessed May 30, 2017].

Francis, C.A., Beman, J.M. & Kuypers, M.M.M., 2007. New processes and players in the nitrogen cycle: the microbial ecology of anaerobic and archaeal ammonia oxidation. *The ISME Journal*, 1(1), pp.19–27. Available at: http://www.nature.com/doifinder/10.1038/ismej.2007.8 [Accessed May 23, 2017].

French, H. et al., 1994. A lysimeter trench for reactive pollutant transport studies. *Future Groundwater Resources at Risk*, 222, pp.131–138. Available at: http://hydrologie.org/redbooks/a222/iahs_222_0131.pdf [Accessed November 8, 2016].

French, H.., Van der Zee, S.E.A.T.. & Leijnse, A., 2001. Transport and degradation of propyleneglycol and potassium acetate in the unsaturated zone. *Journal of Contaminant Hydrology*, 49(1), pp.23–48. Available at: http://www.sciencedirect.com/science/article/pii/S016977220000187X [Accessed May 8, 2017].

French, H. & Binley, A., 2004. Snowmelt infiltration: monitoring temporal and spatial variability using time-lapse electrical resistivity. *Journal of Hydrology*, 297(1), pp.174–186. Available at:

http://www.sciencedirect.com/science/article/pii/S0022169404002082 [Accessed May 29, 2017].

French, H.K. et al., 1996. Melt water from snow affected by potassium acetate and 1,2 propane diol. *Proceedings to the Jens-Olaf Englund Seminar on Protection of groundwater resources against contaminants*, pp.289–300. Available at: file:///C:/Users/Gudny/Downloads/20170522151024.pdf [Accessed May 22, 2017].

French, H.K. et al., 2002. Monitoring snowmelt induced unsaturated flow and transport using electrical resistivity tomography. *Journal of Hydrology*, 267, pp.273–284.

French, H.K., 1999. *Transport and degradation of deicing chemicals in a heterogenous unsaturated soil*. Norges Landbrukshøgskole. Available at: http://agris.fao.org/agris-search/search.do?recordID=NO2000000215 [Accessed November 8, 2016].

Giller, K.E. et al., 1997. Agricultural intensification, soil biodiversity and agroecosystem function. *Applied Soil Ecology*, 6(1), pp.3–16. Available at: http://linkinghub.elsevier.com/retrieve/pii/S0929139396001497 [Accessed May 31, 2017].

Greco, G. et al., 2012. Evaluation of remediation techniques Part 1: Gardermoen site Deliverable D5.1. Available at: http://www.bioforsk.no/ikbViewer/Content/98040/SoilCAM deliverable_D5.1_Part1.pdf [Accessed April 24, 2017].

Hartmanis, M.G.N. & Stadtman, T.C., 1986. Diol Metabolism and Diol Dehydratase in Clostridium glycolicum. *Archives of Biochemistry and Biophysics*, 245(1), pp.144–152. Available at: http://ac.els-cdn.com/0003986186901980/1-s2.0-0003986186901980-main.pdf?_tid=c32829d8-42e6-11e7-b077-00000aab0f6b&acdnat=1495894634_dc565ad688f0a20940ccd28d6feb9c53 [Accessed May 27, 2017].

Hernandez, M.E., Kappler, A. & Newman, D.K., 2004. Phenazines and other redox-active antibiotics promote microbial mineral reduction. *Applied and environmental microbiology*, 70(2), pp.921–8. Available at: http://www.ncbi.nlm.nih.gov/pubmed/14766572 [Accessed May 28, 2017].

Hinks, J., Zhou, M. & Dolfing, J., 2017. Microbial Electron Transport in the Deep Subsurface. In C. Chenard & F. M. Lauro, eds. *Microbial Ecology of Extreme Environments*. Cham: Springer International Publishing, pp. 81–102. Available at: http://link.springer.com/10.1007/978-3-319-51686-8_4 [Accessed May 24, 2017].

Hothorn, T., Bretz, F. & Westfall, P., 2008. Simultaneous Inference in General Parametric Models. *Biometrical Journal*, 50(3), pp.346–363. Available at: http://www.ncbi.nlm.nih.gov/pubmed/18481363 [Accessed May 11, 2017].

Iino, T. et al., 2013. Candidatus Methanogranum caenicola: a Novel Methanogen from the Anaerobic Digested Sludge, and Proposal of Methanomassiliicoccaceae fam. nov. and Methanomassiliicoccales ord. nov., for a Methanogenic Lineage of the Class Thermoplasmata. *Microbes and Environments*,

28(2), pp.244–250. Available at: http://jlc.jst.go.jp/DN/JST.JSTAGE/jsme2/ME12189?lang=en&from=CrossRef&type=abstract [Accessed May 30, 2017].

Jaesche, P., Totsche, K.U. & Kögel-Knabner, I., 2006. Transport and anaerobic biodegradation of propylene glycol in gravel-rich soil materials. *Journal of contaminant hydrology*, 85(3–4), pp.271–86. Available at: http://www.ncbi.nlm.nih.gov/pubmed/16563561 [Accessed April 11, 2016].

Jansson, S.L., Hallam, M.J. & Bartholomew, W. V., 1955. Preferential utilization of ammonium over nitrate by micro-organisms in the decomposition of oat straw. *Plant and Soil*, 6(4), pp.382–390. Available at: http://link.springer.com/10.1007/BF01343647 [Accessed May 25, 2017].

Johnsen, A.R., Wick, L.Y. & Harms, H., 2005. Principles of microbial PAH-degradation in soil. *Environmental Pollution*, 133(1), pp.71–84. Available at: http://www.sciencedirect.com/science/article/pii/S0269749104001587 [Accessed May 23, 2017].

Jørgensen, P. & Østmo, S.R., 1990. Hydrogeology in the Romerike area, southern Norway. *Norges Geologiske Undersøkelse Bulletin*, 418, pp.19–26.

Keeney, D. & Nelson, D., 1982. Nitrogen—inorganic forms A. L. Page, R. H. Miller, & D. R. Keeney, eds. *Methods of soil analysis. Part 2 - Chemical and Microbiological Properties*, pp.643–698. Available at: https://dl.sciencesocieties.org/publications/books/abstracts/agronomymonogra/methodsofsoilan2/643 [Accessed November 8, 2016].

Kitterød, N.-O., 2007. Focused flow in frozen ground increases contamination risk of ground water resources. *Frost in Ground*, 109. Available at: https://folk.uio.no/nilsotto/PUBL/Kitterod_frost_i_jord_2007.pdf [Accessed May 23, 2017].

Klecka, G.M., Carpenter, C.L. & Landenberger, B.D., 1993. Biodegradation of Aircraft Deicing Fluids in Soil at Low Temperatures. *Ecotoxicology and Environmental Safety*, 25(3), pp.280–295. Available at: http://linkinghub.elsevier.com/retrieve/pii/S0147651383710262 [Accessed May 26, 2017].

Kruskal, J.B., 1964. Nonmetric multidimensional scaling: A numerical method. *Psychometrika*, 29(2), pp.115–129. Available at: http://link.springer.com/10.1007/BF02289694 [Accessed May 11, 2017].

Levar, C.E. et al., 2017. Redox potential as a master variable controlling pathways of metal reduction by Geobacter sulfurreducens. *The ISME Journal*, 11(3), pp.741–752. Available at: http://www.nature.com/doifinder/10.1038/ismej.2016.146 [Accessed May 24, 2017].

Lide, D.., 2008. *Handbook of Chemistry and Physics* 88th ed., Boca Raton, FL: CRC Press, Taylor & Francis.

Lissner, H. et al., 2014. Degradation of deicing chemicals affects the natural redox system in airfield soils. *Environmental Science and Pollution Research*, 21(15), pp.9036–9053.

Lißner, H. et al., 2012. *Monitoring and characterisation of flow and transport in field-and laboratory experiments Deliverable D 2.4*, Available at: http://www.bioforsk.no/ikbViewer/Content/102071/Final report_D2.4.pdf [Accessed November 8, 2016].

Lovley, D.R. et al., 1996. Humic substances as electron acceptors for microbial respiration. *Nature*, 382(6590), pp.445–448. Available at: http://www.nature.com/doifinder/10.1038/382445a0 [Accessed May 28, 2017].

Lovley, D.R. & Phillips, E.J.P., 1988a. Manganese inhibition of microbial iron reduction in anaerobic sediments. *Geomicrobiology Journal*, 6(3–4), pp.145–155. Available at: http://www.tandfonline.com/doi/abs/10.1080/01490458809377834 [Accessed May 30, 2017].

Lovley, D.R. & Phillips, E.J.P., 1988b. Novel mode of microbial energy metabolism: organic carbon oxidation coupled to dissimilatory reduction of iron or manganese. *Applied and environmental microbiology*, 54(6), pp.1472–80. Available at: http://www.ncbi.nlm.nih.gov/pubmed/16347658 [Accessed May 25, 2017].

Madigan, M.D. et al., 2014. *Brock Biology of Microorganisms* 14th ed., Glenview, IL, USA: Pearson.

Molstad, L., Dörsch, P. & Bakken, L.R., 2016. Improved robotized incubation system for gas kinetics in batch cultures. *Technical report*. Available at: https://www.researchgate.net/publication/308118692_Improved_robotized_incubation_system_for_gas_kinetics_in_batch_cultures [Accessed May 13, 2017].

Molstad, L., Dörsch, P. & Bakken, L.R., 2007. Robotized incubation system for monitoring gases (O2 , NO, N2O N2) in denitrifying cultures. *Journal of Microbiological Methods*, 71, pp.202–211.

Murray, E. & George, J., 1997. Toxicological Profile for Propylene Glycol. *Agency for Toxic Substances and Disease Registry*, p.176. Available at: https://www.atsdr.cdc.gov/toxprofiles/tp189.pdf [Accessed May 26, 2017].

Muyzer, G., de Waal, E.C. & Uitterlinden, A.G., 1993. Profiling of complex microbial populations by denaturing gradient gel electrophoresis analysis of polymerase chain reaction-amplified genes coding for 16S rRNA. *Applied and environmental microbiology*, 59(3), pp.695–700. Available at: http://www.ncbi.nlm.nih.gov/pubmed/7683183 [Accessed June 1, 2017].

Myers, C.R. & Nealson, K.H., 1988a. Bacterial Manganese Reduction and Growth with Manganese Oxide as the Sole Electron Acceptor. *Science*, 240(4857), pp.1319–1321. Available at: http://www.sciencemag.org/cgi/doi/10.1126/science.240.4857.1319 [Accessed May 25, 2017].

Myers, C.R. & Nealson, K.H., 1988b. Microbial reduction of manganese oxides: Interactions with iron and sulfur. *Geochimica et Cosmochimica Acta*, 52(11), pp.2727–2732. Available at: http://linkinghub.elsevier.com/retrieve/pii/0016703788900415 [Accessed May 30, 2017].

Naganuma, T. et al., 2006. Isolation and Characterization of Pseudomonas Strains Capable of Fe(III) Reduction with Reference to Redox Response Regulator Genes. *Geomicrobiology Journal*, 23(3–4), pp.145–155. Available at: http://www.tandfonline.com/doi/abs/10.1080/01490450600596565 [Accessed May 31, 2017].

Nevin, K.P. & Lovley, D.R., 2002. Mechanisms for accessing insoluble Fe(III) oxide during dissimilatory Fe(III) reduction by Geothrix fermentans. *Applied and environmental microbiology*, 68(5), pp.2294–9. Available at: http://www.ncbi.nlm.nih.gov/pubmed/11976100 [Accessed May 28, 2017].

Newman, D.K. & Kolter, R., 2000. A role for excreted quinones in extracellular electron transfer. *Nature*, 405(6782), pp.94–97. Available at: http://www.nature.com/doifinder/10.1038/35011098 [Accessed May 28, 2017].

Oksanen, J. et al., 2017. vegan: Community Ecology Package. *R package version 2.4-3*. Available at: https://github.com/vegandevs/vegan [Accessed May 11, 2017].

Parker, E.E. & Moffett, E.W., 1954. Physical Properties of Polyester Resins. *Industrial and Engineering Chemistry*, 46(8), pp.1615–1618. Available at: http://pubs.acs.org/doi/pdf/10.1021/ie50536a031 [Accessed May 26, 2017].

R Core Team, 2015. R: A language and environment for statistical computing. *R Foundation for Statistical Computing*. Available at: https://www.r-project.org/ [Accessed May 11, 2017].

Recous, S., Machet, J.M. & Mary, B., 1992. The partitioning of fertilizer-N between soil and crop: Comparison of ammonium and nitrate applications. *Plant and Soil*, 144(1), pp.101–111. Available at: http://link.springer.com/10.1007/BF00018850 [Accessed May 25, 2017].

Recous, S., Mary, B. & Faurie, G., 1990. Microbial immobilization of ammonium and nitrate in cultivated soils. *Soil Biology and Biochemistry*, 22(7), pp.913–922. Available at: http://linkinghub.elsevier.com/retrieve/pii/003807179090129N [Accessed May 25, 2017].

Reguera, G. et al., 2005. Extracellular electron transfer via microbial nanowires. *Nature*, 435(7045), pp.1098–1101. Available at: http://www.nature.com/doifinder/10.1038/nature03661 [Accessed May 28, 2017].

Revil, A. et al., 2015. Self-potential monitoring of the enhanced biodegradation of an organic contaminant using a bioelectrochemical cell. *The Leading Edge*, 34(2), pp.198–202. Available at: http://library.seg.org/doi/10.1190/tle34020198.1 [Accessed May 8, 2017].

Rice, C.W. & Tiedje, J.M., 1989. Regulation of nitrate assimilation by ammonium in soils and in isolated soil microorganisms. *Soil Biology and Biochemistry*, 21(4), pp.597–602. Available at: http://linkinghub.elsevier.com/retrieve/pii/0038071789901351 [Accessed May 25, 2017].

Roesch, L.F.W. et al., 2007. Pyrosequencing enumerates and contrasts soil microbial diversity. *The ISME journal*, 1(4), pp.283–90. Available at: http://www.ncbi.nlm.nih.gov/pubmed/18043639 [Accessed

June 1, 2017].

Samferdselsdepartementet, 1999. St.meld. nr. 31 (1998-99). *028005-040012*. Available at: https://www.regjeringen.no/no/dokumenter/stmeld-nr-31-1998-99-/id192303/sec3 [Accessed May 28, 2017].

Saul, D.J. et al., 2005. Hydrocarbon contamination changes the bacterial diversity of soil from around Scott Base, Antarctica. *FEMS Microbiology Ecology*, 53(1), pp.141–155. Available at: https://academic.oup.com/femsec/article-lookup/doi/10.1016/j.femsec.2004.11.007 [Accessed May 30, 2017].

Schaup, H.W. et al., 1972. Characterization of an RNA ?binding site? for a specific ribosomal protein of Escherichia coli. *MGG Molecular & General Genetics*, 114(1), pp.1–8. Available at: http://link.springer.com/10.1007/BF00268740 [Accessed June 1, 2017].

Schmidt, I. et al., 2002. Aerobic and anaerobic ammonia oxidizing bacteria - competitors or natural partners? *FEMS Microbiology Ecology*, 39(3), pp.175–181. Available at: https://academic.oup.com/femsec/article-lookup/doi/10.1111/j.1574-6941.2002.tb00920.x [Accessed May 23, 2017].

Simpson, E., 1949. Measurement of diversity. *Nature*. Available at: http://psycnet.apa.org/psycinfo/1950-02238-001 [Accessed May 18, 2017].

Smith, B. & Wilson, J., 1996. A consumer's guide to evenness indices. *Oikos*. Available at: http://www.jstor.org/stable/3545749 [Accessed May 10, 2017].

Sogin, M.L. et al., 2006. Microbial diversity in the deep sea and the underexplored "rare biosphere". *Proceedings of the National Academy of Sciences of the United States of America*, 103(32), pp.12115–20. Available at: http://www.ncbi.nlm.nih.gov/pubmed/16880384 [Accessed June 1, 2017].

Solheim, A.L. et al., 2008. Forslag til miljømål og klassegrenser for fysisk-kjemiske parametre i innsjøer og elver, og egnehet for brukerintresser. Available at: http://www.miljodirektoratet.no/old/klif/publikasjoner/2455/ta2455.pdf [Accessed May 22, 2017].

Staley, J. & Konopka, A., 1985. Measurement of in situ activities of nonphotosynthetic microorganisms in aquatic and terrestrial habitats. *Annual Reviews in Microbiology*. Available at: http://www.annualreviews.org/doi/pdf/10.1146/annurev.mi.39.100185.001541 [Accessed June 1, 2017].

Søvik, A.. & Aagaard, P., 2003. Spatial variability of a solid porous framework with regard to chemical and physical properties. *Geoderma*, 113(1), pp.47–76. Available at: http://www.sciencedirect.com/science/article/pii/S0016706102003154 [Accessed June 1, 2017].

Torsvik, V., Goksøyr, J. & Daae, F.L., 1990. High diversity in DNA of soil bacteria. *Applied and*

environmental microbiology, 56(3), pp.782–7. Available at: http://www.ncbi.nlm.nih.gov/pubmed/2317046 [Accessed June 1, 2017].

Torsvik, V. & Øvreås, L., 2002. Microbial diversity and function in soil: from genes to ecosystems. *Current Opinion in Microbiology*, 5(3), pp.240–245. Available at: http://www.sciencedirect.com/science/article/pii/S1369527402003247 [Accessed May 31, 2017].

Toscano, G. et al., 2013. Aerobic biodegradation of propylene glycol by soil bacteria. *Biodegradation*, 24(5), pp.603–613. Available at: http://link.springer.com/10.1007/s10532-012-9609-y [Accessed May 27, 2017].

Toscano, G. et al., 2014. Natural and enhanced biodegradation of propylene glycol in airport soil. *Environmental Science and Pollution Research*, 21(15), pp.9028–9035. Available at: http://link.springer.com/10.1007/s11356-013-1952-y [Accessed April 19, 2017].

Turick, C.E., Tisa, L.S. & Caccavo, F., 2002. Melanin production and use as a soluble electron shuttle for Fe(III) oxide reduction and as a terminal electron acceptor by Shewanella algae BrY. *Applied and environmental microbiology*, 68(5), pp.2436–44. Available at: http://www.ncbi.nlm.nih.gov/pubmed/11976119 [Accessed May 28, 2017].

Tuttle, K., 1997. *Sedimentological and hydrogeological characterisation of a raised ice-contact delta—the preboreal delta-complex at Gardermoen, Southeastern Norway*. University of Oslo, Norway.

Veltman, S., Schoenberg, T. & Switzenbaum, M.S., 1998. Alcohol and acid formation during the anaerobic decomposition of propylene glycol under methanogenic conditions. *Biodegradation*, 9(2), pp.113–118. Available at: http://link.springer.com/10.1023/A:1008352502493 [Accessed April 26, 2017].

Viñas, M. et al., 2005. Bacterial community dynamics and polycyclic aromatic hydrocarbon degradation during bioremediation of heavily creosote-contaminated soil. *Applied and environmental microbiology*, 71(11), pp.7008–18. Available at: http://www.ncbi.nlm.nih.gov/pubmed/16269736 [Accessed May 30, 2017].

Weber, K.A., Achenbach, L.A. & Coates, J.D., 2006. Microorganisms pumping iron: anaerobic microbial iron oxidation and reduction. *Nature Reviews Microbiology*, 4(10), pp.752–764. Available at: http://www.nature.com/doifinder/10.1038/nrmicro1490 [Accessed May 23, 2017].

Wennberg, B. et al., 2015. *Revisjonsrapport : Revisjon ved Oslo Lufthavn AS*,

Willems, A., 2014. The Family Comamonadaceae. In *The Prokaryotes*. Berlin, Heidelberg: Springer Berlin Heidelberg, pp. 777–851. Available at: http://link.springer.com/10.1007/978-3-642-30197-1_238 [Accessed May 30, 2017].

Willetts, A., 1979. Bacterial metabolism of propane-1,2-diol. *Biochimica et Biophysica Acta (BBA) - General Subjects*, 588(3), pp.302–309. Available at:

http://linkinghub.elsevier.com/retrieve/pii/0304416579903386 [Accessed April 24, 2017].

Willetts, A., 1983. Bacterial Metabolism of Aliphatic Diols. Function of Alcohol Oxidases and Catalase in Flavobacterium sp. NCIB 11171. *Microbiology*, 129(4), pp.997–1004. Available at: http://mic.microbiologyresearch.org/content/journal/micro/10.1099/00221287-129-4-997 [Accessed May 27, 2017].

Wintzingerode, F. V., Göbel, U.B. & Stackebrandt, E., 1997. Determination of microbial diversity in environmental samples: pitfalls of PCR-based rRNA analysis. *FEMS Microbiology Reviews*, 21(3), pp.213–229. Available at: https://academic.oup.com/femsre/article-lookup/doi/10.1111/j.1574-6976.1997.tb00351.x [Accessed May 29, 2017].

Woese, C. et al., 1976. A comparison of the 16S ribosomal RNAs from mesophilic and thermophilic bacilli: Some modifications in the sanger method for RNA sequencing. *Journal of Molecular Evolution*, 7(3), pp.197–213. Available at: http://link.springer.com/10.1007/BF01731489 [Accessed June 1, 2017].

Zar, T., Graeber, C. & Perazella, M.A., 2007. Reviews: Recognition, Treatment, and Prevention of Propylene Glycol Toxicity. *Seminars in Dialysis*, 20(3), pp.217–219. Available at: http://doi.wiley.com/10.1111/j.1525-139X.2007.00280.x [Accessed May 26, 2017].

Øvreås, L. et al., 1997. Distribution of bacterioplankton in meromictic Lake Saelenvannet, as determined by denaturing gradient gel electrophoresis of PCR-amplified gene fragments coding for 16S rRNA. *Applied and environmental microbiology*, 63(9), pp.3367–73. Available at: http://www.ncbi.nlm.nih.gov/pubmed/9292986 [Accessed June 1, 2017].

Øvstedal, J. & Wejden, B., 2007. Dispersion of De-Icing Chemicals to the Areas Along the Runways at Oslo Airport Gardermoen. Available at: http://papers.sae.org/2007-01-3351/ [Accessed May 22, 2017].

A. APPENDIX

A.1 Appendix 1 – Samples taken for bacterial analysis

Table A.1: Subsoil refers to soil from Moreppen research station at 1.5 meters below surface (Figure 2.1). Top soil refers to the top 1 meter of the soil in Moreppen research station (Figure 2.2). Both are described in section 2.2.

Sample ID	Soil type	Treatment	Sample ID	Soil type	Treatment	Sample ID	Soil type	Treatment
1-1	Subsoil	Water	13-1	Top soil	Water	DS-1	Subsoil	Storage for 56 days at 5 degrees, sieving at 3.55. Original soil source of samples 1 through 12 and 33. 9th of November 2016.
2-1	Subsoil	Water	14-1	Top soil	Water	TS-1	Top soil	Storage for 56 days at 5 degrees, sieving at 3.55. Original soil source of samples 13 through 24. 9th of November 2016.
3-1	Subsoil	Water	15-1	Top soil	Water	Deep soil from field	Subsoil	Soil directly from field location before sampling. 14th of September 2016. Stored at -20C September-December 2016, and at -80C January 2017 until analysis.
4-1	Subsoil	NH_4Cl	16-1	Top soil	NH_4Cl	Top soil from field	Top soil	Soil directly from field location before sampling. 14th of September 2016. Stored at -20C. September-December 2016, and at -80C January 2017 until analysis.
5-1	Subsoil	NH_4Cl	17-1	Top soil	NH_4Cl			
6-1	Subsoil	NH_4Cl	18-1	Top soil	NH_4Cl			
7-1	Subsoil	PG	19-1	Top soil	PG			
8-1	Subsoil	PG	20-1	Top soil	PG			
9-1	Subsoil	PG	21-1	Top soil	PG			
10-1	Subsoil	PG + NH_4NO_3	22-1	Top soil	PG + NH_4NO_3			
11-1	Subsoil	PG + NH_4NO_3	23-1	Top soil	PG + NH_4NO_3			
12-1	Subsoil	PG + NH_4NO_3	24-1	Top soil	PG + NH_4NO_3			
33-1	Subsoil	PG						

A.2 Appendix 2 – N_2 measurements

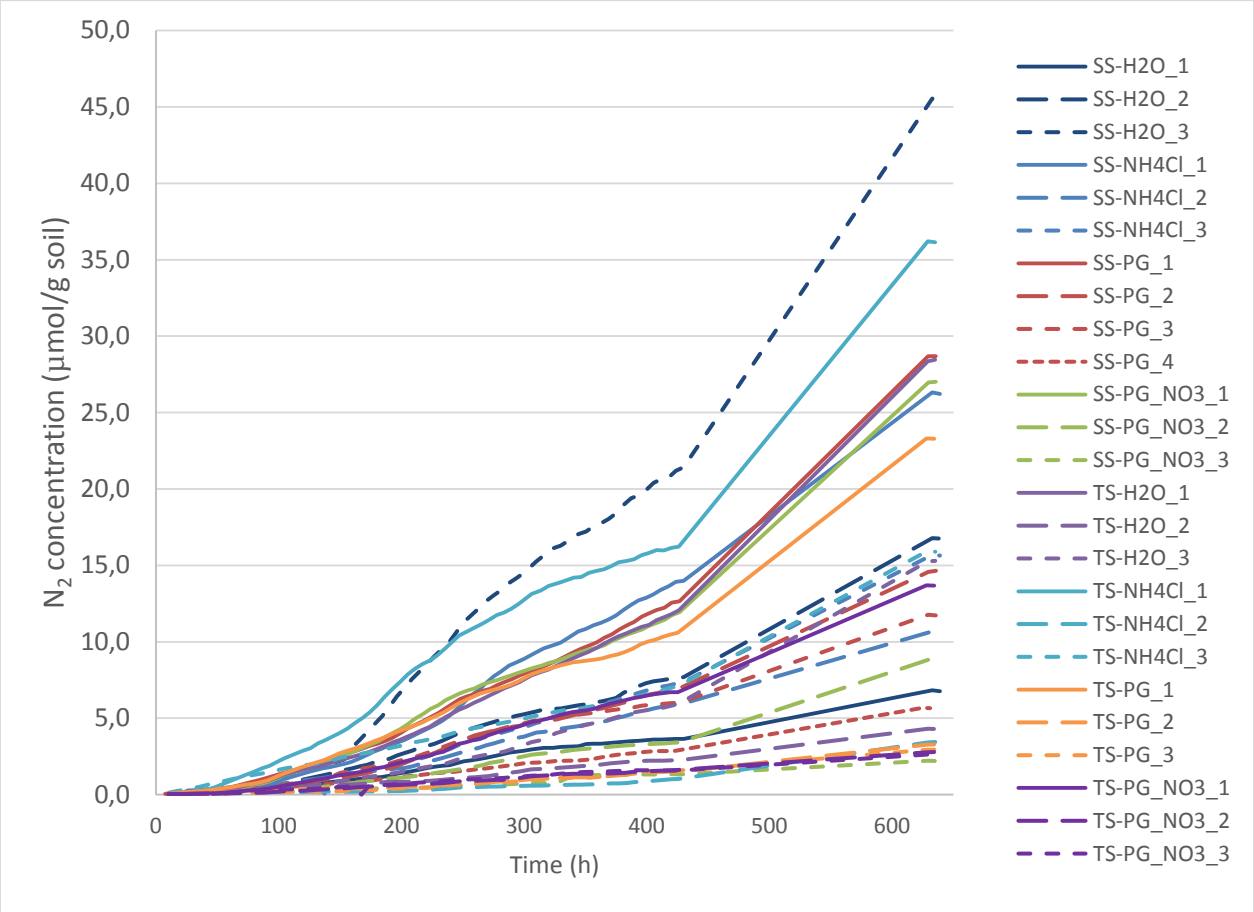

Figure A.1: Nitrogen influx per bottle over time. SS = bottles containing subsoil (Figure 2.1B), TS = bottles containing top soil (Figure 2.2). H2O = soil only added de-ionized water, NH4Cl = soil amended with ammonium chloride, PG = soil amended with propylene glycol, PGNO3 = soil amended with propylene glycol and ammonium nitrate.

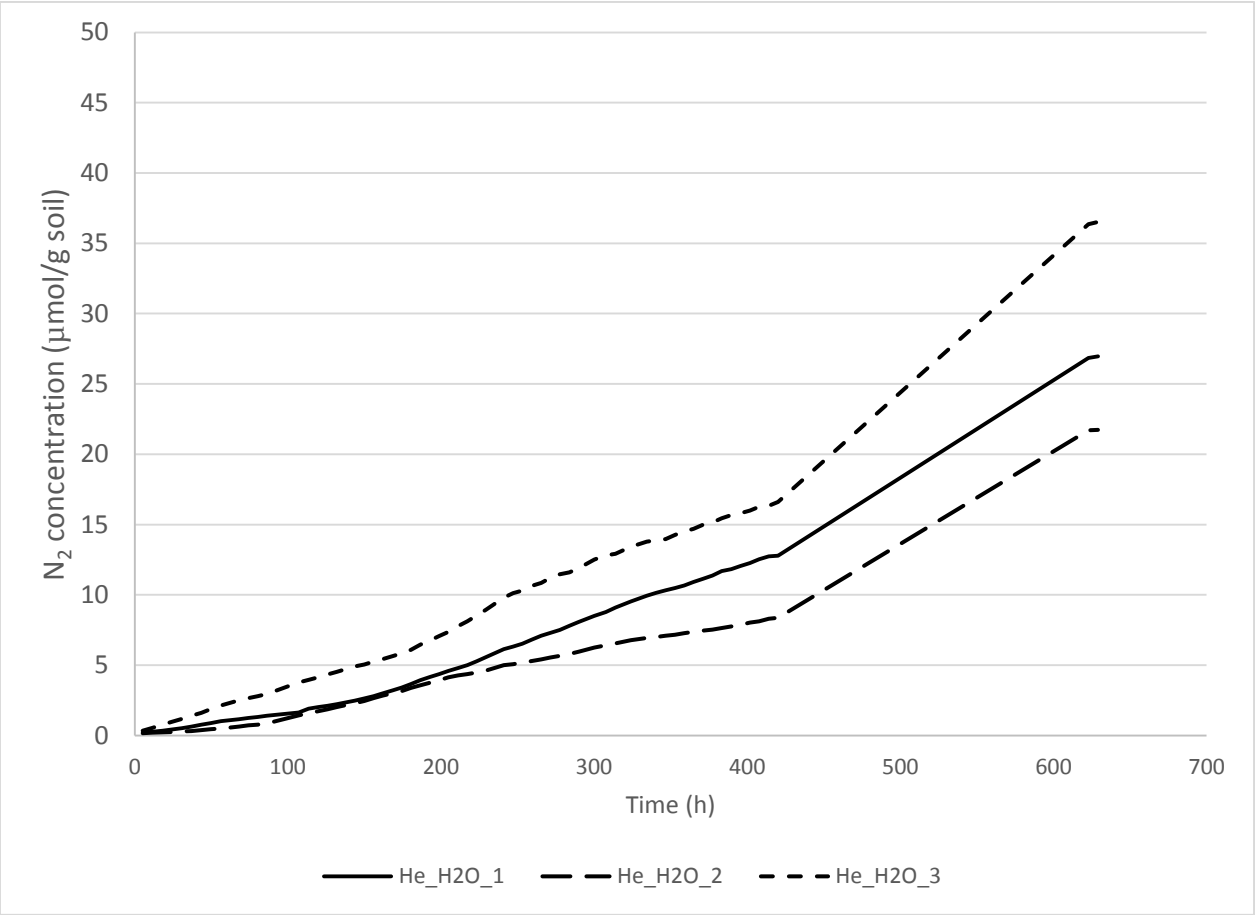

Figure A.2: N_2 influx in three standards without soil. These were added approximately equal volume of DI water as the volume the soil took up in the bottles, 40 mL. Scale in nmol/bottle is divided by 60 g to match the scale of the soil samples.

A.3 Appendix 3 – NO_3^- measurements

Table A.2: Measured initial concentrations of nitrate in the two soil types, and calculated total initial concentrations of NO_3^- amended soils. Average values with one standard deviation listed (n=3).

Soil type	**[NO_3^-] (nmol/g dry soil)**	**[NO_3^-] extra for treatment (nmol/g dry soil)**	**Total [NO_3^-] in NO_3^- amended soils (nmol/g dry soil)**
Subsoil	90 ± 72	170 ± 0.39	260 ± 72
Top soil	160 ± 53	170 ± 0.38	320 ± 53

Table A.3: Measured initial concentrations of nitrite in the two soil types. Average values with one standard deviation listed (n=3).

Soil type	**Initial [NO_2^-] (nmol/g dry soil)**
Subsoil	1.8 ± 1.1
Top soil	1.5 ± 0.61

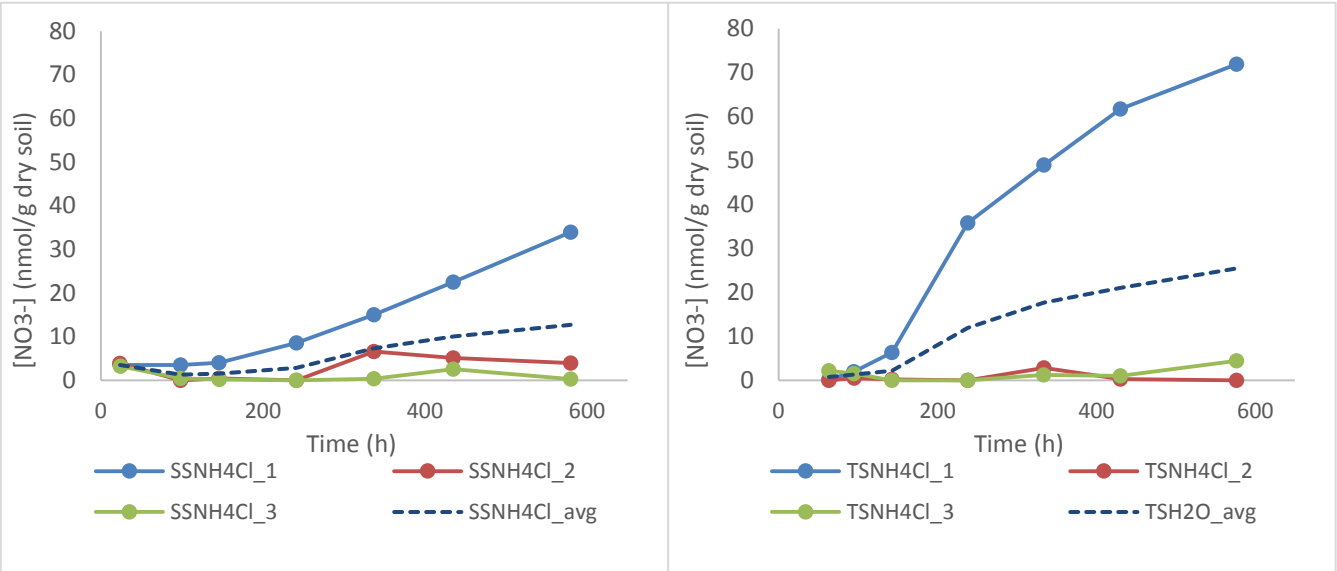

Figure A.3: NO_3^- dynamics in control samples initially amended with 10 µmol ammonia (approximately 160 nmol/g soil), subsoil to the left and top soil to the right. Initial values are omitted for visualization purposes.

Table A.4: Measured concentration of NO_2^- and NO_3^- in the samples over time. Note that this was measured after some time stored frozen, so NO_2^-values are unlikely to be close to the true values.

Sample	Time	$[NO_2^-]$	$[NO_3^-]$	Sample	Time	$[NO_2^-]$	$[NO_3^-]$	Sample	Time	$[NO_2^-]$	$[NO_3^-]$
	h	nmol/g soil			h	nmol/g soil			h	nmol/g soil	
DS_Water_1	23	0,66	3,7	DS_Water_2	24	0,42	4,0	DS_Water_3	24	0,48	4,5
DS_Water_1	98	0,027	0,45	DS_Water_2	98	0,083	0,91	DS_Water_3	98	0,074	1,2
DS_Water_1	146	0,011	0,26	DS_Water_2	146	0,0053	0,32	DS_Water_3	146	0,020	0,52
DS_Water_1	241	0,0	0,57	DS_Water_2	241	0,020	0,38	DS_Water_3	242	0,0051	0,16
DS_Water_1	337	0,0	0,63	DS_Water_2	337	0,0	0,57	DS_Water_3	337	0,0	1,4
DS_Water_1	435	0,0	1,4	DS_Water_2	435	0,011	2,0	DS_Water_3	434	0,0	3,6
DS_Water_1	580	0,0	1,4	DS_Water_2	580	0,0018	2,2	DS_Water_3	580	0,0	7,5
DS_NH4_1	24	0,18	3,5	DS_NH4_2	24	0,51	3,9	DS_NH4_3	24	0,23	3,2
DS_NH4_1	98	0,052	3,5	DS_NH4_2	98	0,02	0,00	DS_NH4_3	99	0,038	0,43
DS_NH4_1	146	0,030	4,0	DS_NH4_2	146	0,01	0,46	DS_NH4_3	146	0,013	0,27
DS_NH4_1	242	0,018	8,6	DS_NH4_2	242	0,00	0,00	DS_NH4_3	242	0,013	0,0
DS_NH4_1	337	0,0	15	DS_NH4_2	337	4,8	6,6	DS_NH4_3	337	0,0	0,40
DS_NH4_1	435	0,0	23	DS_NH4_2	435	1,4	5,2	DS_NH4_3	435	0,0084	2,6
DS_NH4_1	580	0,0	34	DS_NH4_2	580	0,00	4,0	DS_NH4_3	580	0,010	0,32
DS_PG_1	63	0,046	0,27	DS_PG_2	63	0,15	0,85	DS_PG_3	63	0,010	0,10
DS_PG_1	95	0,0	0,024	DS_PG_2	94	0,049	2,2	DS_PG_3	95	0,0	0,46
DS_PG_1	143	0,0	0,0	DS_PG_2	143	0,0055	0,0	DS_PG_3	143	0,0	0,0
DS_PG_1	238	0,0	0,0	DS_PG_2	237	0,029	0,0	DS_PG_3	238	0,0039	0,16
DS_PG_1	334	0,0	0,0	DS_PG_2	333	0,034	0,028	DS_PG_3	333	0,070	0,80
DS_PG_1	431	0,0	0,0	DS_PG_2	430	0,048	0,20	DS_PG_3	431	0,010	0,10

DS_PG_1	577	0,019	0,0	DS_PG_2	576	0,040	4,0	DS_PG_3	577	0,0	0,0
DS_PG_4	59	0,0	0,25								
DS_PG_4	90	0,0	0,32								
DS_PG_4	138	0,012	0,088								
DS_PG_4	233	0,0	0,0								
DS_PG_4	328	0,0	1,2								
DS_PG_4	426	0,0	0,19								
DS_PG_4	572	0,0	0,00								
DS_PG+NO3_1	63	0,45	104	DS_PG+NO3_2	63	6,3	111	DS_PG+NO3_3	64	0,86	96
DS_PG+NO3_1	96	30	92	DS_PG+NO3_2	95	1,5	104	DS_PG+NO3_3	96	0,22	41
DS_PG+NO3_1	143	6,1	15	DS_PG+NO3_2	143	3,9	38	DS_PG+NO3_3	143	1,2	18
DS_PG+NO3_1	239	0,081	0,0	DS_PG+NO3_2	239	0,74	3,8	DS_PG+NO3_3	239	0,22	1,2
DS_PG+NO3_1	334	0,15	0,0	DS_PG+NO3_2	333	0,20	0,70	DS_PG+NO3_3	333	0,19	0,0
DS_PG+NO3_1	432	0,056	0,0	DS_PG+NO3_2	432	0,068	0,14	DS_PG+NO3_3	430	0,051	0,0
DS_PG+NO3_1	577	0,42	0,0	DS_PG+NO3_2	577	0,16	0,0	DS_PG+NO3_3	575	0,48	0,039
TS_Water_1	63	0,016	0,10	TS_Water_2	63	0,021	0,22	TS_Water_3	63	0,018	0,16
TS_Water_1	95	0,0	0,80	TS_Water_2	95	0,0	0,41	TS_Water_3	95	0,0	0,50
TS_Water_1	143	0,0	0,0	TS_Water_2	142	0,0	0,0	TS_Water_3	142	0,0	0,0
TS_Water_1	238	0,0	0,0	TS_Water_2	238	0,0	0,0	TS_Water_3	238	0,0	0,0
TS_Water_1	333	0,0	0,55	TS_Water_2	334	0,0	0,0	TS_Water_3	334	0,0	0,37
TS_Water_1	431	0,0	0,40	TS_Water_2	431	0,0	0,0	TS_Water_3	431	0,0	1,6
TS_Water_1	577	0,0	0,41	TS_Water_2	577	0,0061	0,0	TS_Water_3	576	0,0	12
TS_NH4_1	63	0,030	0,18	TS_NH4_2	63	0,0	0,0	TS_NH4_3	64	0,27	2,2
TS_NH4_1	95	0,0076	2,0	TS_NH4_2	95	0,0	0,55	TS_NH4_3	95	0,040	1,5
TS_NH4_1	143	0,0	6,4	TS_NH4_2	143	0,0	0,20	TS_NH4_3	143	0,0	0,0
TS_NH4_1	238	0,0	36	TS_NH4_2	238	0,0	0,0	TS_NH4_3	238	0,0	0,052
TS_NH4_1	334	0,0	49	TS_NH4_2	334	0,0	2,9	TS_NH4_3	334	0,0	1,2
TS_NH4_1	430	0,0	62	TS_NH4_2	430	0,0	0,33	TS_NH4_3	430	0,0	1,1
TS_NH4_1	577	0,0	72	TS_NH4_2	577	0,0	0,0	TS_NH4_3	576	0,0	4,5
TS_PG_1	63	0,0	0,0	TS_PG_2	62	0,018	0,19	TS_PG_3	63	0,0	0,13
TS_PG_1	94	0,0	0,0	TS_PG_2	94	0,00082	0,0	TS_PG_3	95	0,0	0,0
TS_PG_1	142	0,0	0,0	TS_PG_2	142	0,0060	0,17	TS_PG_3	142	0,0	0,0
TS_PG_1	238	0,0061	0,0	TS_PG_2	237	0,00089	0,0	TS_PG_3	238	0,0028	0,0
TS_PG_1	333	0,0	0,0	TS_PG_2	333	0,0	0,0	TS_PG_3	333	0,0082	0,0
TS_PG_1	430	0,0	0,11	TS_PG_2	430	0,016	2,2	TS_PG_3	428	0,0026	0,0
TS_PG_1	576	0,0	0,0	TS_PG_2	576	0,0019	0,084	TS_PG_3	573	0,040	0,0
TS_PG+NO3_1	63	0,13	61	TS_PG+NO3_2	63	0,09	91	TS_PG+NO3_3	63	0,13	61
TS_PG+NO3_1	94	0,69	58	TS_PG+NO3_2	94	0,44	59	TS_PG+NO3_3	94	0,16	57
TS_PG+NO3_1	142	0,12	12	TS_PG+NO3_2	142	0,79	11	TS_PG+NO3_3	142	0,11	16
TS_PG+NO3_1	238	0,16	0,68	TS_PG+NO3_2	238	0,38	0,81	TS_PG+NO3_3	238	0,18	1,3
TS_PG+NO3_1	333	0,28	0,0	TS_PG+NO3_2	333	0,24	0,0	TS_PG+NO3_3	333	0,10	0,0
TS_PG+NO3_1	430	0,044	0,28	TS_PG+NO3_2	430	0,24	0,0	TS_PG+NO3_3	430	0,42	1,9
TS_PG+NO3_1	576	0,029	0,21	TS_PG+NO3_2	576	0,16	0,0	TS_PG+NO3_3	576	0,23	0,074

A.1 Appendix 4 – Diversity information

Table A.5: Number of reads before and after processing in QIIME, how many of those assigned to a taxonomy, how many different OTUs picked, the sequence length, number of OTUs included from rarefaction, Simpson Diversity Index (SDI) and Chao1 species richness for individual samples.

Sample ID	Total reads	Reads after filtering	Tax. assigned reads	16S rRNA OTUs	Sequence length range (bp)	16S rRNA OTUs after rarefaction	SDI[1]	Chao1[2]
SSfield1	88304	78798	77247	5909	200-320	4528	0,98	11991
SSfield2	85556	73753	72464	4915	200-287	4001	0,98	10965
SSfield3	99795	89802	88241	4929	200-287	3594	0,98	8425
SSstart1	85116	76412	74976	7467	200-287	5826	0,99	16888
SSstart2	111087	100508	98680	11707	200-391	7396	0,99	25362
SSstart3	96522	86069	84452	10634	200-291	7502	0,99	24276
SSH2O1	107266	95974	94220	7958	200-287	5421	0,99	15162
SSH2O2	102323	91947	90558	11836	200-354	7882	0,99	26115
SSH2O3	86653	74569	73629	10022	200-421	7796	0,99	26489
SSNH4Cl1	90495	80864	79665	10128	200-287	7351	0,98	24894
SSNH4Cl2	83660	72523	71512	9606	200-419	7653	0,99	25439
SSNH4Cl3	111186	100220	98747	11886	200-287	7502	0,99	26071
SSPG1	100826	88765	87670	8417	200-280	5894	0,99	17776
SSPG2	107673	94995	93645	9583	200-278	6388	0,98	20942
SSPG3	103816	91620	90434	10539	200-280	7196	0,99	23284
SSPG4	129628	116487	114757	13248	200-395	7528	0,99	24610
SSPGNO31	98409	86480	85933	5897	200-277	4308	0,87	11537
SSPGNO32	104047	93512	92581	7058	200-287	4832	0,89	13021
SSPGNO33	113600	96381	92409	4109	200-287	2767	0,81	6951
TSfield1	57970	52079	50718	4493	200-418	4493	0,98	12852
TSfield2	97375	86738	85568	7057	200-385	5032	0,99	13952
TSfield3	103370	93075	91793	7888	200-317	5321	0,97	15962
TSstart1	105937	95534	94170	11972	200-287	7799	0,99	24105
TSstart2	123930	111426	109544	13799	200-342	8070	0,99	27436
TSstart3	106015	94392	93160	11742	200-326	7739	0,99	25079
TSH2O1	103258	93002	91840	11400	200-293	7603	0,98	24585
TSH2O2	113224	98389	97115	12220	200-293	7884	0,98	26412
TSH2O3	87802	79634	78710	8557	200-410	6463	0,98	19372
TSNH4Cl1	152329	138771	137388	12253	200-391	6362	0,98	18648
TSNH4Cl2	75861	67923	67246	7271	200-391	6065	0,98	17600
TSNH4Cl3	100207	90762	89913	8614	200-406	5898	0,98	18111
TSPG1	96504	86925	86057	8349	200-418	6011	0,98	17781
TSPG2	109094	99226	98411	7675	200-415	5094	0,99	13794
TSPG3	102271	92121	91053	9408	200-391	6476	0,98	18973
TSPGNO31	104480	93750	92877	8896	200-290	5994	0,98	17430
TSPGNO32	111020	99942	98907	10253	200-391	6537	0,99	19070

TSPGNO33	106295	94426	93467	10317	200-391	6893	0,99	21120

[1]Simpson Diversity index (1-D; Simpson, 1949), calculated using all rRNA OTUS after rarefaction.
[2]Chao1 species richness estimator (Chao 1987; Chiu et al. 2014)

Kdføs

Table A.6: From the filtered reads, how many were classified at the different taxonomical ranks based on the GreenGenes database.

Sample ID	Classified at Phylum rank	Classified at Class rank	Classified at Order rank	Classified at Family rank	Classified at Genus rank	Classified at Species rank
SSfield1	98 %	97 %	82 %	36 %	8 %	0,075 %
SSfield2	98 %	97 %	83 %	38 %	7 %	0,20 %
SSfield3	98 %	97 %	84 %	40 %	7 %	0,05 %
SSstart1	98 %	97 %	80 %	45 %	12 %	0,45 %
SSstart2	98 %	97 %	79 %	43 %	10 %	0,36 %
SSstart3	98 %	97 %	80 %	49 %	13 %	0,63 %
SSH2O1	98 %	97 %	80 %	46 %	12 %	0,31 %
SSH2O2	98 %	97 %	77 %	45 %	11 %	0,40 %
SSH2O3	99 %	97 %	79 %	45 %	11 %	0,21 %
SSNH4Cl1	99 %	97 %	80 %	48 %	11 %	0,33 %
SSNH4Cl2	99 %	97 %	78 %	44 %	11 %	0,28 %
SSNH4Cl3	99 %	97 %	77 %	45 %	11 %	0,41 %
SSPG1	99 %	97 %	83 %	52 %	19 %	0,46 %
SSPG2	99 %	98 %	84 %	57 %	24 %	0,55 %
SSPG3	99 %	98 %	82 %	52 %	18 %	0,70 %
SSPG4	99 %	97 %	82 %	50 %	14 %	0,35 %
SSPGNO31	99 %	99 %	92 %	78 %	54 %	0,16 %
SSPGNO32	99 %	98 %	91 %	77 %	52 %	0,39 %
SSPGNO33	96 %	96 %	92 %	85 %	38 %	0,29 %
TSfield1	97 %	90 %	71 %	48 %	14 %	1,3 %
TSfield2	99 %	95 %	80 %	58 %	22 %	2,4 %
TSfield3	99 %	94 %	68 %	37 %	10 %	0,63 %
TSstart1	99 %	95 %	74 %	48 %	15 %	1,3 %
TSstart2	98 %	95 %	78 %	51 %	17 %	1,3 %
TSstart3	99 %	96 %	81 %	55 %	17 %	1,3 %
TSH2O1	99 %	95 %	72 %	49 %	15 %	1,5 %
TSH2O2	99 %	95 %	73 %	48 %	15 %	1,1 %
TSH2O3	99 %	96 %	73 %	50 %	16 %	2,0 %
TSNH4Cl1	99 %	96 %	76 %	51 %	16 %	1,8 %
TSNH4Cl2	99 %	96 %	76 %	51 %	15 %	1,5 %
TSNH4Cl3	99 %	96 %	76 %	52 %	16 %	1,2 %
TSPG1	99 %	95 %	76 %	53 %	17 %	1,2 %
TSPG2	99 %	96 %	80 %	55 %	16 %	1,2 %
TSPG3	99 %	96 %	76 %	52 %	15 %	1,4 %

TSPGNO31	99 %	96 %	78 %	56 %	21 %	1,0 %
TSPGNO32	99 %	96 %	78 %	55 %	15 %	1,1 %
TSPGNO33	99 %	96 %	79 %	55 %	19 %	1,5 %
Total sample set	99 %	96 %	79 %	52 %	17 %	0,86 %

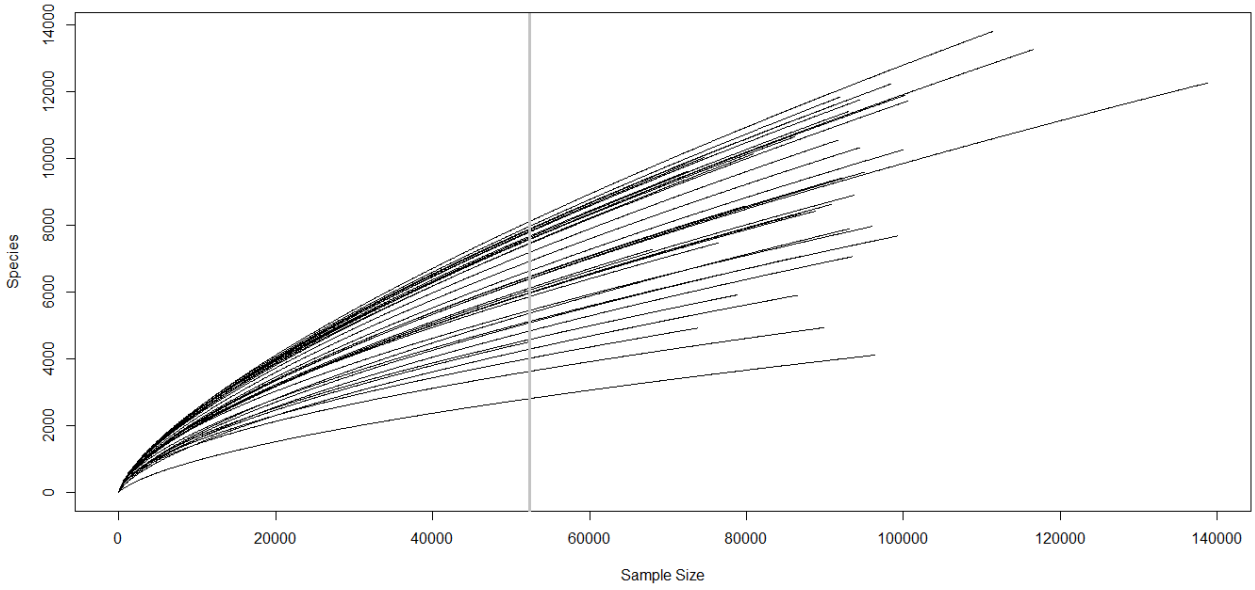

Figure A.4: Rarefaction curves of all samples. The grey line shows the rarefaction cutoff, at 52 079 reads.

Table A.7 lists the top ten most abundant OTUs and their assigned phylogeny/taxonomy according to the GreenGenes database (DeSantis et al. 2006).

Table A.7: The top 10 OTUs and their phylogeny according to GreenGenes database.

%*	**Phylogeny: *Phylum, Class, Order, Family, Genus***
8.1	*Acidobacteria, DA052,* ***Ellin6513***
2.9	*Proteobacteria, Alphaproteobacteria, Rhizobiales,* ***Bradyrhizobiaceae***

2.3	*Chloroflexi, TK10, B07_WMSP1,* ***FFCH4570***
1.7	*'AD3',* ***'JG37-AG-4'***
1.7	*Proteobacteria, Betaproteobacteria, Burkholderiales,* ***Oxalobacteraceae***
1.6	*Proteobacteria, Betaproteobacteria, Burkholderiales, Comamonadaceae,* ***Rhodoferax***
1.5	*Proteobacteria, Gammaproteobacteria, Xanthomonadales,* ***Sinobacteraceae***
1.4	*Proteobacteria, Gammaproteobacteria, Pseudomonadales, Pseudomonadaceae,* ***Pseudomonas***
1.4	*'AD3',* ***'ABS-6'***
1.4	*Acidobacteria, iii1-8,* ***DS-18***

* Fraction of total sample set